University of Southern Queensland

Faculty of Engineering & Surveying

Analysis of Data to Develop Models for Spray Combustion

A dissertation submitted by

Jason Clarke

in fulfilment of the requirements of

ENG4112 Research Project

towards the degree of

Bachelor of Mechanical Engineering

Submitted: October, 2010

Abstract

The design of modern petrol engines has placed an emphasis on lean combustion in order to increase efficiency, reduce operating noise and reduce pollutants. However, the closer the engine operates to the lean combustion limit the higher the possibility of engine misfires occurring. Misfires occur when there is not sufficient droplet density around the spark to allow the evaporation of the droplets and hence the release of fuel to the system.

The advent of injection systems has enabled engineers to control the majority of the parameters of spray combustion, such as droplet size, droplet density and spray pattern. Therefore, the ability to model spray combustion would have wide ranging implications on the automotive industry.

One model which lends itself to the modelling of spray combustion is the Conditional Moment Closure (CMC) model. However, the behaviour of the terms of the CMC model, namely the conditional scalar dissipation, conditional source term and the mixture fraction probability density function (pdf), is not understood well for this case.

A number of Direct Numerical Simulations (DNS) have been performed on different cases of combustion where fuel droplets are present in cold air and a spark is used to evaporate the droplets and initiate a flame kernel. Data was collected and models were developed for the three key terms of the CMC model.

Validation of the first order CMC model was performed by attempting to recreate the behaviour of the DNS data. The performance of the first order CMC model was found to be poor due to the inability of the model to account for fluctuations about the

conditional mean of the quantities. Another conditioning variable, or second-order conditional modelling, may be needed in order for the CMC model to adequately capture the behaviour of spark assisted, spray combustion.

University of Southern Queensland

Faculty of Engineering and Surveying

ENG4111/2 *Research Project*

Limitations of Use

The Council of the University of Southern Queensland, its Faculty of Engineering and Surveying, and the staff of the University of Southern Queensland, do not accept any responsibility for the truth, accuracy or completeness of material contained within or associated with this dissertation.

Persons using all or any part of this material do so at their own risk, and not at the risk of the Council of the University of Southern Queensland, its Faculty of Engineering and Surveying or the staff of the University of Southern Queensland.

This dissertation reports an educational exercise and has no purpose or validity beyond this exercise. The sole purpose of the course pair entitled "Research Project" is to contribute to the overall education within the student's chosen degree program. This document, the associated hardware, software, drawings, and other material set out in the associated appendices should not be used for any other purpose: if they are so used, it is entirely at the risk of the user.

Prof F Bullen

Dean

Faculty of Engineering and Surveying

Certification

I certify that the ideas, designs and experimental work, results, analyses and conclusions set out in this dissertation are entirely my own effort, except where otherwise indicated and acknowledged.

I further certify that the work is original and has not been previously submitted for assessment in any other course or institution, except where specifically stated.

Student Name:

Student Number:

_____ (signature)

_____ (date)

Acknowledgments

This project was supervised by Dr. Andrew Wandel. I would like to thank him for his support and technical expertise without which I could not have completed this project.

I would also like to thank my family for their continuing support.

Jason Clarke

University of Southern Queensland

October 2010

Contents

List of Figures

Chapter 1

Introduction

1.1 Introduction

Increasingly, governments and social pressure have required cars, and therefore engines, to become more efficient and produce less pollutants. Both Australian and American governments have pledged to commit to reducing emissions from cars (Gillard (current August 2010) and Crawley (current May 2010)). Beyond reducing emissions, increased efficiency of cars also translates to benefits for the consumer, with reduced fuel consumption and lower engine noise. For these reasons, both industry and academics have committed large amounts of resources to increasing the efficiency of cars, and perhaps of more interest to this thesis, engines.

In the motor industry today, almost all petrol engines have adopted the use of injectors to supply fuel to the combustion chamber. The use of injectors has allowed a much greater ability to control the parameters of spark assisted spray ignition than carburettored engines. Some parameters which may be adjusted are droplet size, droplet density, spray pattern, spark intensity and duration. The advent of fuel injection has also meant that the mixing of fuel and oxygen now takes place in the combustion chamber.

For the best chemical efficiency, fuel and air should be combusted stoichiometrically.

For stoichiometric mixing, the air to fuel ratio (m_{air}/m_{fuel}) should be 14.7 for octane fuels. However, traditionally, the mixture has been 'rich', or an air to fuel ratio in the range of $12.5 - 13.3$ to reduce the chance of engine misfires. This however leads to unwanted pollutants, such as HC, CO and NO_x. In order to design engines which operate as lean as possible, accurate models of combustion are needed. The focus of this project is to progress the development and implementation of such models.

The modelling of spray combustion is complex and not thoroughly understood. Modelling of gaseous phase combustion is simpler than droplet combustion because the fuel is already present in the correct phase. In spray combustion, however, the droplets must first be evaporated by an area of localised high temperature (which may be created by the spark energy or compression of the gas), and must continue to be evaporated by the flame front in order to continue releasing fuel to the system (Wandel, Chakraborty & Mastorakos 2009). The effect of the evaporation of the droplets with respect to the flow field and temperature must be accounted for when attempting to model two phase combustion.

Currently, there are four main methods used for modelling turbulent reacting flows, such as spray combustion. These are numerical modelling (Direct Numerical Simulations (DNS)), large eddy simulation (LES), turbulent combustion models such as the Conditional Moment Closure (CMC) model and models implemented in Computational Fluid Dynamics (CFD) software. LES still requires development for gaseous combustion. The main disadvantage of numerical modelling is that it is computationally expensive; currently the processing power of computers has not allowed the modelling of spray ignition for volumes larger than the order of 1cm^3. The main disadvantage of CFD is that since little is known about the evaporation of droplets in two phase combustion, models must be developed to incorporate into the CFD software. The models for incorporation into CFD software could potentially be developed from use of the CMC model.

There have been numerous studies into combustion using the CMC model, however most of the studies have relied on numerical data directly obtained from the use of DNS, rather than predefined models. Predefined models for use in CMC modelling are scarce as there is limited understanding of the behaviour of the key coefficients

in the CMC equation in the presence of evaporation. The current study aims to reduce the gap in knowledge by analysing 3-D DNS data to generate models for the key coefficients in the CMC transport equation so that large-scale modelling may be performed for sprays.

The broad objectives of this project are:

- Analyse data from numerical simulations performed by Wandel et al. (2009) to characterise combustion for a small control volume (approximately $1mm^3$) using the CMC model,
- verify the models' accuracy by recreating the data the models were obtained from,
- code the models into a CFD package to allow for a much larger scale of modelling to take place, and
- model combustion in a simple combustion chamber to investigate the effects of changing parameters of spark assisted spray combustion.

1.2 Background and theory

1.2.1 Offer of the project

This project was offered by the faculty under the guidance of Dr. Andrew Wandel. Andrew has a keen interest in the use of CMC methods to characterise combustion. This project is an extension of research conducted by Andrew, from which a large amount of data has been generated. This data has been used in the published paper Wandel et al. (2009), but all the necessary quantities needed to solve the CMC model are also present in the data.

1.2.2 Importance of fuel efficiency and low emissions

In recent years, there has been a widespread political and social push for car manufacturers to increase fuel efficiency and reduce emissions. Fuel efficiency is a measure

of the specific fuel consumption of an automobile per kilometre travelled. Emissions refer to the production of harmful pollutants, such as HC, CO and NO_x. Generally, fuel efficiency and level of emissions are linked; an increase in fuel efficiency results in a decrease in the production of pollutants.

Increasing the fuel efficiency of a vehicle has been, and continues to be, the focus of much research (Taymaz, Cakir & Mimaroglu (2005) and Nabi (2010)). There are many positives associated with increasing efficiency. Among these are: reduced fuel consumption (resulting in lower costs of running and longer range of the car), reduced engine noise, and fewer pollutants. Commercially, the production of efficient cars is of great importance as the majority of consumers value fuel efficiency when buying a new car.

There are numerous methods of increasing the brake thermal efficiency of a car. Brake thermal efficiency is a measure of the output power of a car converted from the energy stored by the fuel, and takes into account the thermal efficiency of the engine cycle, the mechanical efficiency and the chemical efficiency. Thermal efficiency may be increased by increasing the efficiency of the combustion cycles (typically Otto or Diesel cycle) by increasing compression ratio or decreasing the heat loss from the combustion to the cooling system. Mechanical efficiency can be increased by reducing any mechanical losses, such as friction. The chemical efficiency can be increased by ensuring all fuel that enters the combustion chamber is consumed by the combustion. The findings of this project could lead to an increase in the chemical efficiency of an engine, but the findings could also flow on to reducing mechanical losses.

1.2.3 Background on two phase systems

This project focuses on spark assisted spray combustion, which is found in fuel injected petrol engines. The presence of two phases (namely fuel in liquid, or droplet form, and air in gaseous form) presents quite a problem when trying to model combustion. In fact, the interaction of two phases without combustion is a complex phenomena and has been the focus of many studies (Bini & Jones (2008) and Lebas, Menard, Beau, Berlemont & Demoulin (2009)).

There are many difficulties associated with trying to predict the behaviour of two-phase mixing. Among these are: the effect of turbulence on the mixing rate, the evaporation of the liquid phase, droplet breakdown and the tendency of the droplets to coalesce. These phenomena also prove to be computationally complex.

These problems are amplified somewhat with the mixing occurring concurrently with combustion. For combustion to take place, energy in the form of a spark must be added to the system. This also has the effect of evaporating fuel droplets and releasing fuel to the system. The presence of fuel and oxidiser in gaseous phase, along with heat from the spark, allows a flame kernel to develop. Once the flame kernel has grown to a sufficient size and heat to stabilise, the spark may be removed. The flame kernel advances throughout the rest of the combustion chamber, first evaporating any droplets nearby, and then consuming them in the combustion. Several factors influence the ability of the flame kernel to proceed throughout the combustion chamber. If the droplet size is too big, too little fuel is evaporated to allow combustion to proceed. Likewise, if the droplet spacing is too big, fuel may become too sparse. If the spark is removed prematurely, the flame kernel may not be hot enough to become self sustained. The ability to model two-phase combustion systems would allow the investigation of the parameters which would encourage the most efficient combustion.

When trying to model two-phase systems, the required outputs are most often the mass fractions of each species, and temperature across the domain. The mass fractions of each species are hard to model, because the rate of reaction between the fuel and the oxidiser are highly non-linear functions of the mass fractions of fuel and oxidiser, and the local temperature (Klimenko & Bilger 1999). Further complexity arises from turbulence in the combustion chamber. This causes areas of highly differing rates of mixing and therefore the spatial location of combustion in the domain is largely unpredictable. Also contributing to the difficulty of modelling spray combustion in comparison to single phase systems is that some energy (in the form of a spray or advancing flame front) is needed to evaporate droplets and thus release fuel to the system.

Due to the complexity of attempting to model two-phase systems, and in particular spray combustion, rigorous and accurate modelling methods are required. One such

approach is performing a DNS.

1.2.4 Direct Numerical Simulation (DNS)

DNS is a method of solving the Navier-Stokes equations numerically to describe fluid flow. In a similar fashion to CFD, a given control volume is meshed (divided up into a number of nodes) and the defining equations are solved at these points. However, given that the Navier-Stokes equations are solved directly and without the use of pre-defined models, the grid size must be much smaller than that used in CFD software. For example Wandel et al. (2009) performed a DNS with a control volume with 128^3 nodes. The control volume was cubic with length 1.675mm. This equates to approximately 1.31×10^{-5}m between adjacent nodes. The simulation, performed on a recent, commercially available computer, took a period of days to solve.

The computational time required for DNS is further increased when a chemical reaction (such as combustion) occurs. While there has been some research into reducing the computing requirements of the chemical reaction of n-heptane fuels (Lu, Law, Yoo & Chen 2009), performing DNS on combustion any larger than the order of 1cm^3 is too computationally demanding. While there has been widespread use of DNS to model the behaviour of certain systems (Wang & Rutland (2007) and Sreedhara & Huh (2007)), and it is a useful tool for verifying the results of other less demanding models, DNS is of little use when modelling large scale systems, such as spray ignition. Therefore, other methods of modelling large scale systems are needed. One of these methods is the CMC model.

One of the advantages of using DNS is the ability to record vast amounts of data relating to the combustion. This data, if analysed properly, can allow for a very thorough understanding of the behaviour of the combustion. The data may also used to develop models for certain aspects of the combustion which may be used in the CMC model.

1.2.5 Conditional Moment Closure model

The CMC model is used for the prediction of turbulent reacting flows. Combustion may be considered a turbulent reacting flow as the burning of fuel and oxidiser is a chemical reaction. The main advantage of the CMC model over DNS is that because it uses predefined models, rather than solving the Navier-Stokes equations and reaction equations directly, it is much less computationally intense and therefore can be used to model much larger systems.

At the core of the theory behind the CMC model is that fundamental quantities of combustion, such as species mass fractions, enthalpy and temperature, is conditional on the mixture fraction (or 'is a function of' the mixture fraction) (Klimenko & Bilger 1999). The mixture fraction is defined as the proportion of the mixture that was originally fuel. The general form of the first order CMC model for homogenous cases is:

$$\frac{\partial \langle Y_\alpha | Z \rangle}{\partial t} = \langle N | Z \rangle \frac{\partial^2 \langle Y_\alpha | Z \rangle}{\partial Z^2} + \langle W | Z \rangle + \langle S | Z \rangle \tag{1.1}$$

where:

- The angle brackets denote the quantity to the left of the vertical bar is conditional upon the quantity to the right (is the average of the left given a particular value of the right),
- Z = mixture fraction, or proportion of the mixture that was originally fuel,
- $\langle Y_\alpha | Z \rangle$ = mass fraction of fuel or oxidiser,
- $\langle N | Z \rangle$ = conditional scalar dissipation (equivalent to viscosity),
- $\langle W | Z \rangle$ = conditional chemical source term (gain/loss due to chemical reactions),
- $\langle S | Z \rangle$ = conditional generation due to droplet evaporation.

For stoichiometric combustion of n-heptane (as analysed in this project), the mean mixture fraction over the whole combustion chamber should equal 0.062.

The scalar dissipation, chemical source and generation due to droplet evaporation are all quantities which must be modelled. The models for these terms may be derived from DNS data, experimental data or analytical equations. One of the aims of this project is to develop models for these three terms by analysing DNS data generated as a by-product of the work undertaken in Wandel et al. (2009).

The CMC model is versatile due to its ability to be used for many different forms of combustion, as well as the ability to predict many quantities such as mass fraction of fuel and oxidiser, temperature and enthalpy. Depending on the nature of the combustion, the form of the CMC model may change (Klimenko & Bilger 1999).

One of the main advantages of using the CMC model is that the quantities do not need to be modelled with respect to their spatial coordinates, rather the quantities are only conditional upon the mixture fraction. By reducing the number of independent variables, the time necessary to model a system using CMC methods is dramatically less than if DNS were to be used. For example, in the work performed as part of this project, the time saved when modelling an equivalent system using CMC over DNS was an order of magnitude of approximately 17000.

Given that the calculated values, such as mass fractions and temperature, are conditional upon the mixture fraction, the distribution of mixture fraction throughout the domain needs to be known in order to calculate the average values of those quantities. The average value of any of the quantities calculated with the CMC model is given by

$$\langle Y_\alpha \rangle = \int_0^1 \langle Y_\alpha | Z \rangle \, P(Z) dZ \tag{1.2}$$

where $P(Z)$ is the mixture fraction probability density function. Therefore, in order for the CMC model to be useful, and therefore for the ability to verify the CMC model against other methods, the probability density function must also be known. While some forms of the mixture fraction probability density function are given in literature (Sreedhara & Huh 2007), it may also be determined when performing a DNS. Therefore, as with other terms of the CMC equation such as scalar dissipation, the mixture fraction pdf may be modelled from data obtained by performing a DNS.

1.2.6 Terms of the CMC model

There are three main terms of the CMC model which require modelling. These are conditional scalar dissipation, conditional chemical source and conditional generation due to droplet evaporation.

The mathematical equation defining the scalar dissipation is:

$$N = D(\nabla Z \cdot \nabla Z) \tag{1.3}$$

where D is the diffusivity and Z is the mixture fraction. The conditional scalar dissipation is equivalent to viscosity. Scalar dissipation is typically high at large values of mixture fraction, as combustion occurs in rich areas. The combustion releases fuel to the surrounding air, causing large variations in mixture fraction, and therefore large gradients of mixture fraction. This in turn causes the scalar dissipation to be large.

The conditional generation due to droplet evaporation is a term which refers to the contribution of the evaporation of droplets into gaseous phase to the mass fraction of fuel. As the droplets are evaporated from the high temperature caused by either the spark or the flame kernel, more fuel is released into the system in gaseous phase. Therefore, more fuel is present which causes the mass fraction of fuel to increase. The conditional generation due to droplet evaporation is greater in rich areas where combustion is more likely to take place.

The chemical source term, $\langle W|Z \rangle$ can be approximated by an Arrhenius equation and is a function of the mass fractions of fuel and air, and the temperature. Because the CMC model solves for the mass fractions as well as temperature, $\langle W|Z \rangle$ can be calculated as the combustion proceeds. The chemical source term used is different depending on which quantity is being solved for.

The mixture fraction probability density function may also be determined from DNS data. Because the mixture fraction can be determined at every node in the DNS, the relative probability of each value of mixture fraction occurring within the domain can be ascertained.

1.2.7 Limitations and assumptions of the first order CMC model

The first order CMC model is useful under many circumstances for modelling combustion. The equation presented above (1.1) is a first order CMC model because there is only one conditioning variable, mixture fraction. However, in certain cases, two conditioning variables may be needed to fully capture the behaviour of the combustion.

One of the assumptions implicit in the use of the first order CMC model is that the conditional species mass fractions are strongly correlated, or

$$\langle Y_\alpha Y_\beta | Z \rangle = \langle Y_\alpha | Z \rangle \langle Y_\beta | Z \rangle + \left\langle Y''_\alpha Y''_\beta | Z \right\rangle \tag{1.4}$$

where the final term, $\left\langle Y''_\alpha Y''_\beta | Z \right\rangle$ or the conditional variance, is assumed to be negligible. If the species mass fractions are strongly correlated, the conditional average rate of reaction can be predicted using the conditional moments and the final term of equation (1.4) may indeed be considered negligible.

In single phase systems, it has been found that under most circumstances that the mass fractions of fuel and oxidiser are strongly correlated and as such the first order CMC model accurately predicts the behaviour. In systems where local extinction and re-ignition occurs, the mass fractions become less correlated and a higher order version of the CMC equation is required. It is unclear whether the use of the first order CMC model will accurately model two-phase combustion.

Single phase combustion which experiences local extinction and re-ignition has been successfully modelled using a doubly-conditioned CMC model (Kronenburg & Papoutsakis 2005). Significant variation in the values of mass fractions conditional upon mixture fraction was found around the points at which extinction and re-ignition occurred. The result of the high variance was that the first order CMC equation was unable to fully predict the reaction rate at these critical points. In order to account for the significant variation about the mean, a second conditioning variable was introduced. This second conditioning variable was sensible enthalpy.

There are two main factors which may influence the ability of a first order CMC model to accurately predict spark assisted spray combustion. It is unclear whether the presence of two phases will require the use of a second conditioning variable. There is also some

doubt that a first order CMC model will be able to account for significant variations in the mean occurring in areas adjacent the spark.

The use of a doubly-conditioned CMC model is beyond the scope of this project, but the work presented here will be able to ascertain the validity or otherwise of the first order CMC at modelling spark assisted spray combustion.

1.2.8 Objectives relating to DNS and CMC

This project will focus on characterising the terms of the single order CMC equation presented in (1.1). The mixture fraction probability density function will also be characterised. The data required to successfully create models for the CMC terms has been recorded as outputs from a DNS performed by Wandel et al. (2009). DNS data is available for several cases of combustion, which will be used to assess the adaptability of the models created.

The first order CMC equation will then be solved numerically, and with the same boundary and initial conditions as was used in the DNS. The quantities that will be solved for are conditional temperature and the conditional mass fractions of fuel and oxidiser. These values will then be checked against the values computed in the DNS.

The two main conclusions that are hoped to be drawn from this work are:

1. That all conditional quantities present in the single order CMC model can be modelled accurately over the whole life of the combustion, and that these models may easily be adapted for different cases of combustion.
2. To prove or disprove that the first order CMC model can be successfully applied to spark assisted spray combustion.

If both of these objectives can be met, further work may focus on:

1. Using the models to predict the behaviour of much larger systems, either through implementation of the models in CFD software or the creation of a program, or

2. If the first order CMC model is not sufficient, using the techniques presented in this thesis to characterise the quantities of the CMC model with respect to two conditioning variables as per the requirements of the doubly-conditioned CMC model.

1.2.9 Application of the CMC model to CFD software

The CMC model could potentially be integrated into CFD software in order to model large, dynamic systems. CFD software has the ability to accurately predict the flow field of a system, however currently the models used may not be suitable for spray combustion. The flow field refers to the velocity and pressure of the system.

Because the outputs obtained from CFD software (velocity, pressure) are inputs into the CMC equation, and the outputs obtained from the CMC model (temperature, density) are inputs into the CFD software, the two could be coupled in order to predict the behaviour of large, dynamic combustion systems. The coupling of CFD and CMC can be depicted graphically in figure 1.1.

Each completion of the cycle is equivalent to one timestep. The integration of CMC models into CFD software could potentially prove to be very valuable, more so with the increasing computation power available. It could possibly be used to model combustion in an engine or other large, complex systems.

1.3 Literature review

Literature published on the modelling of turbulent combustion of two phase systems has been restricted to the last 15 years as the processing power required to perform numerical simulations has become available. Most literature concerning DNS and CMC models for spray combustion is published by two bodies, the Combustion Institute and Combustion and Flame journal. Currently, there is somewhat of a void in the area of using DNS data to model the terms of the CMC model.

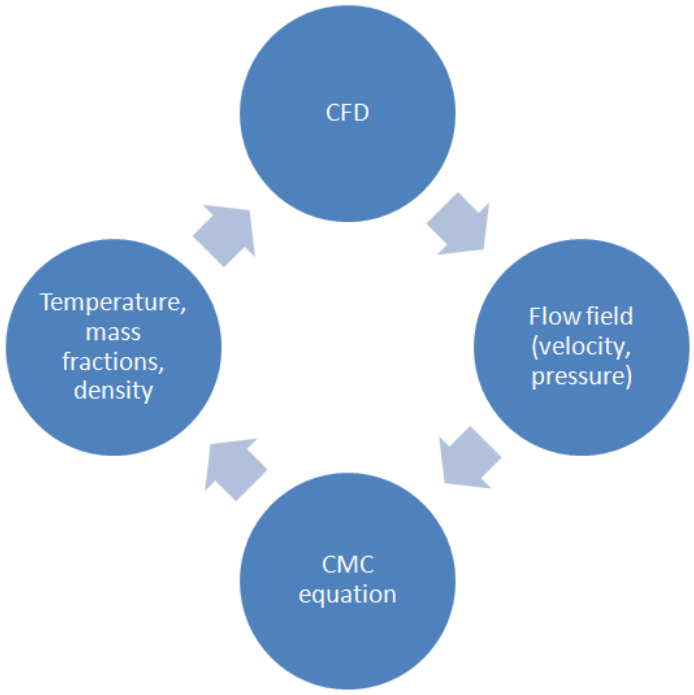

Figure 1.1: Flowchart showing the coupling of CMC and CFD.

The CMC model and its uses

The most definitive article on the subject is Klimenko & Bilger (1999), "Conditional moment closure for turbulent combustion". This article aims to review all of the preceding knowledge of the application of the CMC model to "turbulent reacting flows, with particular emphasis on combustion".

The article provides a comprehensive overview of the methods of developing approximations of the mixture fraction probability density function (pdf) for use in the CMC model. A combination of β, δ and Gaussian functions is used to model the pdf. However, this information is not needed in this project as data necessary to model the pdf forms part of the data collected from the DNS simulations and therefore will be modelled as per the other quantities.

In this article, the proposed CMC equation is

$$\frac{\partial Q}{dt} + \langle \mathbf{v}|Z\rangle \cdot \nabla Q + \frac{\mathrm{div}(\rho_Z \langle \mathbf{v}"Y"|Z\rangle P(Z))}{P(Z)\rho_Z} - \langle N|Z\rangle \frac{\partial^2 Q}{\partial Z^2} = \langle W|Z\rangle \tag{1.5}$$

where the second and third terms of the left hand side are, for the purposes of this project, negligible. This equation is largely consistent with that presented in Mortensen & Bilger (2009).

The work of Klimenko & Bilger (1999) highlights the main void in current literature; applying models derived from DNS data to the CMC equation.

Mortensen & Bilger (2009) derive equations necessary for CMC modelling for single phase systems, two phase systems and separated flow systems, with an emphasis on two phase flows. The article succinctly outlines the difficulty of modelling two phase systems: "Mainstream approaches to modelling gas phase chemistry in sprays usually assume that it can be treated in much the same way as in single phase systems. Little attention has been given to the possible effects of strong mixture fraction variations in the neighbourhood of the evaporating droplets on the chemistry in a turbulent spray flame. Potentially, CMC has the advantage that it can handle complex chemistry and such effects of the fine scales of the mixing."

The CMC equation derived for two phase combustion is

$$\begin{aligned}\frac{\partial Q_\alpha}{\partial t} &= -\langle u_i|Z\rangle \frac{\partial Q_\alpha}{\partial x_i} \\ &\quad + \langle N|Z\rangle \frac{\partial^2 Q_\alpha}{\partial Z^2} + \langle W_\alpha|Z\rangle - \frac{1}{\langle\theta\rangle \rho_Z p} \frac{\partial \langle\theta\rangle \rho_Z p \langle u_i'' Y_\alpha''|Z\rangle}{\partial x_i} \\ &\quad + \left[Q_{1,\alpha} - Q_\alpha - (1-Z)\frac{\partial Q_\alpha}{dZ}\right] \frac{\langle \Pi|Z\rangle}{\langle\theta\rangle} \\ &\quad - \frac{1}{\langle\theta\rangle \rho_Z p} \frac{\partial (1-Z)\rho_Z p \langle Y_\alpha'' \Pi''|Z\rangle}{\partial Z}\end{aligned} \tag{1.6}$$

where the first, fourth and sixth terms on the right hand side can be considered negligible. Here Q_α is any conditional quantity such as Y_f, Y_o, T and h (enthalpy) and certain terms, such as $\langle W|Z\rangle$, are to be used in their correct form with respect to the quantity being solved for. The article suggests that experimental methods for resolving some of these terms is likely to be unsuccessful and advocates the use of DNS to fully evaluate all of the necessary terms.

In addition to the terms shown in the general form of the CMC, equation (1.1), the use of this form of the CMC model requires the use of the term $Q_{1,\alpha}$. This term relates to the behaviour of the quantity being solved for, Q_α, inside the droplets. For example,

if the temperature was being solved for, $Q_{1,\alpha}$ is the temperature of the droplets. As with other terms of the CMC model, this term may be determined from DNS data.

Uses of doubly conditioned CMC modelling

The use of doubly conditioned CMC modelling is becoming better understood as cases where the assumptions of first order CMC modelling is invalid are investigated. One such case of combustion that is not accurately modelled with the first order CMC model is combustion in which local extinction and reignition occurs. Doubly-conditioned CMC modelling is more complex than first order CMC modelling (as is used in this thesis) as quantities such as scalar dissipation are conditional upon two variables. Kim, Huh & Bilger (2002) investigated the application of doubly-conditioned CMC modelling to combustion with local extinction and reignition.

The main focus of the work in Kim et al. (2002) was to investigate the ability of the doubly-conditioned CMC model to predict the reaction rates of hydrocarbon fuel. A very simple two step mechanism was used as an approximation of the reaction of the fuel and oxidiser. "Two step mechanism" refers to the number of reactions required for the fuel to fully react with the oxidiser. For example, a two step mechanism results in one intermediate species, with in turn reacts with the oxidiser to form the products.

The results of the singly and doubly conditioned CMC were compared with DNS results. The quantities investigated were the species mass fractions (including the intermediate species) and the reaction rates. It was found that the doubly-conditioned CMC model accurately predicted the reaction rates and species mass fractions, regardless of the presence of local extinction and reignition. The first order CMC model predicted the behaviour of some, but not all, quantities.

Kronenburg & Papoutsakis (2005) also investigated the use of doubly-conditioned CMC modelling to identify localised extinction and reignition of the flame kernel. In this report, the conditioning variables were mixture fraction and sensible enthalpy. Modelling of local quenching and reignition make investigation of flammability limits, flame stabilisation and wall quenching possible.

A DNS was performed with parameters such that local extinction and reignition would occur, and in some cases global extinction would occur. Terms such as scalar dissipation, mass fractions, rate of evaporation and temperature from both the singly- and doubly-conditioned CMC models were compared with the DNS data. In most circumstances the doubly-conditioned CMC captured the behaviour of extinction and reignition quite accurately while single order CMC had some trouble predicting reignition.

This article demonstrates some of the flaws associated with first order CMC modelling. If behaviour occurs which causes a significant variation of the singly conditioned quantities about the mean, the addition of another conditioning variable is needed. While the events which cause this behaviour (extinction and reigntion) are not present in the DNS data which has been captured for this project, other events such as the addition and removal of the spark and evaporation of droplets may have a similar effect.

Uses of DNS

Wang & Rutland (2007) used solely DNS to study the ignition of turbulent n-heptane jets. The affect of changing two parameters, droplet radius and velocity, was investigated. Important findings from the article were that evaporative cooling due to the evaporation of the spray and turbulent mixing are both important phenomena which affect the ignition of the jet. This research differs from that being investigated in this project because this project has a focus on combustion chambers rather than jets.

Other types of combustion

Fairweather & Woolley (2004) attempt to verify the results obtained from combustion of a turbulent, single phase hydrogen jet with experimental results. The form of the CMC which was used was not disclosed. Two different turbulence closure methods were used to determine which would produce the most accurate predictions.

Kim & Mastorakos (2006) performed first order CMC studies on the combustion of

CH_4-air counterflow streams. The form of the CMC model used was

$$\frac{\partial Q_\alpha}{\partial t} = -\langle u_i|Z\rangle \frac{\partial Q_\alpha}{\partial x_i} + \langle N|Z\rangle \frac{\partial^2 Q_\alpha}{\partial Z^2} + \langle W_\alpha|Z\rangle - \frac{1}{\overline{\rho}\widetilde{P}(Z)} \frac{\partial}{\partial x_i}(\langle u_i'' Y_\alpha''|Z\rangle \overline{\rho}\widetilde{P}(Z)) \quad (1.7)$$

where the first and fourth terms of the right hand side are considered negligible. This is the simplest form of the CMC model advocated in literature and will form the basis for the preliminary investigation of the accuracy of the models derived from DNS data in this report.

Some of the quantities that are predicted with the use of the CMC model are the mean mixture fraction profile at several points axially along the jet, the conditional mass fractions of the fuel and oxidiser, the conditional temperature and the mean temperature axially along the jet. The model is deemed to be quite accurate in the prediction of the above quantities, however the authors do have some reservations about the ability of the model to predict the release of nitrous oxides.

While this article is of little use in the context of this project, it does serve to demonstrate the ability of the CMC model to predict a variety of reactions. It also highlights the relative ease of the prediction of single phase systems.

Specific terms of the CMC model

Sreedhara & Huh (2007) investigated the conditional statistics of spray combustion for two dimensional control volumes, with an emphasis on two dimensional turbulence. A two dimensional control volume of length 2πcm with 192^2 grid points was used. The effect of varying the Sauter Mean Radius (SMR), the level of turbulence and droplet velocity was investigated. A β-function pdf was proposed and validated for the mixture fraction. A linear fit for the conditional evaporation rate was compared against the DNS data.

While this article aims to demonstrate the effect of different parameters on the evaporation and combustion within the control volume, the results are of little value to the current work for a number of reasons. Several source terms were investigated, but were not conditional upon the mixture fraction as is required for use in the CMC model. The source terms were presented as averages across the whole domain versus time. Another

factor which may affect the validity of the results is how turbulence was defined within two dimensions; two dimensional DNS requires the use of artificial turbulence whereas turbulence is a three dimensional phenomenon. Furthermore, the results obtained in their DNS differ from the results studied in this project as they solved an autoignition problem.

Massebeuf, Bedat, Helie, Lauvergne, Simonin & Poinsot (2006) attempted to quantify the conditional source term due to droplet evaporation and conditional scalar dissipation rate which appear in the mixture fraction variance equation (and hence predict the mixture fraction in a turbulent, two phase combustion). Models were proposed for these quantities. The work in the article is similar to that of this thesis; deriving models for CMC quantities.

Coupling of CMC and CFD

The coupling of the CMC model and CFD software has been performed on compression ignition in diesel engines (Wright (2010) and De Paola, Mastorakos, Wright & Boulouchos (2008)). There has yet to be an investigation of spark ignition using this method.

Wright (2010) outlines the basic steps required for the coupling of CMC models and CFD software, as well as verifying the process against some experimental data. A first order CMC model was used, and the CFD software used was STAR-CD.

The coupling of the CMC model and CFD was similar to that shown in figure 1.1. The CFD software, given input parameters such as initial temperature, density, velocity, mass fractions and velocity, solves for the flow field. The CMC model then takes those outputs (such as turbulence) as input parameters and solves for the conditional species mass fractions, temperature and enthalpy. A β-function approximation for the mixture fraction pdf is assumed, and is used to return the averages of the calculated values back to the CFD software. The process is then repeated.

The second part of the article compares the results of the simulation with experimental results performed in Koss, Bruggemann, Wiartalla, Backer & Breuer (2010). The

ignition delay (the time required for the fuel to ignite under compression) and mean pressure rise were the quantities which were compared. The results showed that the use of CMC and CFD was able to capture some of the behaviour of the compression ignition. The accuracy of the results may have been affected by a number of factors. The use of first order CMC may have had some effect on the ability to predict the spatial location of some of areas of ignition, and on other combustion phenomena such as behaviour at physical boundaries and local extinction and reignition. Also, the initial conditions of the system would have been approximated to some extent which may have led to some error.

The work in De Paola et al. (2008) shows a much more thorough discussion of the results of coupling CMC and CFD for the simulation of an autoignition system. A heavy duty diesel engine, for which experimental and numerical analysis has been performed, was chosen. A first order, three dimensional version of the CMC model was used.

Some of the challenges of the modelling of a complex physical system, such as the combustion chamber of a diesel engine, are discussed. Amongst these difficulties are: accurately predicting the initial flow conditions as the air enters the combustion chamber, and the subsequent injection of fuel through the injector; the effect of turbulence on combustion; the complex nature of the chemical reactions; and the effects of the physical boundaries such as the piston crown and cylinder walls. Some discussion of how to overcome these difficulties is present.

Again, the CFD software used was STAR-CD. Due to symmetry, a segment representing one eighth of the combustion chamber was modelled. The use of the combustion chamber as the control volume led to the volume and shape of the control volume constantly changing as the piston oscillates between Top Dead Centre and Bottom Dead Centre. How this change in volume was accounted for by the CFD software was discussed. As the piston moves to the bottom of the stroke, and the expansion chamber expands, some of the expansion is accounted for by the expansion of the mesh. However, once the grid length surpasses a certain pre-defined length, another horizontal layer of nodes is added to the grid. The mesh is then stretched again until another layer of nodes is needed. The result of this is that at TDC there were 3680 cells and at BDC, 26945 cells.

The grid for the CMC model was different to that of the CFD grid. A pre-defined, structured physical grid which encompassed the whole of the CFD mesh (the largest of which occurs at BDC) was overlaid onto the CFD mesh. An algorithm was used to determine which of the CMC cells were located within the control volume at any time, and which were located outside of the control volume. The cells outside of the control volume were discarded. The cells located within the control volume were coupled with their corresponding CFD cells. The form of the CMC equation which accounts for physical boundaries was used for cells located on the boundary.

The main method of validating the simulation against experimental data was the mean pressure versus crank angle. The use of CMC coupled with CFD managed to accurately predict the peak pressure which occurs slightly after TDC. The increase in pressure is due to the combustion.

While the focus of the literature presented above is often quite narrow and tends to focus on specific behaviour of different types of combustion, the methods used to calculate results is often similar to that which will be used in this report. As the CMC model lends itself to the simulation of many different types of combustion, it is envisaged that the work completed in this report will have broad implications towards further modelling some of the phenomena described above.

1.4 Consequential Effects

It is envisaged that this project will positively impact the engineering community, in both the academic and industrial fields. In the academic field, it will provide a progression towards more accurately modelling spray combustion using the CMC model. In the automotive industry, it may be used as a design tool.

In the academic field, there is significant effort currently being put into developing accurate models for spray combustion, as per the articles discussed in the literature review. The analysis of DNS data to propose models for use in CMC would offer researchers another avenue of predicting the terms of the CMC model, which are currently limited. This could potentially pave the way for academics to concentrate resources elsewhere

when trying to model certain phenomena or systems.

A greater understanding of spray combustion could lead to the application of the CMC model to other systems. Some systems that are currently being investigated in literature are jets, internal combustion engines and the combustion of counter-flow streams.

By applying the CMC model to CFD software, it would allow much more large-scale modelling of real world combustion. This offers the advantage of being able to model the large scale systems before they are tested experimentally (in a similar fashion to the modelling of fluid flow over a wing before being tested in a wind tunnel).

In relation to industry, it is hoped that this project may prove to be a successful design tool. The design of injectors could be improved by designing for a spray which gives the best combustion. Three parameters that could be tweaked using the proposed model would be droplet size, droplet density and spray pattern. The spark size and location could also be incorporated.

There are also many articles which focus on improving injector design for the most efficient design. One article of interest is Reynolds & Evans (2003), "Improving emissions and performance characteristics of lean burn natural gas engines through partial stratification". The ever increasing research and implementation of stratified-charge spark and compression ignition is of particular significance to the work being undertaken in this project.

Stratification refers to the process of concentrating the injected fuel about the spark while having the rest of the combustion chamber lean. The resulting air to fuel ratio averaged over the whole of the chamber is lean, which cannot be achieved with regular homogenous charge spark ignition. In the process of combustion, the spark ignites the rich region of air-fuel mixture adjacent to the spark plug, which forms a stable flame kernel. This then propagates throughout the lean areas of the combustion chamber. There are two main advantages of using full or partial stratification. These are increased efficiency at light loads and reduced emissions.

The use of stratification allows the use of much leaner mixtures than is currently possible using homogenous charges. The effect of this is that engine output can be reduced by

reducing the fuel injected into the chamber without throttling the air intake. The pumping losses incurred by having to pump air through a constricted throttle can affect the efficiency of the engine at low loads quite markedly, therefore varying the engine output without using a throttle is advantageous.

The test system for the work in Reynolds & Evans (2003) consisted of a single cylinder, naturally aspirated 4-stroke engine running on natural gas. In order to provide a portion of the charge as a concentrated rich mass about the spark plug, a custom spark plug injector was used. About 5 per cent of the mass of fuel was injected this way, giving a partial stratified charge. The other fuel was injected using the existing injection system and was lean. Using this system, they were about to achieve significant (up to 7%) reductions in the brake specific fuel consumption (a measure of fuel consumed per brake power output).

The partial stratification system also offers reduced levels of emissions, and in particular, reduced levels of NO_x. The production of nitrous oxides is formed in the hot exhaust gases before they leave the combustion chamber. One method of reducing the formation of NO_x is reducing the temperature of the exhaust gases. This is another advantage of full or partial stratification; the temperature is high in close proximity to the spark plug, but as the flame front advances to the boundaries of the cylinder it cools due to the sparse fuel. It was found that an optimum air to fuel ratio could be found whereby HC and CO emissions were low (due to most of the fuel being burnt) and NO_x emissions were low (due to the cool outer region of the combustion chamber).

Ultimately, it was found that there was a limit to how much the engine output could be controlled by controlling the air-to-fuel ratio (AFR). The mixture around the spark had to be sufficiently rich to allow a flame kernel to form, and the outer, homogenous region had to be sufficiently rich to sustain the flame kernel as it progressed towards the cylinder wall. Using a mixture which was too lean would result in misfires and a reduction in efficiency and increase in the release of HC and CO. The point at which this starts occurring is called the 'lean misfire limit'.

Using the CMC model with data obtained from DNS would be a very suitable design tool for developing a stratified charge system. The CMC model can accurately predict

when a flame kernel extinguishes, as well as the temperature in the combustion chamber. This could lead to the design of more efficient engines, and allow engineers to predict the efficiency and amount of emissions an engine produces before a prototype is produced.

Chapter 2

Analysis of the DNS data

2.1 Overview of the DNS data

Wandel et al. (2009) performed DNS on a small, three dimensional control volume in order to investigate the characteristics (droplet size and spacing) that would lead to full combustion of a fine mist of fuel. The fuel investigated was n-heptane. Navier-Stokes equations were used to determine fluid movement. The control volume was a cube, with 128 nodes along each edge, with the following characteristics:

- Boundaries is the y- and z-directions were periodic (droplets which flow out of the boundary re-enter through the opposite boundary).
- Boundaries in the x-direction were "partially non-reflecting" (gradient at the boundary is zero, droplets do not re-enter).
- Droplets were uniformly distributed throughout y and z co-ordinates, and between $L/4$ and $3L/4$ in the x-direction.
- The spark was centred in the control volume, and deposited energy for a predetermined period of time.

As a process of this DNS, quantities required for the CMC model were saved throughout

the duration of the combustion. This data is the basis for the first part of this thesis, analysis of data to develop models for spray combustion.

There are three main regimes ("zones") that may be observed in a successful burn when a spark is turned on, then off:

- Initial zone ($< 7\mu$s): Little fuel vapour exists, combustion is almost non-existent, there is a rapid release of fuel to the system as the spark evaporates fuel.
- Intermediate zone ($7 - 165\mu$s): The spark is either still on, or there is a strong residual effect from the spark and the droplet evaporation rate becomes steady-state.
- Final zone ($> 165\mu$s): No residual effect from the spark exists, droplet evaporation is steady-state for the remaining droplets (many are completely evaporated), flame propagation is strong.

For the purposes of fully characterising the data, another stage was introduced. This stage occurs before the initial stage, and for this very brief period, all quantities approximate the initial conditions before the spark begins evaporating fuel. This stage will be referred to as zone 0.

2.2 Selection of the DNS data

There were eleven different sets of DNS data from which to choose. The combustion differed in two ways; the overall equivalence ratio and the droplet size. The equivalence ratio, ϕ, is a ratio between the mass fraction of fuel that is supplied to the system and the mass fraction of fuel required for stoichiometric burning. For example, an equivalence ratio of two suggests that there is twice the amount of fuel present than is needed for stoichiometric burning.

For the purposes of modelling the terms of the DNS data, a case in which combustion acts as expected and did not prematurely extinguish would provide a good starting

point. In order to determine if the combustion indeed continued for the length of the simulation, the maximum temperature in the domain was plotted versus time. The maximum temperature was recorded when the DNS was performed.

2.2.1 The effect of the equivalence ratio on combustion

As mentioned previously, in spark ignition systems, the equivalence ratio of the system may greatly affect the ability of the spark to form a stable flame kernel. If the mixture is too lean, not enough fuel will be evaporated for the flame to consume. If the mixture is too rich, not enough oxidiser may be present. Figure 2.1 shows the maximum temperature in the domain over the length of the simulation for various values of equivalence ratio. The initial diameter of the droplets is held almost constant in each case.

A normalised temperature equal to one refers to the adiabatic flame temperature, or the maximum temperature the combustion alone can sustain. The maximum temperature may be greater than one due to the additional energy from the spark.

The graph for the equivalence ratio of 0.5 shows little or no combustion. The normalised temperature is initially zero, indicating that no energy has been released to the system yet. As time progresses, the temperature increases as the spark starts releasing energy. At the peak of the curve, the spark is removed and the system gradually cools back to its original state. The graph suggests that little or no combustion occurs, because it seems that there is no other energy released to the system but the spark (the subsequent graphs show a deviation upwards from the shape of the graph shown for $\phi = 0.5$).

The maximum temperature shown in the case of equivalence ratio equal to one again shows little combustion. There is some suggestion that there are small, localised areas of burning (as evidenced by the slighter higher peak temperature than $\phi = 0.5$), but these areas do not get sufficiently hot to produce a stable flame kernel.

For the system with an equivalence ratio of $\phi = 1.5$, a flame kernel is formed and continues to burn until the normalised time is approximately 0.275, at which point it extinguishes. This can be seen by the tail of the graph gradually returning to the initial temperature of 0.

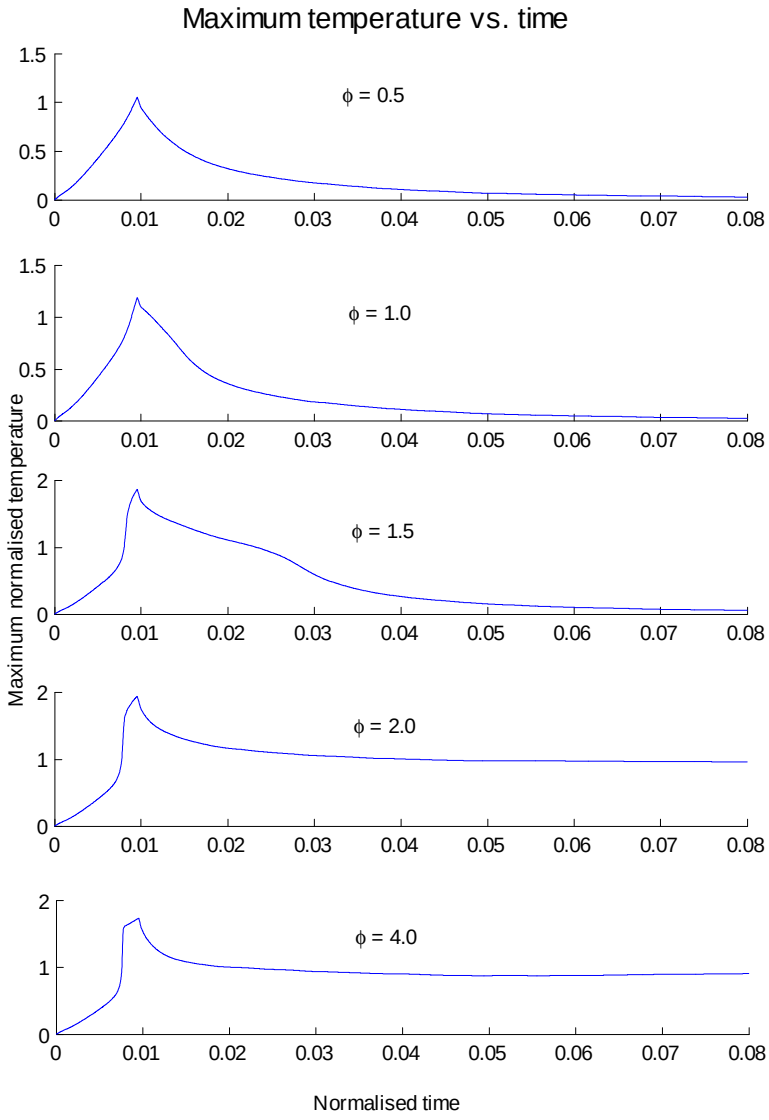

Figure 2.1: DNS results for the maximum temperature within the domain for five cases of equivalence ratio with droplet diameter constant.

The graphs for $\phi = 2$ and $\phi = 4$ show that the flame kernel becomes self sufficient and does not extinguish before the end of the simulation. This can be seen by the maximum temperature becoming steady at approximately 1.0 after the spark has been removed.

These graphs show the impact of the mass fractions of fuel and oxidiser on the effectiveness of the burn. If the system is too lean, the flame is indeed extinguished as not enough fuel vapour can be supplied. Of particular interest is the behaviour of equivalence ratios 1 and 1.5; while these mixtures were stoichiometric or rich, the combustion was still not effective. This suggests that the droplet size may have been too great.

2.2.2 The effect of droplet size on combustion

Figure 2.2 shows the maximum temperature for combustion with an equivalence ratio of 2 but with differing droplet sizes.

The droplet sizes are:

- Small: 2.783μm
- Medium: 3.936μm
- Large: 4.821μm.

It can be seen that for a given equivalence ratio, the droplet diameter may have an effect on the ability of combustion to proceed. In the case where $\phi = 2$, the largest droplet diameter cannot sustain the flame kernel.

2.2.3 Selection of the DNS data

In order to characterise the terms of the CMC equation, a case of combustion which is representative of most combustion will be selected. It is hoped that these models will be readily adaptable to any other combustion, whether the air to fuel ratio, droplet size or any other parameters are changed. It is also hoped that the models will also be

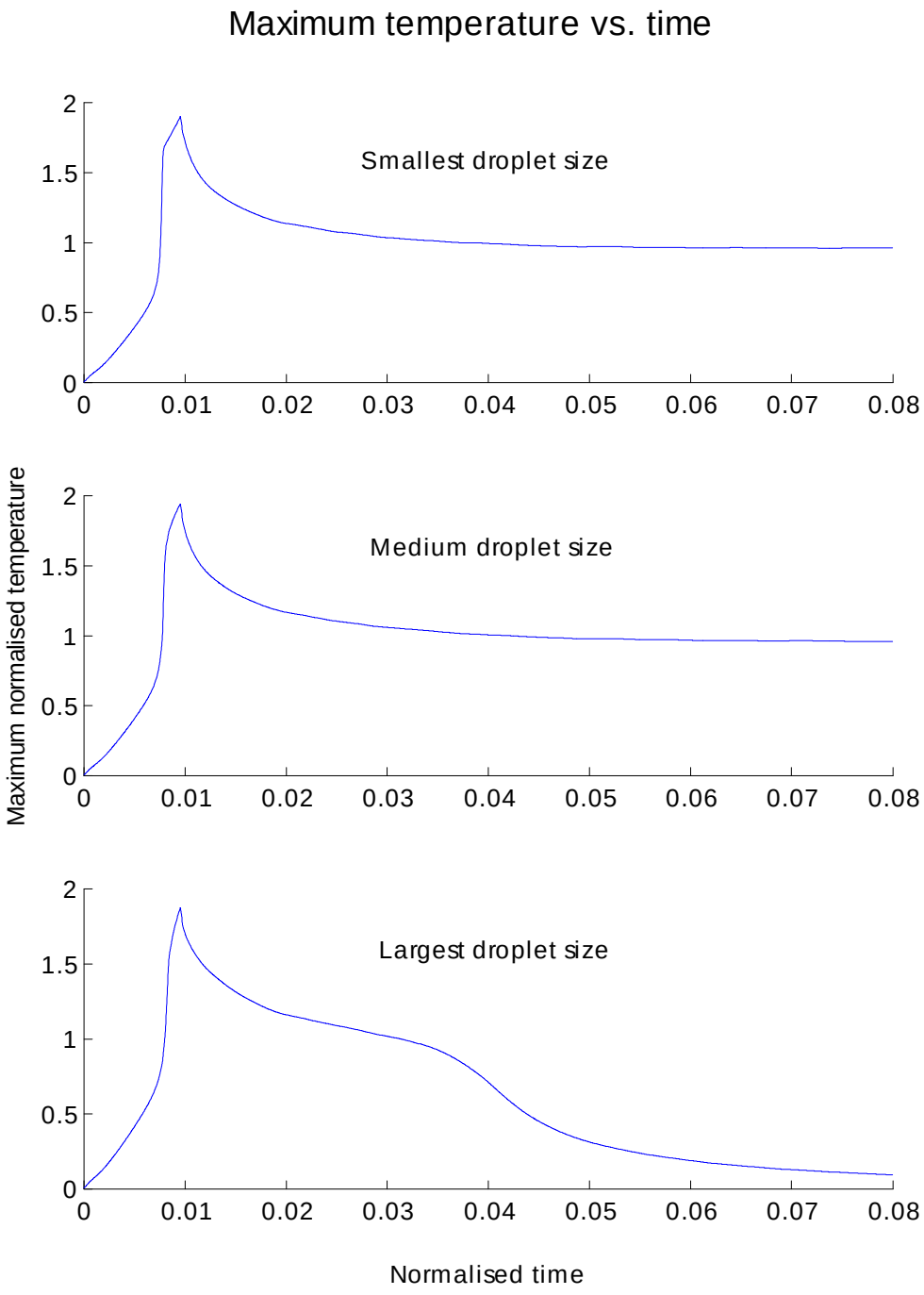

Figure 2.2: Maximum temperature across the domain with a constant equivalence ratio and varying droplet diameter.

able to predict the behaviour of prematurely ending combustion up until the flame is extinguished.

The combustion which was chosen for initial analysis in this project is combustion with an equivalence ratio of two and a droplet diameter of 3.936μm.

2.3 Overview of important quantities

The three quantities that will be calculated using the CMC model are conditional temperature and conditional mass fractions of both the fuel and the oxidiser. The mixture fraction probability density function may then be used to find the mean values of these quantities at any point in time. The following graphs show the data for each of these quantities taken from the DNS. They give some insight on how the combustion behaves.

2.3.1 Conditional temperature

Figure 2.3 shows a plot of the conditional normalised temperature over the life of the combustion. The conditional temperature highlights the main values of mixture fraction in which combustion is taking place. The stoichiometric mixture fraction in this case is $Z = 0.062$. At low values of mixture fraction (and hence localised lean areas within the mixture), the temperature is low and almost equal to the initial temperature before the spark was added. However, the temperature increases as the regime becomes richer, and tends to peak and then plateau at high values of mixture fraction. This suggests that combustion as expected is occurring in the rich areas while in the lean areas no combustion occurs. Of particular interest is that combustion seems to occur only at mixture fractions higher than stoichiometric. This agrees with the data shown previously which suggested that of all the DNS data produced, only those simulations with an equivalence ratio of two or higher could sustain combustion for the length of the simulation. Given that most petrol engines today achieve consistent combustion with mixture fractions approaching stoichiometric, it would suggest that the droplet diameter of the given DNS data is larger than can be expected in real engines.

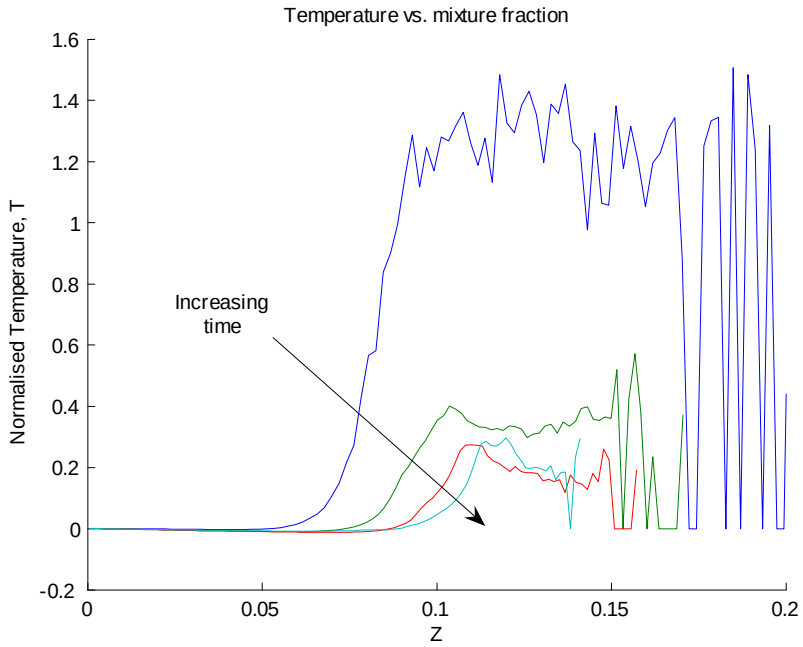

Figure 2.3: Conditional temperature over the life of the combustion.

Recall that the conditional temperature is the mean of all the temperatures within the domain given a particular value of mixture fraction. It was shown in figure 2.2 that the maximum temperature in the domain at all times is approximately equal to one, which contrasts with the mean temperature shown in figure 2.3 which is much lower. This suggests that there is high variability of the conditional temperature.

Counter-intuitively, with increasing time, the conditional temperature decreases. However, the high temperature of the first curve occurs while the spark is still present. When the spark is removed, the temperature decreases and stabilises. It also seems that as time progresses, the ability of the combustion to occur in lean regions is reduced. This is due to the reduced temperature of the flame kernel with respect to the spark; the high temperature of the spark is able to produce fuel more rapidly and thus in areas of low droplet density is more likely to burn the fuel. Once the flame kernel stabilises, it is only able to progress to rich areas of the domain.

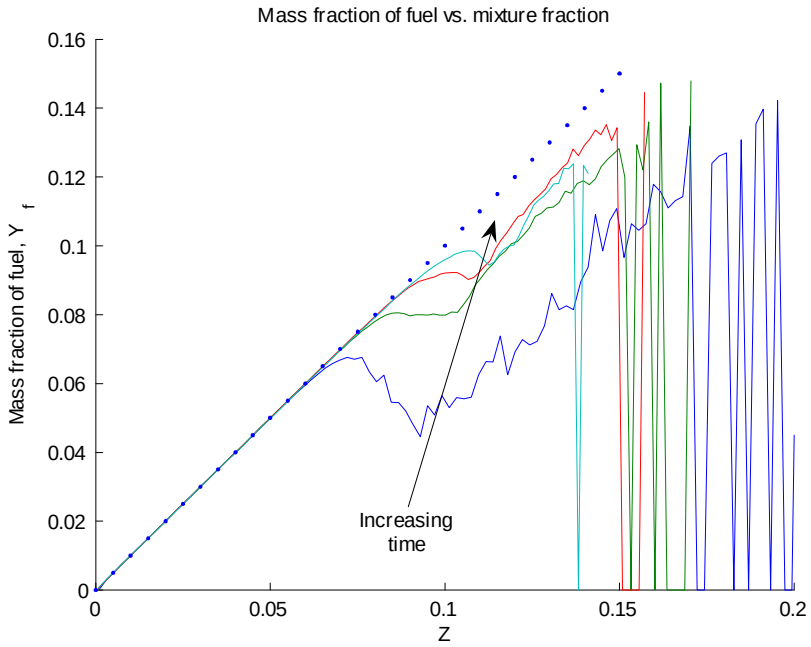

Figure 2.4: Conditional mass fraction of fuel, all zones.

2.3.2 Conditional mass fraction of fuel

Figure 2.4 shows the conditional mass fraction of fuel as the combustion proceeds. The blue dots represent the initial mass fraction of fuel before the spark is added. The oscillation at high values of Z is due to statistical error inherent in the process used to capture data from the DNS. In many ways, this graph reaffirms the inferences that can be made from the graph of the conditional temperature.

Initially, before combustion occurs, by definition the mass fraction of fuel is equal to the mixture fraction. As combustion proceeds and the fuel is consumed due to it burning in air, the mass fraction of fuel is reduced. Eventually, it is expected that most of the fuel has been consumed and the mass fraction of fuel approaches zero.

As can be seen, the fuel is consumed in the rich regions of the domain, while the fuel present in the lean areas is relatively untouched. This confirms that combustion only takes place in rich areas, and in this case the rate of combustion occurs most rapidly at approximately $Z > 0.09$.

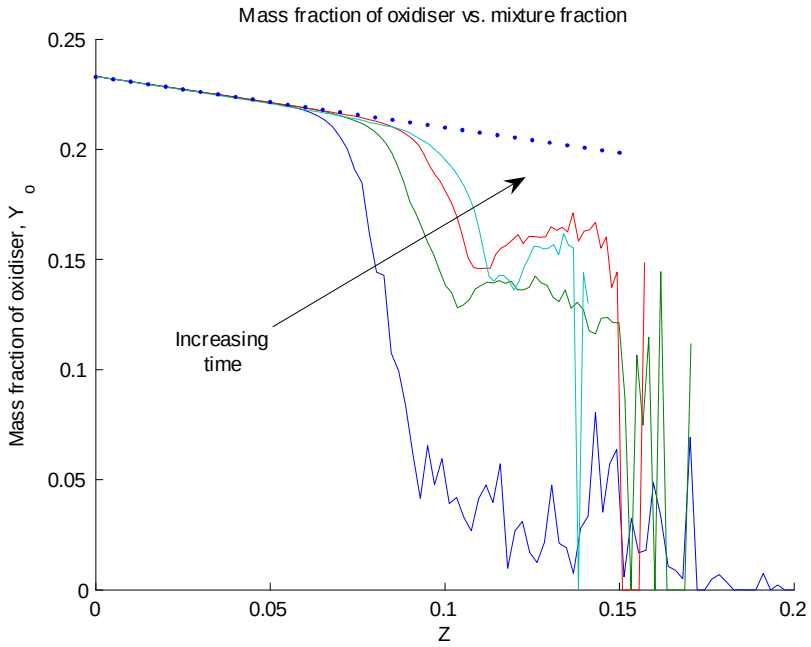

Figure 2.5: Conditional mass fraction of oxidiser, all zones.

Similarly to the conditional temperature, the graph is to an extent counter-intuitive. It seems to suggest that as time progresses, the mass fraction of the fuel increases. However, this is not the case; at low values of time before the spark has evaporated much fuel, the probability of high mixture fractions is very low. However, in the few areas which have become rich, the combustion rate is high because the spark is providing a very high source of energy. Therefore, at small values of time, the mass fraction of fuel at high mixture fractions is quickly diminished. As more time progresses and the spark is removed, the composition of the combustion chamber becomes more homogenous and there are many rich regions. Therefore, the 'creation' of the fuel may be attributed to the evaporation of droplets.

2.3.3 Conditional mass fraction of oxidiser

The conditional mass fraction of oxidiser is shown in figure 2.5. Again, the blue dots denote the initial mass fraction. The mass fraction of oxidiser acts in a similar way to the mass fraction of fuel. More oxidiser is consumed at high mixture fractions where

combustion occurs, but does not react with the fuel at low mixture fractions.

Again, the system seems to 'produce' oxidiser. However, since the probability of high values of mixture fraction at small values of time is very low, the actual amount of oxidiser consumed is also very low. As time progresses the probability of high mixture fraction increases and this contributes to curves moving towards higher mixture fractions.

2.3.4 Mean mass fractions

Figure 2.6 shows the average mass fractions of fuel and oxidiser versus time over the length of the simulation. As can be seen, the mass fraction of fuel increases with time as the spark, and then flame front, evaporate more fuel into gaseous form. As this mass of fuel is released, the mass fraction of oxidiser is reduced. It can be seen that the average mass fraction of fuel increases over the length of the simulation. However, after time, it is expected that the mass fraction of fuel would decrease to almost zero as both the fuel and oxidiser are consumed as they react. While the DNS has not been allowed enough time to run to start capturing the decay of the system, this behaviour is reflected in the above graphs. As time increases, the rate of change of mass fraction decreases. This suggests that while fuel is still being released to the system from the evaporation of droplets, more and more of this fuel is being consumed by the combustion. Eventually, the rate of consumption will be greater than the rate of supply and the mass fraction of fuel will start approaching zero. Because the oxidiser is already in gaseous form, no oxidiser is generated by the addition of heat. The consumption of oxidiser is approximately linear.

The rate of generation of fuel is greatest at early stages. This coincides with the addition of the spark, which releases quite a substantial amount of fuel to the system to allow the formation of the flame kernel.

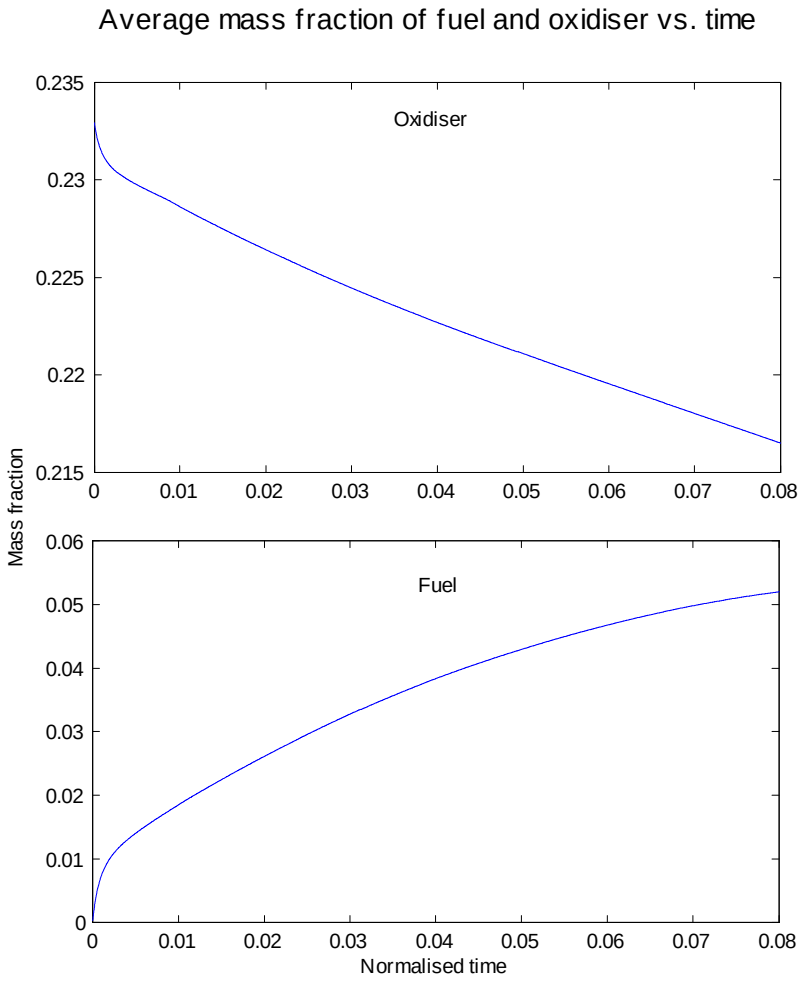

Figure 2.6: Average mass fraction of fuel and oxidiser with respect to time.

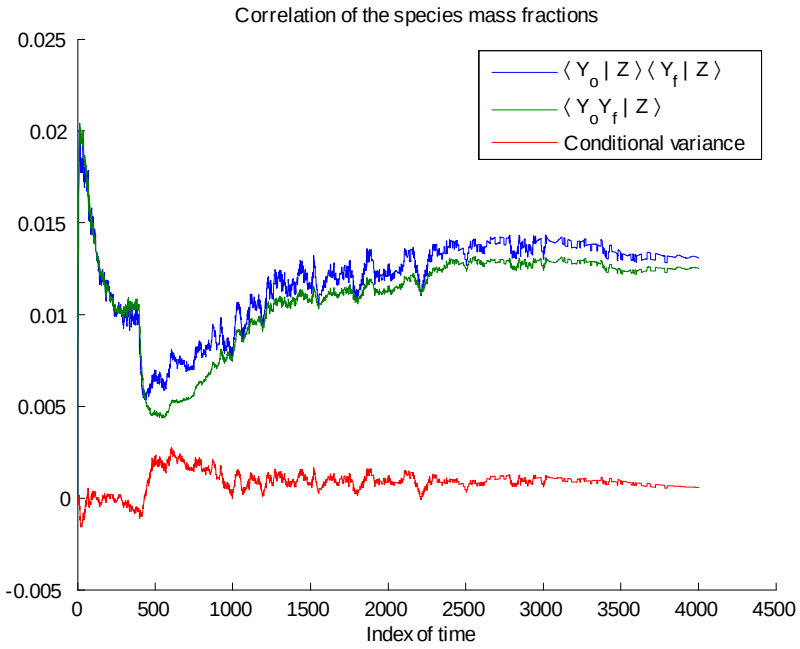

Figure 2.7: Conditional variance between the species mass fractions.

2.3.5 Validation of the correlation between the species mass fractions

One of the assumptions of the first order CMC model is that the species mass fractions are strongly correlated. It is expected that this should hold true, because as combustion takes place, both quantities should be reduced relative to one another. For example, fuel cannot burn without the consumption of some oxidiser.

Because the DNS data contains the calculated values of conditional mass fraction of fuel and oxidiser, the validity of this assumption may be tested. Figure 2.7 shows the terms of equation (1.4) plotted at all the values of time. As can be seen, the mass fractions of fuel and oxidiser show a reasonable amount of correlation, with the greatest difference between the terms occurring at about the $500th$ timestep. This probably coincides with the formation of a flame kernel.

The assumption of correlation between the mass fractions of the two species is valid and should not adversely affect the results of the CMC model.

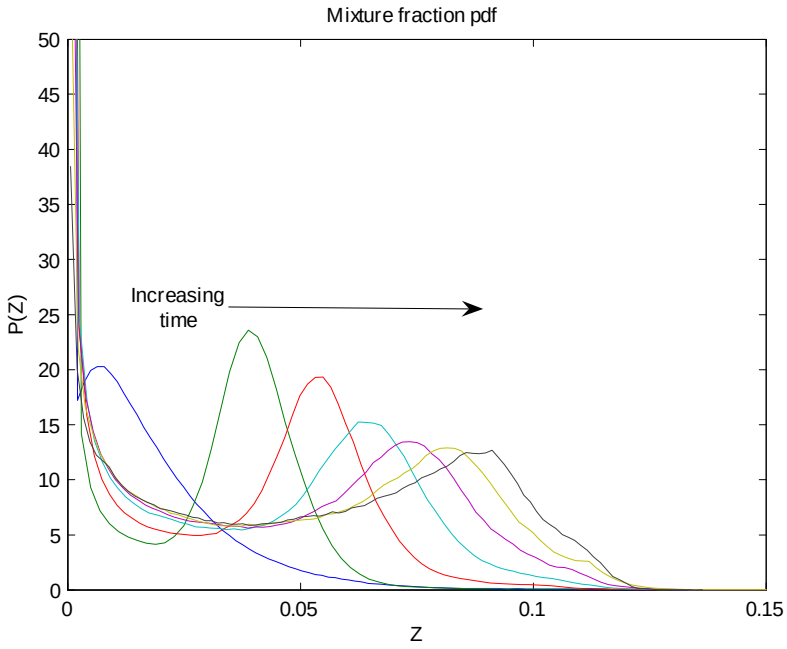

Figure 2.8: Mixture fraction pdf, all zones.

2.4 Overview of the CMC terms

2.4.1 Mixture fraction probability density function

Figure 2.8 shows the mixture fraction pdf, $P(Z)$, throughout the control volume. Initially, the mixture fraction pdf shows that most fuel was still unavailable to the system as the droplets were yet to evaporate. This is evidenced by the peak of the curve of the first timestep occuring at $Z \approx 0.01$. However, as combustion progresses, more fuel is available to the system, which is shown by the progression of the peak up to $Z \approx 0.09$.

As the fuel evaporates, large regions develop that become rich. The variation in mixture fractions is due to the presence of localised high mixture fractions, such as areas adjacent to the droplets in which the mixture fraction is high due to evaporation of the droplets. Areas where fuel is sparse occur due to the spacing between the droplets. The fuel rapidly diffuses away from the droplets, as indicated by the probability of locations having an equivalence ratio of 2 being insignificant (the stoichiometric mixture fraction was $Z_{stoich} = 0.062$).

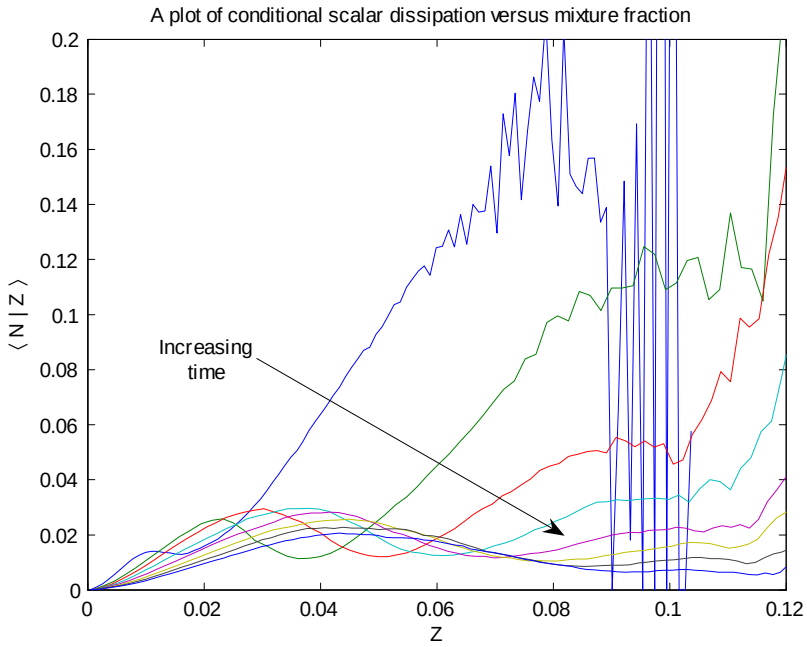

Figure 2.9: Conditional scalar dissipation, all zones.

2.4.2 Conditional scalar dissipation

A plot of conditional scalar dissipation over the length of the combustion is shown in figure 2.9. As previously mentioned, the scalar dissipation is defined as $N = D(\nabla Z \cdot \nabla Z)$ where D is the diffusitivity and ∇Z is the gradient of Z. The scalar dissipation is large for large values of Z because this corresponds to areas immediately adjacent the droplet surfaces, which provide the source of Z. Throughout combustion, a peak progressively shifts from low values of Z to high values of Z, which indicates the development of the flame front, which eventually stabilises.

The large fluctuations in the data for large values of Z are due to statistical errors, corresponding to low values of probability. Therefore, as a general rule, values of Z corresponding to $P(Z) < 0.1$ will be neglected.

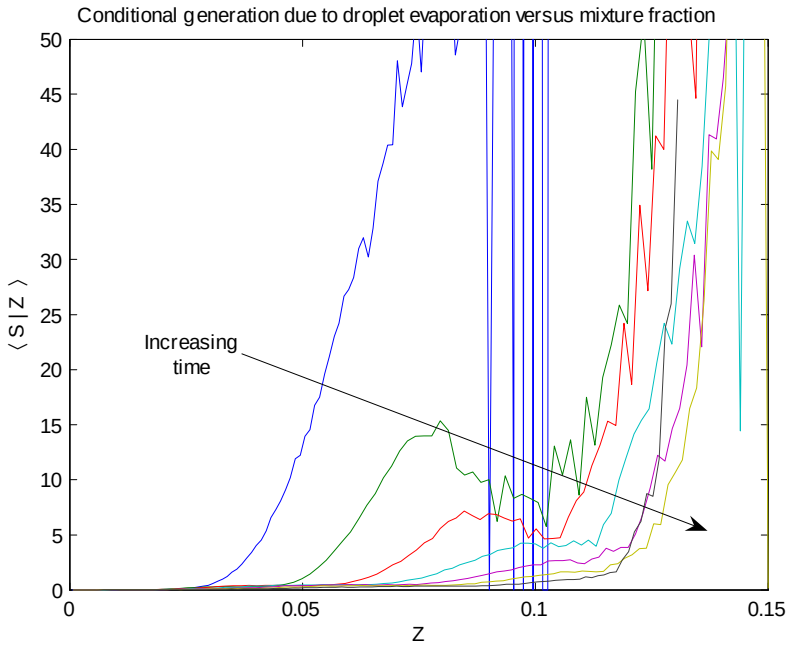

Figure 2.10: Conditional generation due to droplet evaporation, all zones.

2.4.3 Conditional generation due to droplet evaporation

A plot of the conditional generation due to droplet evaporation, $\langle S|Z\rangle$, versus mixture fraction for the length of combustion is shown in figure 2.10. The conditional generation due to droplet evaporation is a term which refers to the contribution by the evaporation of droplets to the mass fraction of fuel. As can be seen from figure 2.10, the rate of generation due to droplet evaporation eases with time. This is because at initial stages during combustion, a strong source of energy is present in the control volume in the form of a spark. The spark evaporates many surrounding droplets and thus the generation due to droplet evaporation is quite high. During the intermediate stage of combustion, the spark is removed but combustion becomes self sustained due to the advancement of the flame front. Again, evaporation is quite high and fuel is still being released to the system as a gas. However, the rate of evaporation becomes somewhat slower. In the final stage of combustion, the flame front is still providing energy for the evaporation of droplets, but the amount of droplets present to evaporate is small as most fuel has been expended in previous stages of the combustion.

2.5 Characterisation of the CMC terms

This case is the first case being investigated, and as such will be named case 1. Subsequent analysis will focus on different cases of combustion to investigate whether the parameters of the CMC model can be readily modelled under different combustion conditions.

2.5.1 Mixture fraction pdf

From analysis of the mixture fraction pdf data presented in figure 2.8, it is evident the functions are not self similar and seem to be a function of time. In this state, $P(Z)$ is difficult to characterise. The functions can be made self similar by creating the Favre pdf, defined as $\tilde{P} = \langle \rho | Z \rangle \, P(Z) / \langle \rho \rangle$ where $\langle \rho | Z \rangle$ is the conditional density and $\langle \rho \rangle$ is the mean density. The mixture fraction was also normalised by the mean mixture fraction. The approach of normalising the quantities by a mean quantity will be adopted throughout the analysis as average values are quite readily predicted at any point during the combustion and this should make the model generally applicable for any case.

The graphs of the Favre pdfs for each zone and their corresponding fitted functions are shown in figure 2.11.

As zone 0 refers to combustion at very small values of time, before significant changes are made to the probability density function by the evaporation of fuel, the pdf resembles the intial distribution. As defined in the DNS, initially the distribution takes the form of a β-function pdf. The formula for a β-function pdf is:

$$B(Z_n) = \frac{1}{b-a} \frac{\Gamma(\alpha+\beta)}{\Gamma(a)\Gamma(b)} \left(\frac{Z_n - a}{b-a} \right)^{\alpha-1} \left(\frac{b - Z_n}{b-a} \right)^{\beta-1} \tag{2.1}$$

with α and β the shape parameters while $a < Z_n < b$ is the range where $B(Z_n) > 0$. Z_n is the normalised mixture fraction.

The fit describing the Farve pdf for zone 0 is $\tilde{P} = A.B(Z_n)$. The parameters for use

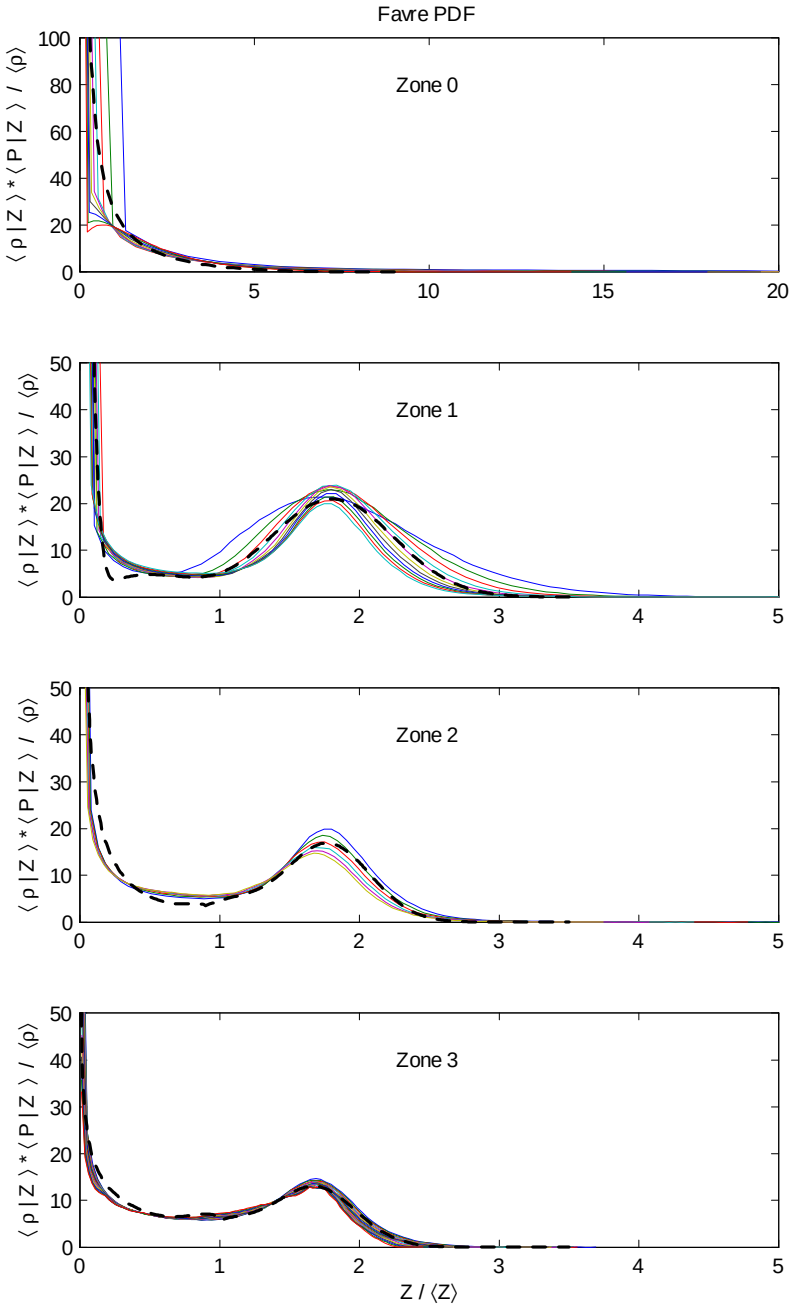

Figure 2.11: Favre averaged mixture fraction for each of the zones with their respective fits shown as dashed lines.

in the β-function (equation (2.1)) are:

$$\begin{aligned} A &= 902.40 \\ \alpha &= 0.0381 \\ \beta &= 2.9051 \\ a &= 0 \\ b &= 8.0. \end{aligned}$$

The use of a single β-function produces a good fit, with the errors in the location of the β-function near $Z = 0$ being due to the rapidly increasing mean mixture fraction. However, the error will be negligible as zone 0 represents a very small period in time in comparison to the length of the combustion.

The use of a β-function to describe the mixture fraction pdf is a common practise when using the CMC model (Girimaji 1991). The use of a sole β-function pdf at any point during the combustion has produced solid results, but the use of DNS data to characterise the mixture fraction pdf allows this aspect of the CMC model to be much more accurate. It will be seen from further analysis that as time progresses, the mixture fraction pdf evolves to become quite different from the initial β-function.

The plot of the zone 1 pdf shows the effect of the spark evaporating droplets to release fuel to the system. A Gaussian peak can be seen to form at $Z/\langle Z\rangle \approx 1.75$ in addition to the β-function pdf, which still dominates the behaviour for $Z/\langle Z\rangle < 0.5$. Further analysis reveals a secondary Gaussian peak at $Z/\langle Z\rangle \approx 0.5$. The function to describe the behaviour for zone 1 is a composite function of the form:

$$f(Z_n) = A_0 B(Z_n) + A_1 G_1(Z_n) + A_2 G_2(Z_n) \tag{2.2}$$

where A_i are constants, $B(Z_n)$ is a β-function pdf and $G(Z_n)$ is a Gaussian pdf.

A Gaussian pdf is solely a function of the mean, μ, and standard deviation, σ:

$$G(Z_n) = \frac{1}{\sqrt{2\pi\sigma^2}} \exp\left(-\frac{[Z_n - \mu]^2}{\sigma^2}\right). \tag{2.3}$$

For zone 1, the coefficients of the composite function shown in equations (2.1), (2.2) and (2.3) are:

$$
\begin{aligned}
A_0 &= 18.9137 \\
\alpha &= 0.9529 \\
\beta &= 5.6558 \\
a &= 0 \\
b &= 0.3 \\
\sigma_1 &= 1.8091 \\
\mu_1 &= 0.1943 \\
A_1 &= 23.1701 \\
\sigma_2 &= 0.4700 \\
\mu_2 &= 0.1073 \\
A_2 &= 3.7370.
\end{aligned}
$$

The resulting fit can be seen in figure 2.11. Some error is evident around the primary peak, while the composite pdf does not predict the interface between the β-function pdf and secondary Gaussian pdf for $Z \approx 0.25 \langle Z \rangle$. In addition, there is some transient development around the secondary peak which is not completely captured by the primary Gaussian pdf. The degree to which these errors will affect the recreation of the probability density function will be seen when the CMC model is validated.

In zone 2, the Favre pdf becomes more self-similar as the rate of combustion and evaporation approaches an equilibrium. As with zone 1, the function to describe the pdf is a composite function as defined in equation (2.2). The variables for use in equation (2.2) are:

$$
\begin{aligned}
A_0 &= 27.6222 \\
\alpha &= 0.1536 \\
\beta &= 1.6190 \\
a &= 0 \\
b &= 0.9 \\
\sigma_1 &= 1.7726 \\
\mu_1 &= 0.0930 \\
A_1 &= 12.8574 \\
\sigma_2 &= 1.0515 \\
\mu_2 &= 0.0573 \\
A_2 &= 2.3901.
\end{aligned}
$$

In zone 2, the system becomes more stable and the secondary Gaussian function has more effect on the final function. The mean mixture fraction is relatively stable during this period, so the peak near $Z = 0$ is reasonably accurately predicted, while there are some errors for $Z/\langle Z \rangle < 1$.

In zone 3, the system becomes stable and therefore the Favre averaged pdfs during this time are self-similar. Again, the composite function (equation (2.2)) is used to characterise the zone with:

$$
\begin{aligned}
A_0 &= 9.8762 \\
\alpha &= 0.5639 \\
\beta &= 1.4709 \\
a &= 0 \\
b &= 1.0 \\
\sigma_1 &= 1.6781 \\
\mu_1 &= 0.0881 \\
A_1 &= 9.6339 \\
\sigma_2 &= 1.0251 \\
\mu_2 &= 0.0515 \\
A_2 &= 2.7235.
\end{aligned}
$$

The β-function pdf again over-predicts the tail towards the secondary Gaussian pdf.

Overall, the fits are quite good and should lead to the accurate prediction of the mean values of any conditional quantities. Before use, the functions will need to be normalised to ensure that the area under the graph is equal to one. This step will be performed later, when the data is recreated.

2.5.2 Conditional scalar dissipation

As with the mixture fraction pdf, the conditional scalar dissipation is not self similar over the life of the combustion and seems to be a function of time. This is rectified by normalising the conditional scalar dissipation by the mean scalar dissipation. The resulting plot of $\langle N|Z\rangle \,/\, \langle N\rangle$ versus $Z/\langle Z\rangle$ is shown in figure 2.12.

Zones 0, 2 and 3 are, for most values of Z, self similar. The conditional scalar dissipation undergoes a transition in zone 1 where a peak and trough form progressively.

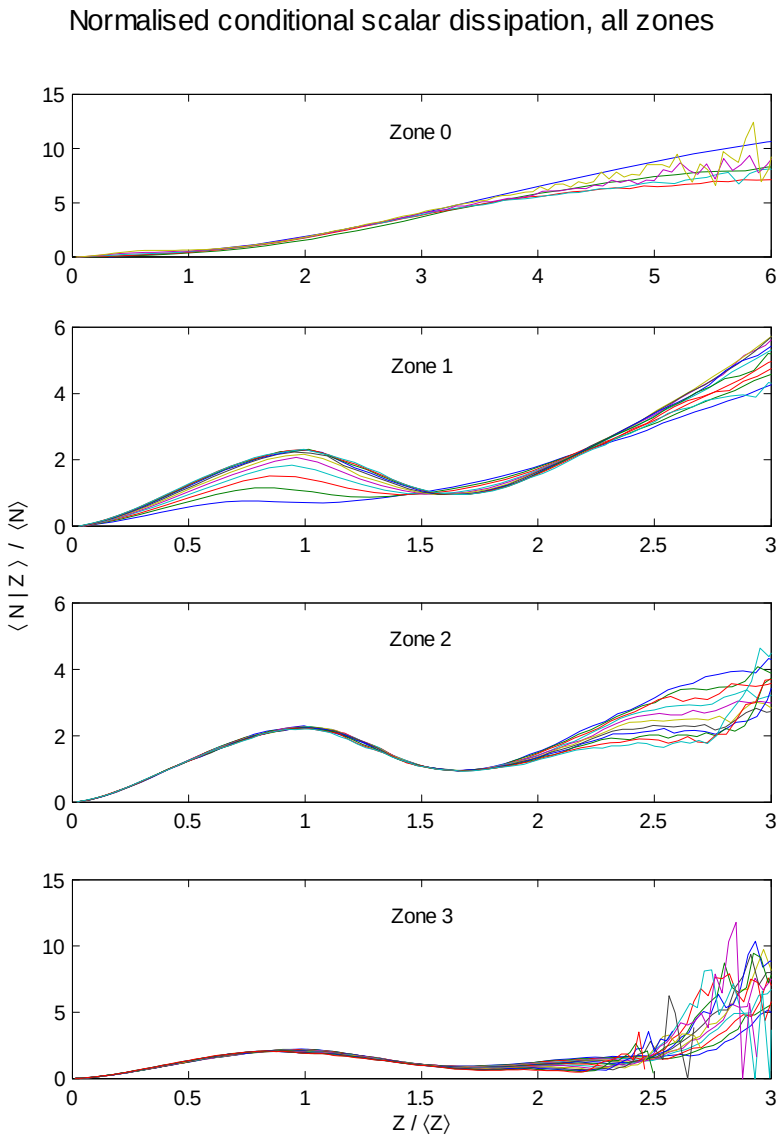

Figure 2.12: Behaviour of the conditional scalar dissipation for each zone.

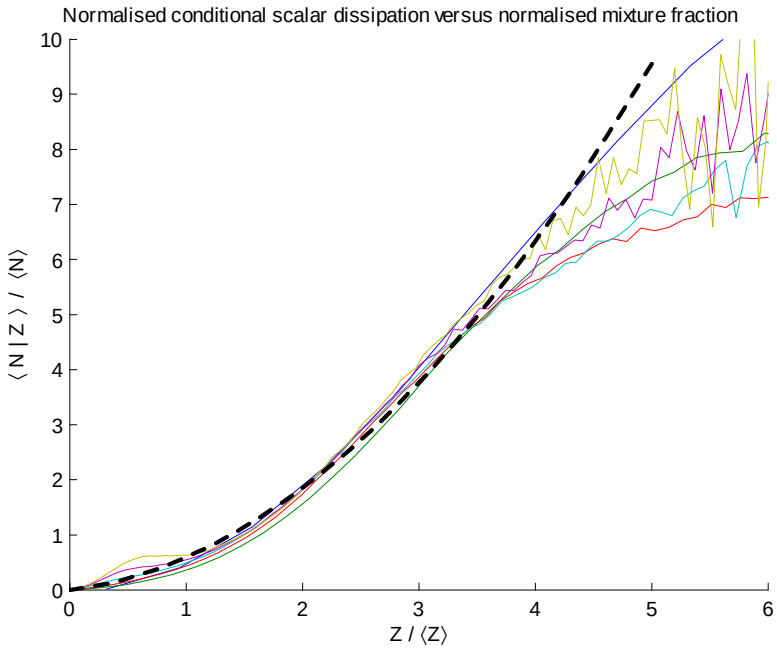

Figure 2.13: Fit for the conditional scalar dissipation, zone 0.

Zone 0

Figure 2.13 shows the conditional scalar dissipation versus normalised mixture fraction for zone 0. For clarity, large values of Z, which correspond to erroneous values of $\langle N|Z\rangle$, are omitted. The value of $Z/\langle Z\rangle = 4$ corresponds to a probability of $P(Z) \approx 1$. However, the total probability for $P < 1$ is very small, which indicates that the behaviour at those mixture fractions will have little impact on the system.

This is a higher probability than the target previously set of 0.1, but has been deemed to be appropriate given that the data becomes erratic at values of Z larger than this.

The fit for zone 0 is a second order polynomial with a forced condition of passing through the origin. The function is

$$f(Z_n) = 0.3282Z_n^2 + 0.2706Z_n. \tag{2.4}$$

The fit is quite good up to $Z/\langle Z\rangle = 4$, which corresponds to a probability of approximately one. All lower probabilities can be ignored.

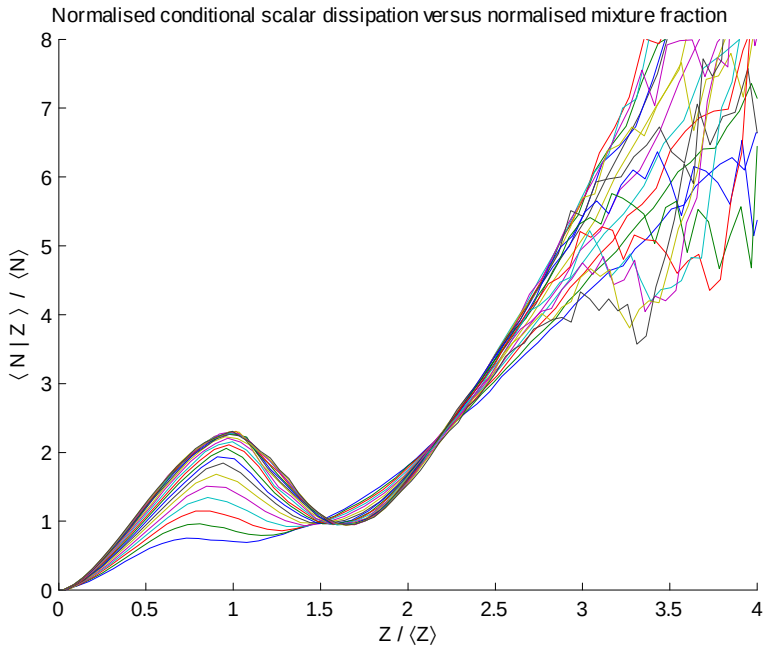

Figure 2.14: Conditional scalar dissipation, zone 1. Note the transient behaviour.

Zone 1

Shown in figure 2.14 is a plot of the normalised conditional scalar dissipation versus normalised mixture fraction for zone 1. Zone 1 requires a more rigorous approach given that the conditional scalar dissipation is a function of time as well as mixture fraction. There are, however, two distinguishing features of the curve which if characterised, would allow a function (or number of functions) to be constructed. These are the local minima and maxima. One cubic spline can be constructed between the known points of the origin and the maxima, and another between the maxima and the minima. The locations of the maxima and minima were determined for all points in time and their positions with respect to time were plotted.

A plot of the position of the local maxima with respect to time is shown in figure 2.15. The bottom plot can be thought of as the x position (Z) and the top plot the y position ($\langle N|Z\rangle$) of the maxima throughout time. Zone 1 corresponds to normalised time less than 2.73.

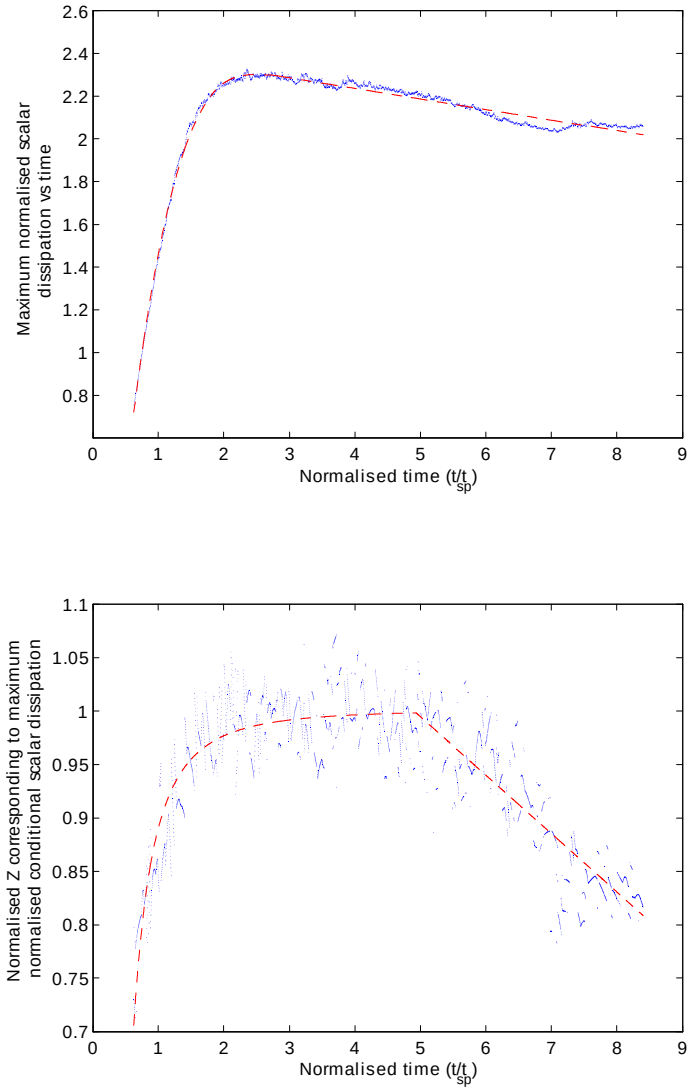

Figure 2.15: Position of the local maxima with respect to time.

The function for the Z position of the maxima with respect to time is:

$$\frac{Z_{max}}{\langle Z \rangle} = \begin{cases} \frac{-0.1267}{t_n^2} + \frac{0.0169}{t_n} + 1.0 & t_n \leq 4.9349 \\ -0.0457 t_n + 1.2681 & t_n \geq 4.9349 \end{cases} \tag{2.5}$$

where t_n is the time normalised by the length of the spark, $t_n = t/t_{sp}$.

The function for the $\langle N|Z \rangle$ location of the maxima is shown below.

$$\frac{\langle N_{max}|Z \rangle}{\langle N \rangle} = \begin{cases} 0.2080 t_n^3 - 1.6240 t_n^2 + 4.2158 t_n - 1.3385 & t_n \leq 2.7290 \\ -0.0498 t_n + 2.4351 & t_n \geq 2.7290 \end{cases} \tag{2.6}$$

A plot of the position of the minima with respect to time is shown in figure 2.16. The function for the Z position of the minima with respect to time is:

$$\frac{Z_{min}}{\langle Z \rangle} = \begin{cases} \frac{-0.3634}{t_n^2} + \frac{0.1320}{t_n} + 1.65 & t_n \leq 4.9349 \\ 0.0307 t_n + 1.5105 & t_n \geq 4.9349 \end{cases} . \tag{2.7}$$

The function for the $\langle N|Z \rangle$ location of the minima is shown below.

$$\frac{\langle N_{min}|Z \rangle}{\langle N \rangle} \tag{2.8}$$
$$= \begin{cases} 0.0639 t_n^5 + 0.6724 t_n^4 + 2.777 t_n^3 - 5.6151 t_n^2 + 5.5234 t_n - 1.1451 & t_n \leq 2.729 \\ 0.0003 t_n^4 - 0.0076 t_n^3 + 0.0519 t_n^2 - 0.1382 t_n + 1.0739 & t_n \geq 2.729 \end{cases}$$

Two cubic splines will be used to characterise $\langle N|Z \rangle$ up to the local minima. Each of these cubic splines can be fully characterised because four pieces of information are known; the position of the minima and maxima, and the gradient of zero at the minima and maxima. The following matrix operation can be used to find the coefficients of the cubics.

$$y = Ax^3 + Bx^2 + Cx + D \tag{2.9}$$

$$MX = Y$$
$$\begin{bmatrix} x_1^3 & x_1^2 & x_1 & 1 \\ x_2^3 & x_2^2 & x_2 & 1 \\ 3x_1^2 & 2x_1 & 1 & 0 \\ 3x_2^2 & 2x_2 & 1 & 0 \end{bmatrix} \begin{bmatrix} A \\ B \\ C \\ D \end{bmatrix} = \begin{bmatrix} y_1 \\ y_2 \\ y_1' \\ y_2' \end{bmatrix} \tag{2.10}$$

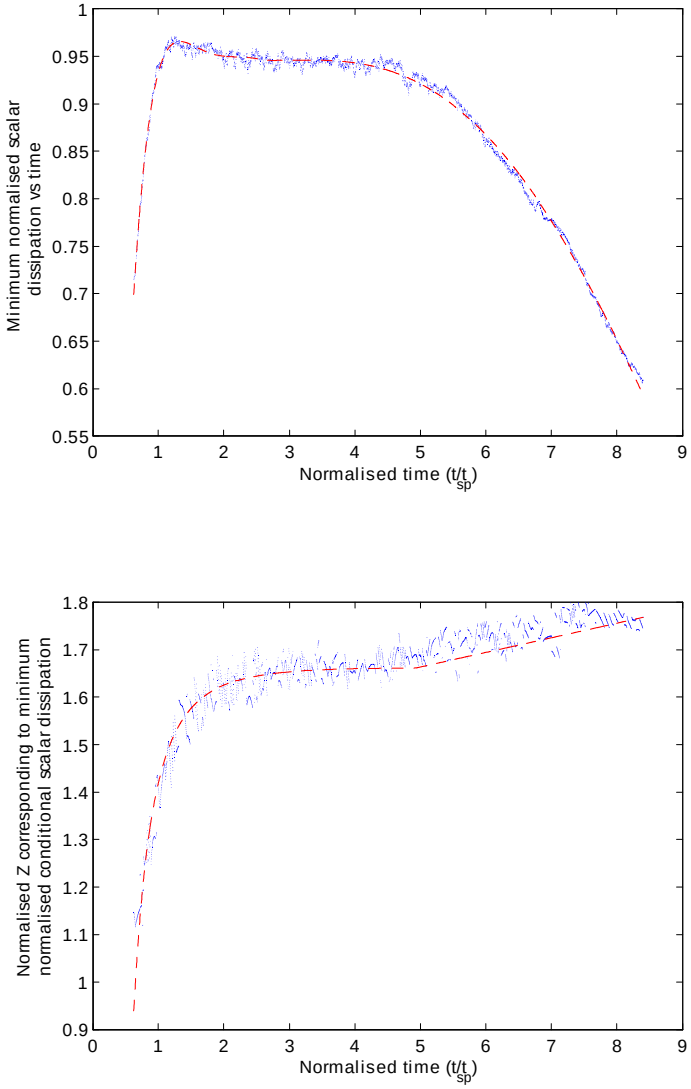

Figure 2.16: Position of the local minima with respect to time.

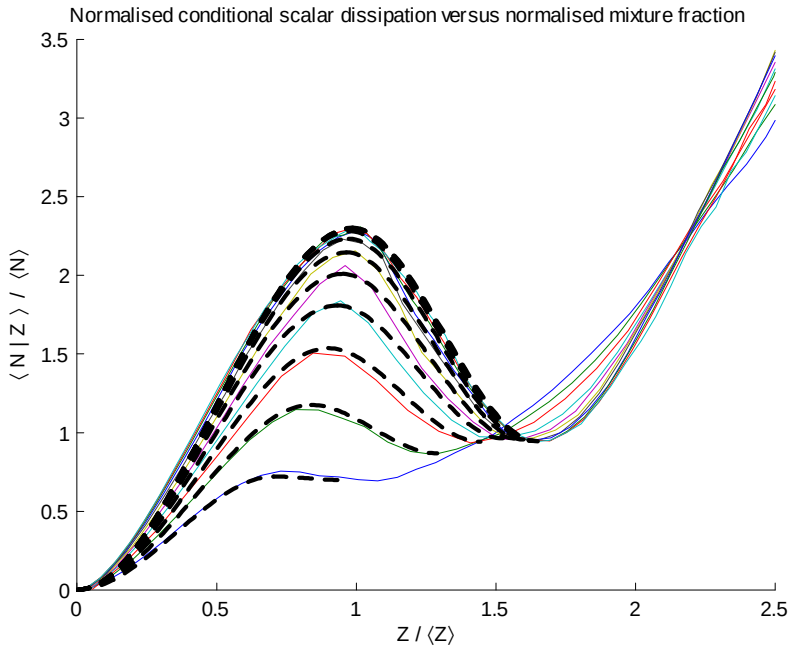

Figure 2.17: Conditional scalar dissipation, zone 1. Resultant fits up to the local minima.

where (x_n, y_n) is the position of the minima or maxima, and $(x_n, y_n^{'})$ is the gradient at the minima or maxima. By definition, the gradient at the maxima and minima is zero.

Using this approach, the function is approximated as shown in figure 2.17. The fit achieved is quite good.

The trailing part of the curve can be approximated with a quadratic. It can be seen from figure 2.17 that the tail of all the curves seem to pass through one point located at approximately $(2.19, 2.22)$. A quadratic can now be created from the three known pieces of data; the position of the minima, the zero gradient at the minima, and the point which all curves pass through, $(2.19, 2.22)$. Therefore, using the following matrix operations, the coefficients of the quadratic can be found.

$$y = Ax^2 + Bx + C \tag{2.11}$$

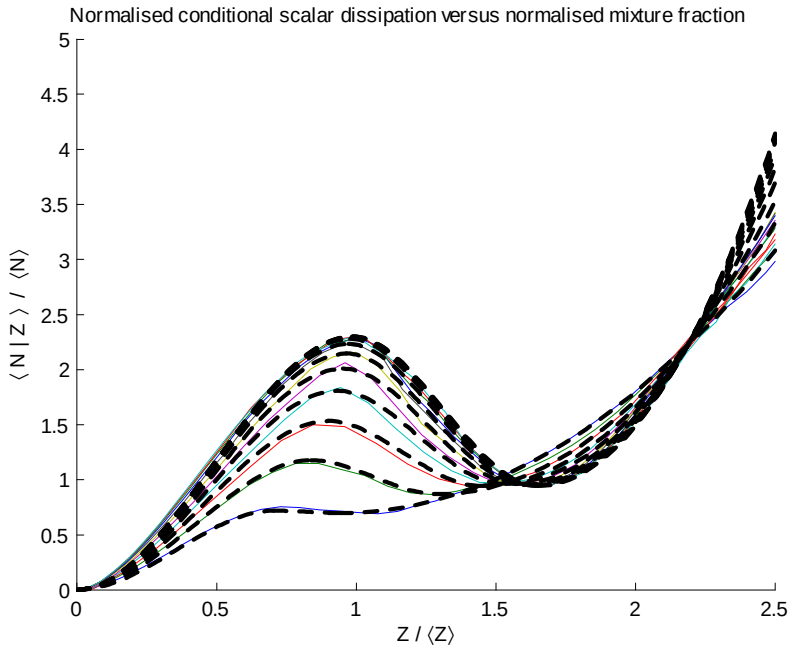

Figure 2.18: Resultant fit for the conditional scalar dissipation, zone 1.

$$MX = Y$$

$$\begin{bmatrix} x_{min}^2 & x_{min} & 1 \\ 2x_{min} & 1 & 0 \\ x_p^2 & x_p & 1 \end{bmatrix} \begin{bmatrix} A \\ B \\ C \end{bmatrix} = \begin{bmatrix} y_{min} \\ 0 \\ y_p \end{bmatrix} \tag{2.12}$$

The position of the minima is (x_{min}, y_{min}) and the position of the common point between all curves is (x_p, y_p). The resultant fit is shown in figure 2.18. The overall fit for each curve is very good.

Zone 2

The plot of conditional scalar dissipation versus mixture fraction for zone 2 is shown in figure 2.19. In contrast to zone 1, the curves are self similar up until the local minima, at which point the curves seem to diminish with time. As with zone 1, the curves will be split into three distinct parts and cubic splines fitted to these parts. A plot showing the first two cubic splines fitted to the curves is shown in figure 2.20. This represents

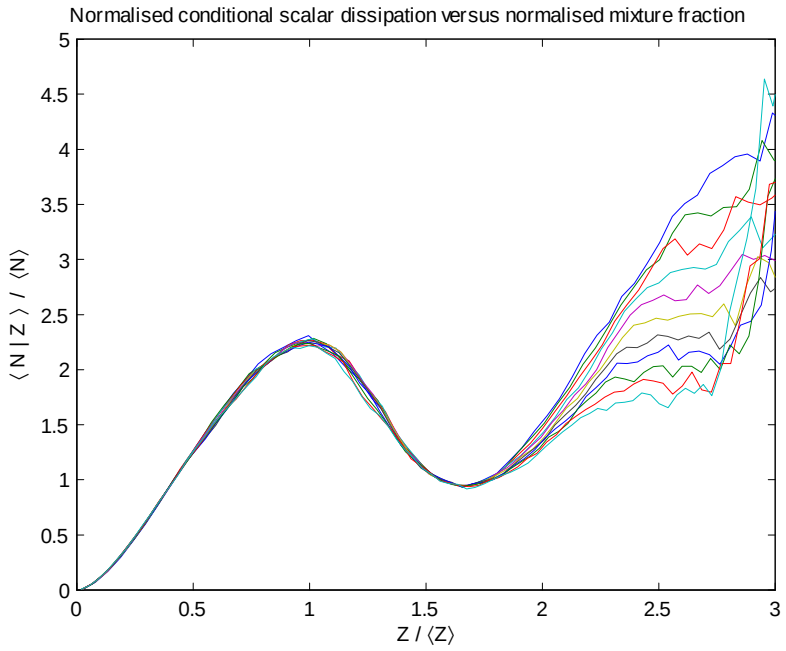

Figure 2.19: Conditional scalar dissipation, zone 2.

a good fit. The functions for the cubic splines are

$$\frac{\langle N|Z\rangle}{\langle N\rangle} = \begin{cases} -3.8549Z_n^3 - 5.3555Z_n^2 + 0.7545Z_n & Z_n < 1 \\ -8.6253Z_n^3 - 34.4747Z_n^2 + 42.7351Z_n - 14.7307 & 1 \leq Z_n \leq \frac{5}{3} \end{cases} . \quad (2.13)$$

Note that the splines are continuous, as both pass through the maxima and have zero gradients at the maxima.

The third section of the curve is not self similar and becomes erratic at values of $Z > 2.3$. This data can be ignored because the probability of $Z > 2.3$ occurring in the domain is less than 0.1. Again, cubic functions are fitted to the curve, however now at all points in time to account for the curves not being self similar. The result is shown in figure 2.21.

The fits seem reasonable up to values of Z greater than 2.3. The splines also seem to be quite similar in shape, which gives reason to believe a function of the form $y = abcd.x^3 + bcd.x^2 + cd.x + d$ may be used, where a, b and c are constants and d is a function of time.

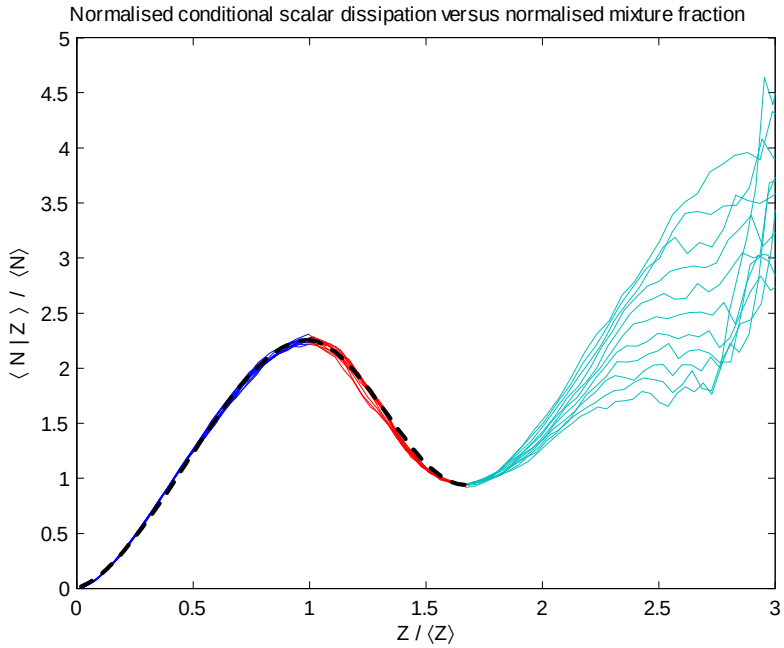

Figure 2.20: Fit for the zone 2 conditional scalar dissipation until the local minima.

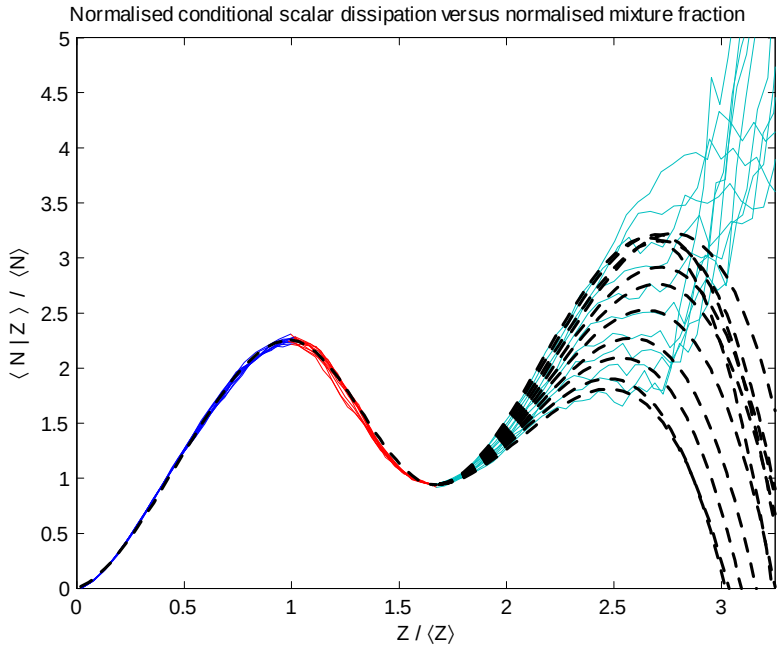

Figure 2.21: Fits obtained for the tail of the zone 2 curves. These fits have not been characterised.

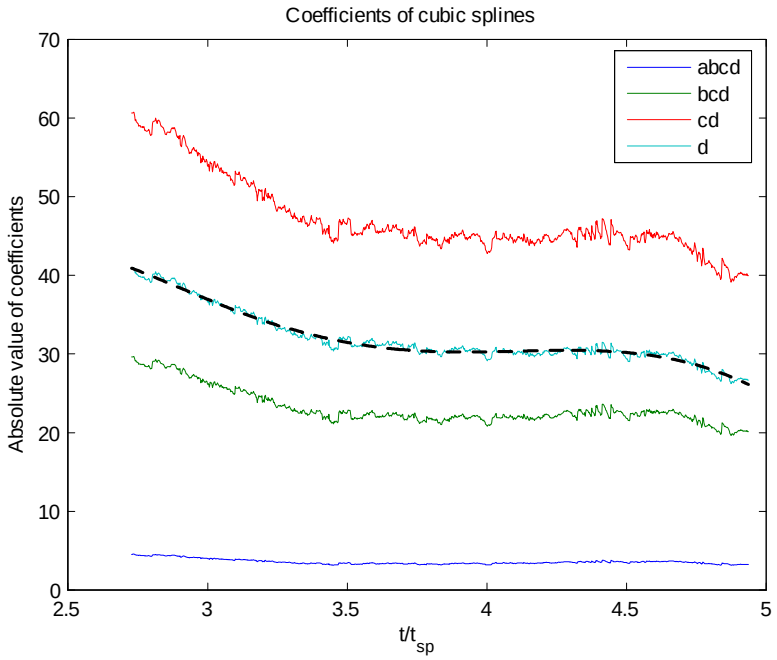

Figure 2.22: Coefficients of the cubic splines shown in figure 2.21. The fit for coefficient d is shown as the dashed line.

The absolute values of $abcd$, bcd, cd and d are shown in figure 2.22. The coefficients indeed seem to be multiples of one another, with d a function of time. The function of coefficient d versus time was found to be a fifth order polynomial. The coefficients are:

$$\begin{aligned} a &= -0.1554 \\ b &= -0.4908 \\ c &= -1.4781 \\ d &= 0.0010t_n^5 - 0.0215t_n^4 + 0.1806t_n^3 - 0.7244t_n^2 + 1.3818t_n - 0.9617 \end{aligned} \quad (2.14)$$

where t_n is the normalised time.

The resulting cubics produced using this method are shown in figure 2.23. Note that the graphs do not pass through the minima. Steps may be taken to ensure that the function passes through the minima. It is proposed that while d is a function of time, c is function of d in order to force the curves through the minima. The equation describing c is:

$$c = \frac{y_{min} - d}{abd.x_{min}^3 + bd.x_{min}^2 + d.x_{min}} \quad (2.15)$$

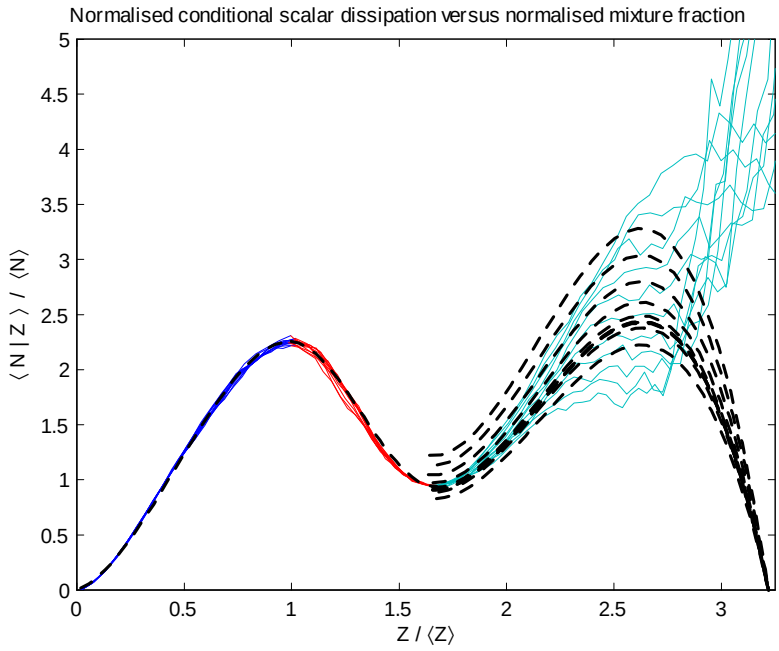

Figure 2.23: Fit for the tail of the curves using coefficients shown in equation 2.14. Note the inability to accurately predict the location of the minima.

where (x_{min}, y_{min}) is the location of the minima.

Using these values of the coefficients, figure 2.24 is produced. Note that now all splines pass through the minima. Some error is introduced into the fit, but they are still reasonable given that high values Z correspond to relatively low probabilities. In future characterisations of the DNS data, a single cubic through the transient behaviour of the tail of the curves would probably suffice. Given that this project aims to investigate some of the methods of characterising all the terms of the DNS data, the above was a good investigation of some of the various techniques which may need to be used in order to characterise the data with the best possible accuracy.

Zone 3

Figure 2.25 shows zone 3 of conditional scalar dissipation. It is evident that the curves are not as self similar as in zone 2 as the rate of combustion diminishes. Currently, two cubics and a quadratic function are used to characterise the curves. At the moment,

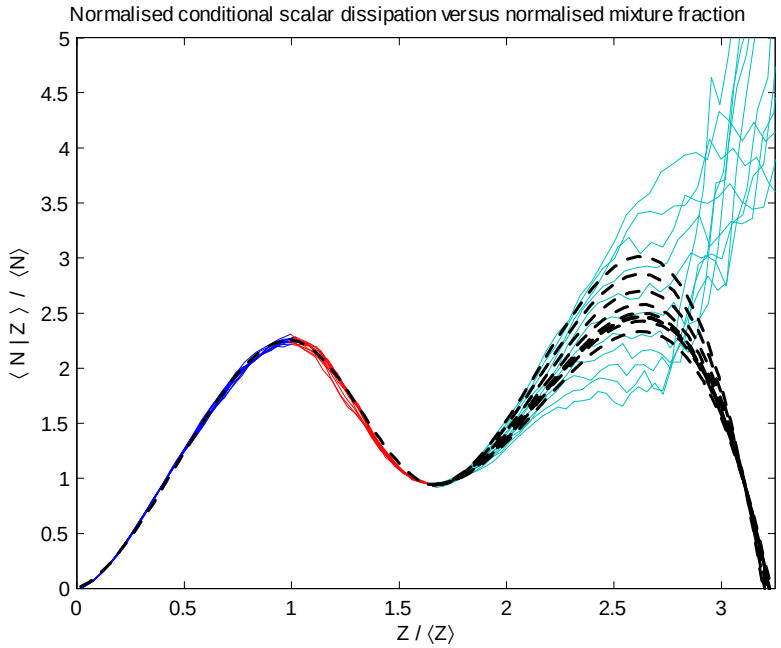

Figure 2.24: The final fit for the conditional scalar dissipation, zone 2, after the cubic splines are forced through the local minima.

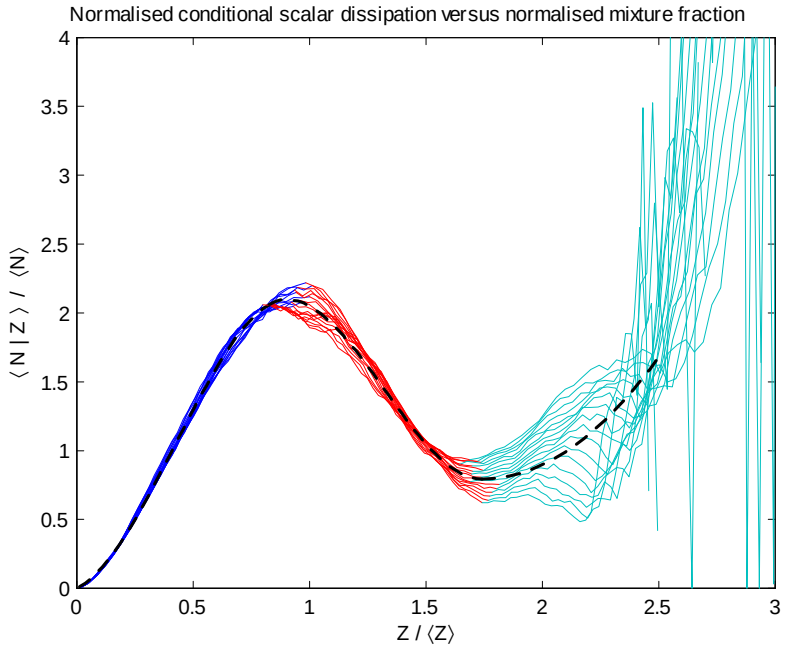

Figure 2.25: Fit obtained for the conditional scalar dissipation, zone 3.

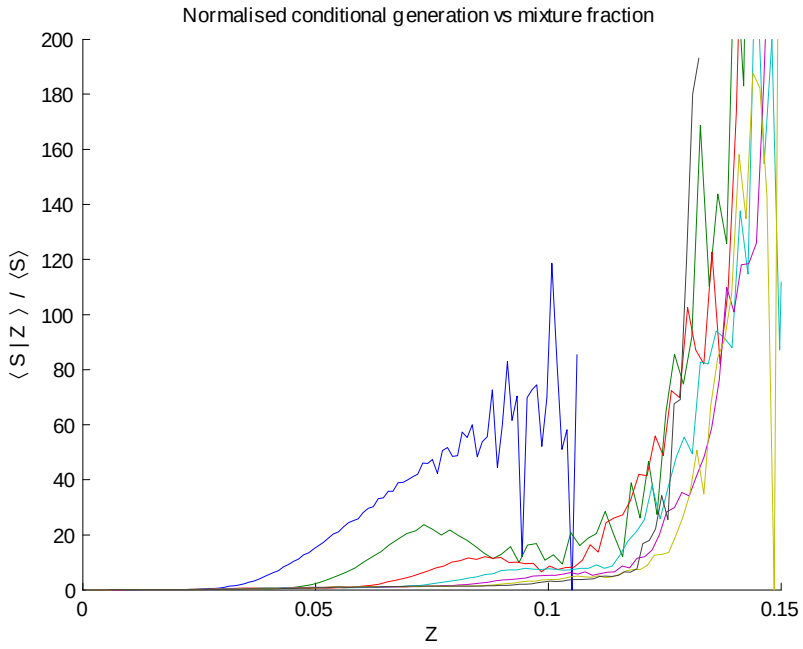

Figure 2.26: Conditional generation due to droplet evaporation, all zones.

this fit is satisfactory, but future work may lead to more accurately describing $\langle N|Z\rangle$ over the last stage of combustion. Whether more work needs to be undertaken will be determined by the ability of the use of the CMC equation to accurately reproduce the behaviour of the combustion in zone 3.

The functions used to describe the fit are:

$$\frac{\langle N|Z\rangle}{\langle N\rangle} = \begin{cases} -4.7032Z_n^3 + 5.9381Z_n^2 + 0.7958Z_n & Z_n < 0.9042 \\ 4.4909Z_n^3 - 17.8044Z_n^2 + 21.1823Z_n - 5.8180 & 0.9042 \leq Z_n \leq 1.7389 \\ 1.5274Z_n^2 - 5.3118Z_n + 5.4109 & Z_n > 1.7389 \end{cases} . \tag{2.16}$$

2.5.3 Conditional generation due to droplet evaporation

Figure 2.26 shows the normalised conditional generation due to droplet evaporation versus the mixture fraction over the life of combustion. As can be seen, $\langle S|Z\rangle$ seems to be a transient function for all zones, regardless of which quantities are normalised. The fit for zone 0 is shown in figure 2.27.

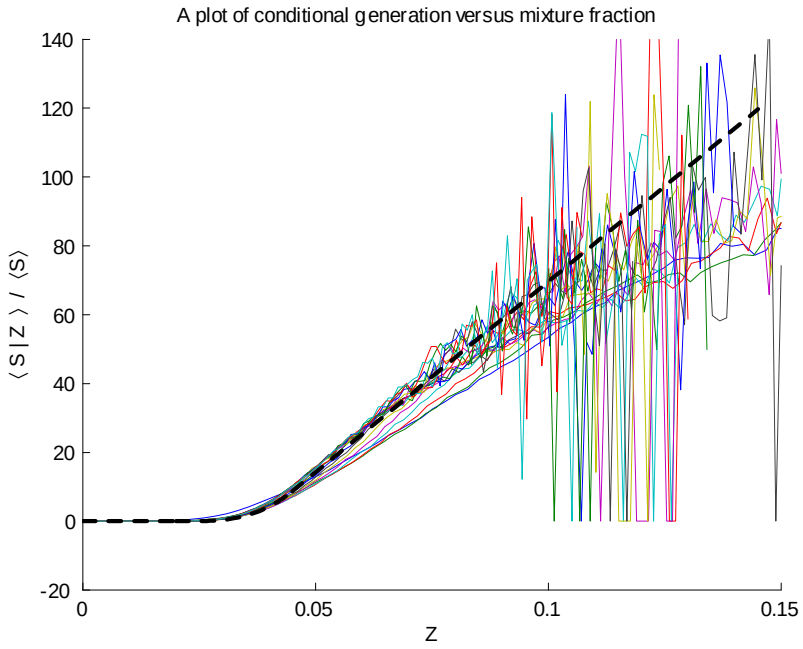

Figure 2.27: Fit of the conditional generation, zone 0.

The curves for zone 0 are quite similar, therefore one function will be used to describe all points in time in zone 0. The equations describing the fit are shown in equation (2.17). Note that in this instance Z is not normalised.

$$\frac{\langle S|Z\rangle}{\langle S\rangle} = \begin{cases} 0 & Z < 0.02 \\ 6.68Z^3 - 0.430Z^2 + 0.009Z - 0.0001 & 0.02 \leq Z \leq 0.045 \\ 1125Z - 42.2 & Z > 0.045 \end{cases} \tag{2.17}$$

The curves for the rest of the zones are shown in figure 2.28. The graph shows that all of the curves pass through roughly the same route, before branching upwards. Therefore, the model that is proposed is a combination of one non-transient function and a transient function.

The non-transient, 'base' function can be described with the use of an error function. The portion of the curves which branch off of the error function will be approximated as straight lines, and the erratic behaviour and the ends of the straight lines will be neglected due to low probability. The fit can easily be determined by the greater of the error function and the linear function.

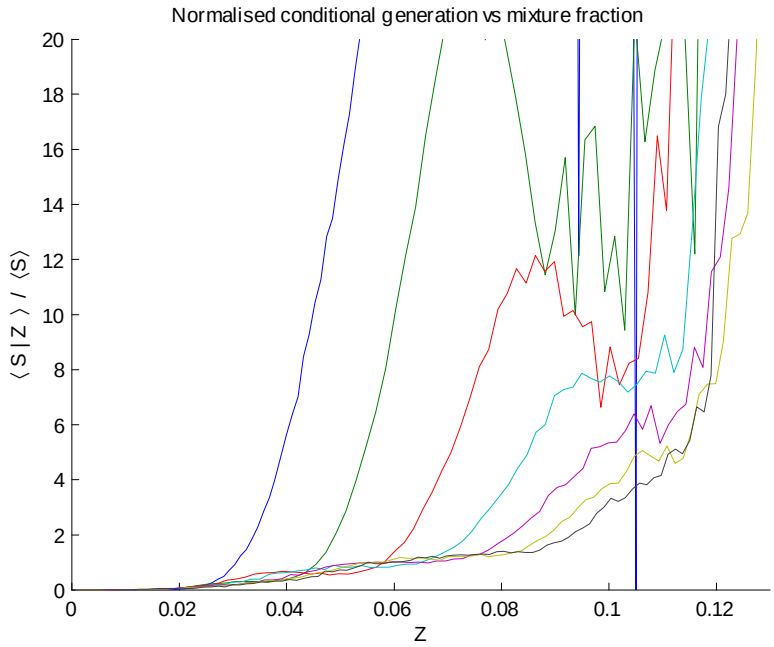

Figure 2.28: Conditional generation, zones 1–3. Note the transient behaviour.

The error function is defined as:

$$\frac{\langle S|Z\rangle}{\langle S\rangle} = 0.7\left\{1 + \mathrm{erf}(38.9[Z - 0.0477])\right\}. \tag{2.18}$$

The coefficients of the straight lines in the form $y = M(x - c)$ are shown in figure 2.29. The fits describing M and c are:

$$M = -2.60t_n^3 + 58.6t_n^2 - 458.0t_n + 1364 \tag{2.19}$$

$$c = 0.0001t_n^3 - 0.0021t_n^2 + 0.0172t_n + 0.0247 \tag{2.20}$$

The gradient (M) at $t_n < 1.0$ is overestimated, however the fit should prove to be adequate. The behaviour of coefficient c is captured quite well.

The fits are shown in figure 2.30. As predicted, the error is greatest at the start of zone 1, and the fit becomes more accurate at the end of the combustion.

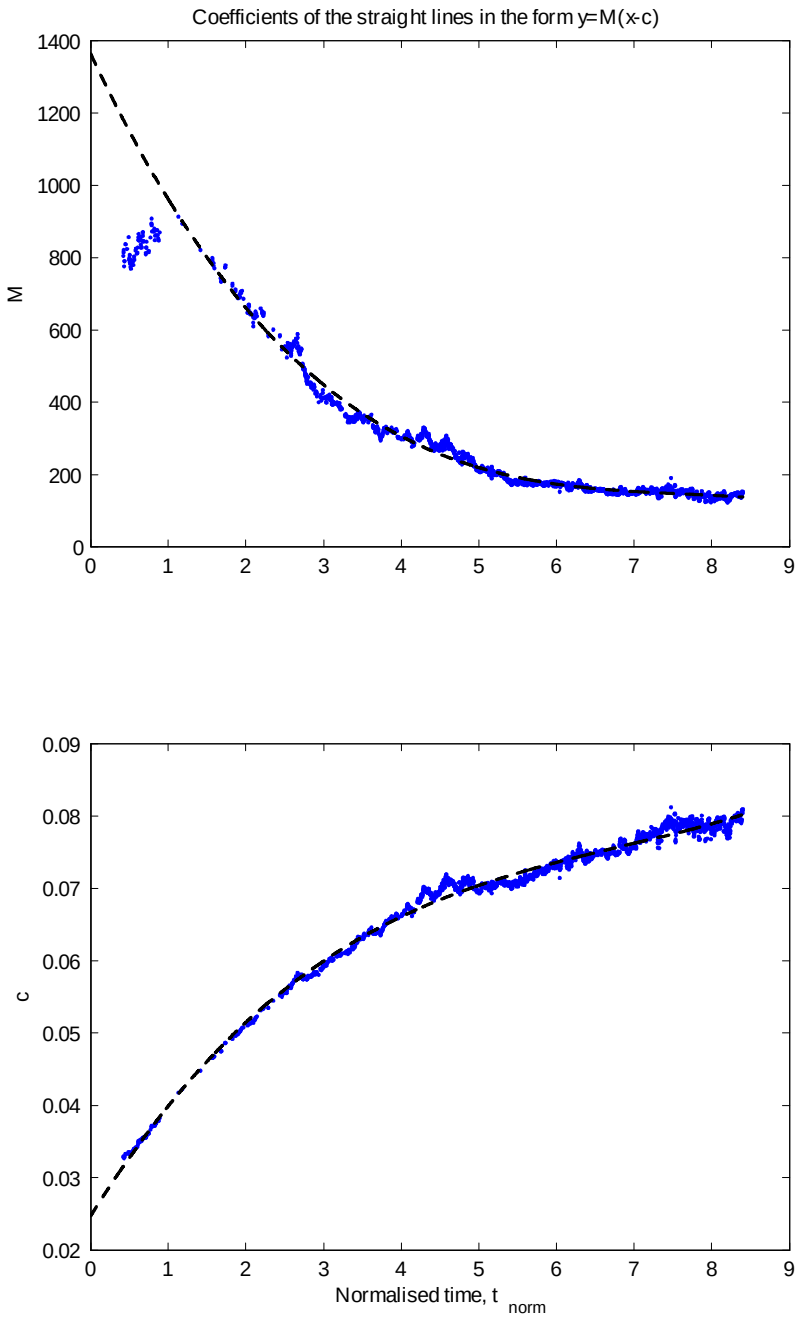

Figure 2.29: Linear coefficients in the form $y = M(x - c)$.

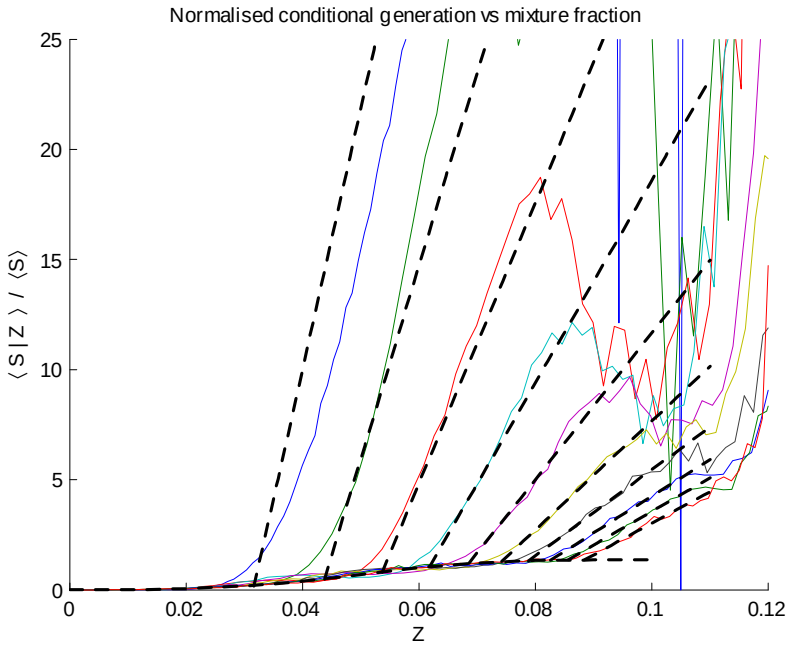

Figure 2.30: Fit for the conditional generation, zones 1–3.

2.6 Other cases

2.6.1 Droplet diameter decreased

As mentioned previously, the above data is of equivalence ratio of 2 and droplet diameter, $d = 3.936\mu$m. However in order to be of any significant use to the engineering community, combustion with different parameters (such as droplet size and spacing) must also be able to be characterised. The following is based on combustion with an equivalence ratio of 2 and droplet diameter of 2.783μm. This case will be named case 2. In this case, the stages of combustion occur at the following points in time:

- Initial stage ($< 4.6\mu$s),
- Intermediate stage ($4.6 - 126\mu$s),
- Final stage ($> 126\mu$s).

The tendency of this system to reach each of the stages quicker reflects the higher surface area of fuel droplets (due to decreased droplet size but similar mass of fuel initially) allowing for more rapid evaporation of droplets. The progress of the wave front is also more rapid due to less energy having to be expended in releasing more fuel to the system. The final stage of combustion for this case tends not to highlight the system reaching an equilibrium, but rather the system starts to decay.

As will be shown, the characterisation of each of the terms of the CMC model is very similar to that shown in the first case investigated.

Mixture fraction pdf

The mixture fraction pdf for each of the four zones is shown in figure 2.31, along with the fits to describe those zones. It can be seen that the mixture fraction pdf is very similar to that investigated in the first case. This allows for the application of each of the techniques and functions used in the earlier work. This is very positive as the MATLAB scripts used to find the best fit for each of the zones can be readily transferred between different types of spray combustion.

The equation describing the fit for zone 0 is a β-function. The shape parameters for the β-function pdf (as defined in equation (2.1)) are:

$$\begin{aligned} A_0 &= 258.9835 \\ \alpha &= 0.1373 \\ \beta &= 3.0578 \\ a &= 0 \\ b &= 8. \end{aligned}$$

There is some transient behaviour nearing the end of this time period as the rate of fuel being evaporated in locations around $Z \approx 1.5$ increases. This causes a slight error in the fit around this location, however this should prove to be of little concern. This fit similar to that of the previous case of combustion.

The fit for zone 1 also takes the same form as the fit for zone 1, case 1; a combination

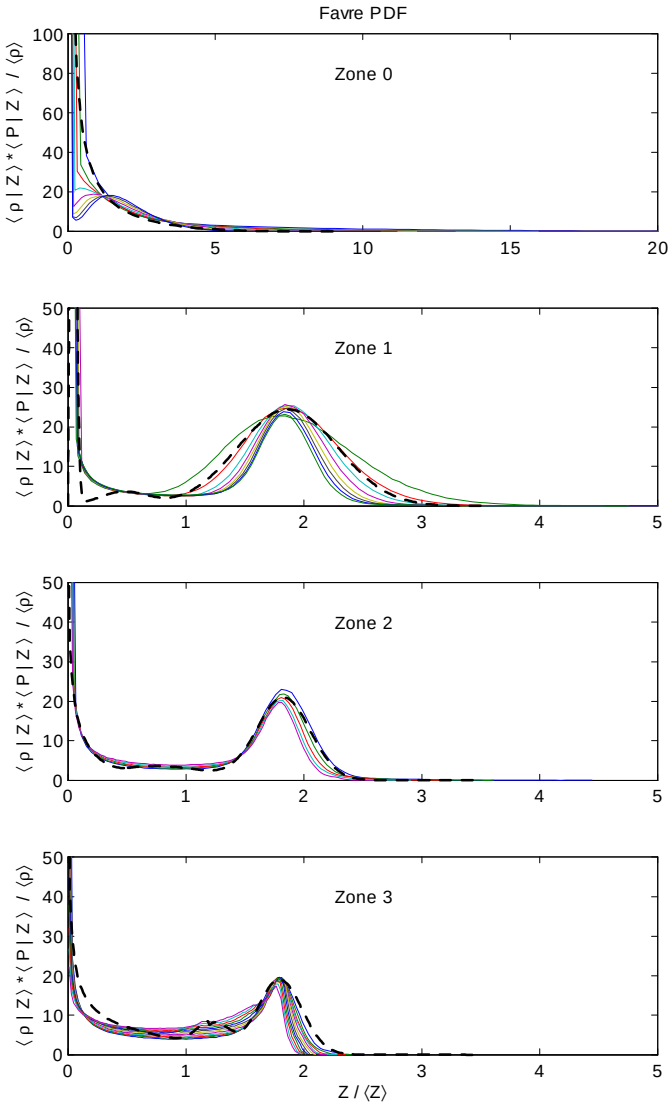

Figure 2.31: Favre averaged mixture fraction for each of the zones with their respective fits, case 2.

of a β-function and two Gaussian functions. The parameters for use in equations (2.2), (2.1), and (2.3) are:

$$\begin{aligned}
\sigma_1 &= 1.8686 \\
\mu_1 &= 0.2943 \\
A_1 &= 32.6270 \\
\sigma_2 &= 0.4791 \\
\mu_2 &= 0.0205 \\
A_2 &= 0.7024 \\
A_0 &= 13.7697 \\
\alpha &= 4.5292 \\
\beta &= 46.7537 \\
a &= 0 \\
b &= 0.5.
\end{aligned}$$

The model of the pdf for zone 1 shows some error around $Z \approx 0.25$ where the β-function underestimates the behaviour. This may require more rigorous modelling. There is also some error around the primary Gaussian peak as the system takes some time to stabilise.

The coefficients for zone 2 are shown below.

$$\begin{aligned} A_1 &= 10.1456 \\ \sigma_1 &= 1.826 \\ \mu_1 &= 0.040995 \\ A_2 &= 3.5553 \\ \sigma_2 &= 0.92423 \\ \mu_2 &= 0.12977 \\ A_0 &= 5.086 \\ \alpha &= 0.51619 \\ \beta &= 1.6062 \\ a &= 0 \\ b &= 0.5 \end{aligned}$$

The fit for zone 2 is quite good. The behaviour of the system is the least transient in zone 2 and this is reflected in the pdf for zone 2.

The coefficients for zone 3 are shown below.

$$\begin{aligned} A_1 &= 9.058 \\ \sigma_1 &= 1.7962 \\ \mu_1 &= 0.036009 \\ A_2 &= 2.5516 \\ \sigma_2 &= 1.2464 \\ \mu_2 &= 0.01671 \\ A_0 &= 10.9368 \\ \alpha &= 0.50151 \\ \beta &= 1.3151 \\ a &= 0 \\ b &= 1.2 \end{aligned}$$

The fit for zone 3 is not particularly good but should prove sufficient. The decay of the system causes the primary peak to become more pronounced and this has not been

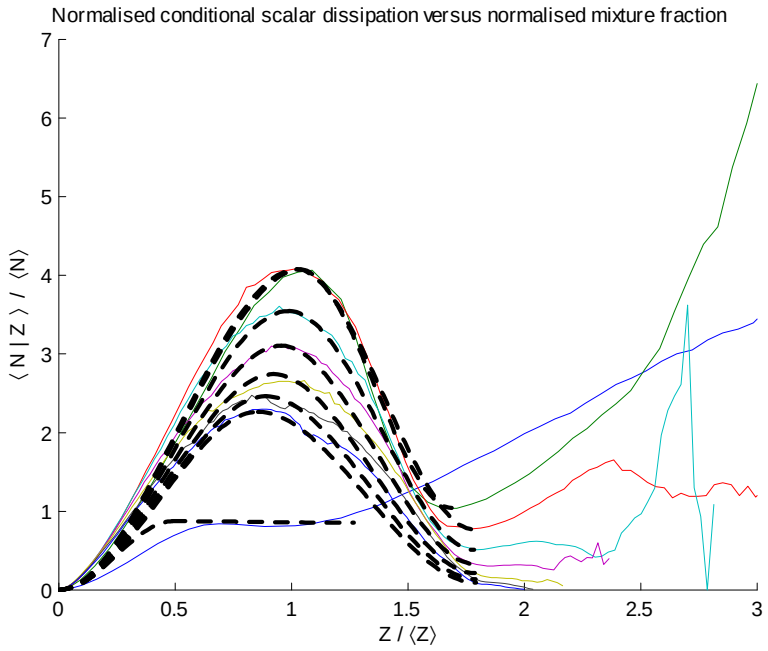

Figure 2.32: Fits for the conditional scalar dissipation, all zones, case 2. Fits for the tail are omitted.

captured well with the Gaussian fit. The secondary peak tends to become more elongated and this also has not been described well. Because this zone represents decaying combustion, these errors should have a minimal effect on subsequent calculations.

Conditional scalar dissipation

The fits for the conditional scalar dissipation for all zones is shown in figure 2.32. As can be seen, it was possible to define $\langle N|Z\rangle$ for all zones by defining the x and y locations of the maxima and minima, and joining the origin and those known points with two cubic splines. This approach was used for zone 1 of case 1.

The technique of defining the location of the maxima and minima and then joining those points with cubic splines has proven to be quite successful. In fact, pending the results of this case, future modelling of all zones of the conditional scalar dissipation may rely on this technique. The MATLAB script required for this process is quite simple and could be easily adapted to different cases of combustion.

The function for the Z position of the maxima with respect to time is shown in equation (2.21).

$$\frac{Z_{max}}{\langle Z \rangle} = \begin{cases} \frac{-0.0754}{t_n^2} + \frac{0.1088}{t_n} + 1.0 & t_n \leq 1.994 \\ -0.0317 t_n + 1.0988 & t_n \geq 1.994 \end{cases} \tag{2.21}$$

The function for the $\langle N|Z \rangle$ location of the maxima is shown below.

$$\frac{\langle N_{max}|Z \rangle}{\langle N \rangle} = \begin{cases} 0.6183 t_n^3 - 3.8297 t_n^2 + 7.8970 t_n - 1.1221 & t_n \leq 1.994 \\ 0.0376 t_n^2 - 0.7221 t_n + 5.5902 & t_n \geq 1.994 \end{cases} \tag{2.22}$$

The function for the Z position of the minima with respect to time is shown in equation (2.23).

$$\frac{Z_{min}}{\langle Z \rangle} = \begin{cases} \frac{0.0763}{t_n^2} - \frac{0.4752}{t_n} + 2.0 & t_n \leq 1.994 \\ 0.0021 t_n + 1.7767 & t_n \geq 1.994 \end{cases} \tag{2.23}$$

The function for the $\langle N|Z \rangle$ location of the minima is shown below.

$$\frac{\langle N_{max}|Z \rangle}{\langle N \rangle} \tag{2.24}$$

$$= \begin{cases} 0.5338 t_n^5 - 3.5124 t_n^4 + 9.0283 t_n^3 - 11.3505 t_n^2 + 6.7720 t_n - 0.3549 & t_n \leq 1.994 \\ -0.0024 t_n^3 + 0.0603 t_n^2 - 0.5364 t_n + 1.7445 & t_n \geq 1.994 \end{cases}$$

These points, and the origin, are joined with the use of two cubic splines. The methods used for achieving this are the same as shown for case 1. Depending on the accuracy required, the last part of the curves may be approximated by a straight line. For the purposes of this project, this part of the curve was neglected. These values being small confirms the assertion that evaporation has been completed.

Again, the models which were derived for case 2 are quite similar to those derived for case 1. Therefore, without too much further alteration of the MATLAB scripts, a universal script may be created which would greatly decrease the time required for the modelling of the DNS data.

Conditional generation due to droplet evaporation

The fit for the conditional generation due to droplet evaporation is shown in figure 2.33. The fit for zone 0 is not included in this analysis. As can be seen, the fit for zones 1

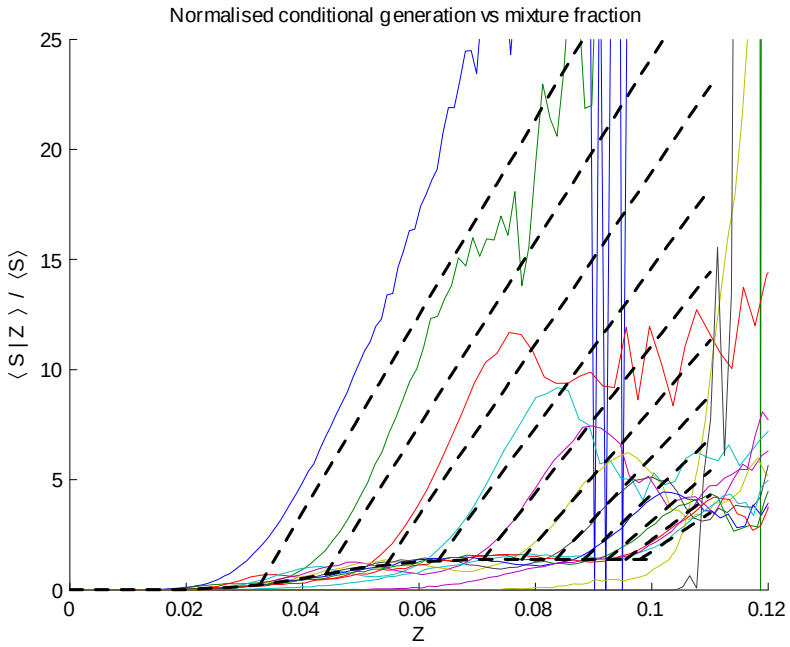

Figure 2.33: Fit for the conditional generation, zones 1–3, case 2.

to 3 take the same form as that of case 1.

The error function is defined as:

$$\frac{\langle S|Z\rangle}{\langle S\rangle} = 0.7\left\{1 + \mathrm{erf}(64.88[Z - 0.0434])\right\}. \tag{2.25}$$

The coefficients of the straight lines are again a function of time. Using a straight line of the form $y = M(x - c)$, the values of M and c are shown below.

$$M = 0.8603t_n^2 - 68.66t_n + 466.6 \tag{2.26}$$

$$c = -1.5089 \times 10^{-5}t_n^3 - 0.00263t_n^2 + 0.0267t_n + 0.0246 \tag{2.27}$$

As with the other quantities of the CMC model, the fits for the conditional generation due to droplet evaporation are very easily transferred between different cases of combustion.

2.6.2 Droplet diameter increased

The droplet diameter in the third case analysed was $4.821\mu m$. This system was chosen for analysis due to the combustion becoming prematurely quenched due to the inability of the flame kernel to supply gaseous fuel to allow combustion to proceed. The input parameters which led to this case were high droplet diameter and greater distance between droplets.

This type of combustion was investigated in order to find if the above procedures can be applied to this case. The inclusion of these results are too lengthy to include in this document, however all the required conditional values were modelled quite accurately as per the other two cases shown above.

The main points to note were that while the combustion was still occurring, the system behaved just as the other cases investigated above. All of the zone changes were slower due to the inability of the flame front to quickly evaporate the large droplets. The extinction of the flame was quite abrupt; there was some transient decay as the combustion neared the end of its life but was restricted to a relatively small amount of time.

2.6.3 Comments on the characterisation of the terms

As shown in the above analysis, all terms of the CMC have been modelled. No particular term, or particular case of combustion, proved to be overly difficult to characterise. This work achieves one of the main objectives of this project: to analyse DNS data to create models for the first order CMC equation.

The accuracy of all of the fits is quite good. Some transient behaviour has caused some amount of error, the magnitude of which will be determined when the CMC model is validated. However, in the current form of the functions, it is expected that none of the zones in any of the cases of combustion would be directly responsible for creating large errors in the CMC model.

The similarities of the CMC terms in each of the different cases of combustion is en-

couraging. This suggests that in future work, one universal MATLAB script for each CMC term would be able analyse most, if not all, cases of combustion correctly. This would greatly reduce the number of man hours necessary to develop models.

Chapter 3

Validation of the first order CMC model

The validity of the first order CMC model may be determined by checking the outputs of the CMC model (conditional temperature and conditional mass fractions of both species) with the values of those quantities obtained from the DNS. If the values of the conditional quantities calculated with the CMC model are validated, the overall mean of these quantities can then be validated against the DNS data. This will determine if the mixture fraction pdf is valid or needs further work.

In order to validate the CMC model by comparing the results to that of the DNS, all of the assumptions used in the DNS must also be used in the CMC model. These include initial and boundary conditions.

The MATLAB script which was used to validate the first order CMC model is given in Appendix B.

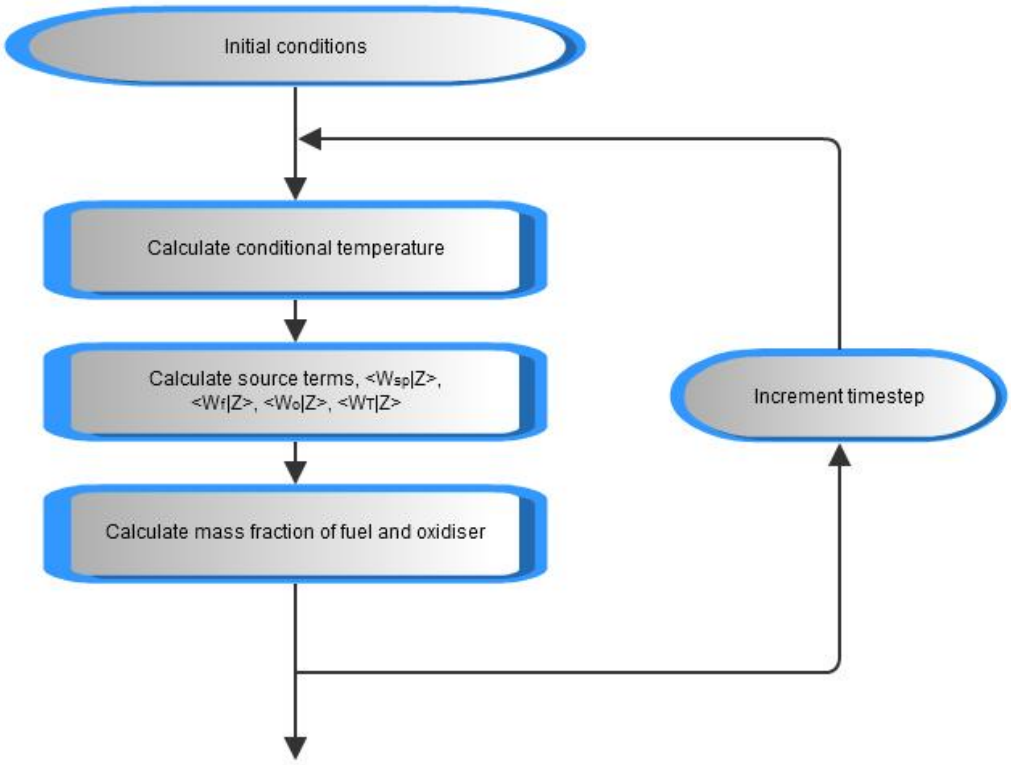

Figure 3.1: Flowchart showing the steps taken when calculating the required quantities using the CMC model.

3.1 Recreation of the data

3.1.1 Order of calculation

In order to calculate the value of any one of the quantities (conditional temperature, mass fraction of fuel, mass fraction of oxidiser) at any point in time, all three of the quantities must be known at that particular time or one timestep previous. A schematic of how the calculation of the quantities progresses with time is shown in figure 3.1.

The data to be recreated has three dimensions, the independent variables Z and t and the dependent variable, either T, Y_f or Y_o (temperature or species mass fractions). As shown in figure 3.1, the model will have three steps:

1. Calculate the conditional temperature,
2. Calculate the source term, $\langle W|Z \rangle$,
3. Calculate the conditional mass fraction of the fuel and the oxidiser.

Each of these steps will require a different equation to model. The conditional temperature and mass fractions may be calculated using a form of the CMC model, while the source term is calculated using a combination of the DNS data and predefined models.

3.1.2 Mixture fraction and time

The mixture fraction, Z, and time, t, are independent variables and therefore will be determined prior to any calculations taking place.

The following values of mixture fraction and time will be used:

- $0 \leq Z \leq 0.15$, $\Delta Z = 0.005$
- $0 \leq t \leq 0.08$, $\Delta t = 0.00002$

The upper range of Z, $Z = 0.15$ was chosen because evaluation of the data showed that for most points in time, the mixture fraction was unlikely to be richer than this value. Also, the mixture fraction probability density function indicates that the probability of regions that rich is quite small and therefore has little bearing on the behaviour of the system. Using a step of $dZ = 0.005$ allows for 31 values of Z. This was chosen to maintain a balance between satisfactory accuracy and calculation time.

The determination of the time domain and timestep was linked to the values used in the DNS. The use of the relatively small timestep of $dt = 0.00002$ results in 4001 timesteps, which is quite large and causes the computation time to be relatively large. However, using the same timesteps for both the CMC and DNS calculations allows for the direct comparison of the output quantities at any point in time, and thus allows for easier analysis of the accuracy of the CMC model.

3.1.3 Calculation of temperature

The normalised temperature is obtained using an equation similar to that shown in equation (1.6) with negligible terms neglected, or

$$\frac{\partial \langle T|Z\rangle}{\partial t} = \langle N|Z\rangle \frac{\partial^2 \langle T|Z\rangle}{\partial Z^2} + \langle W_T|Z\rangle + \left[T_d - \langle T|Z\rangle - (1-Z)\frac{\partial \langle T|Z\rangle}{dZ}\right] \langle S|Z\rangle (\Delta x)^3 \tag{3.1}$$

where T_d is the normalised mean temperature of the droplet liquid, and for the purposes of validating the first order CMC model, is obtained from the DNS data. The value $(\Delta x)^3$ refers to the number of nodes in the original DNS data, and is equal to $\frac{1}{128^3}$. All other terms of this equation have been modelled using the DNS data.

Because no exact solution may be found for the above equation, numerical methods are needed. The explicit finite difference method may have some stability issues, so the implicit method was used.

The equivalent implicit numerical form of this equation is:

$$\begin{aligned}
&\left(\frac{-N_{i-1}^{k+1}}{(\Delta Z)^2} + \frac{(Z_{i-1}-1)\,S_{i-1}^{k+1}(\Delta x)^3}{2\Delta Z}\right) T_{i-1}^{k+1} + \left(\frac{1}{\Delta t} + \frac{2N_i^{k+1}}{(\Delta Z)^2} + S_i^{k+1}(\Delta x)^3\right) T_i^{k+1} \\
&- \left(\frac{N_{i+1}^{k+1}}{(\Delta Z)^2} + \frac{(Z_{i+1}-1)\,S_{i+1}^{k+1}(\Delta x)^3}{2\Delta Z}\right) T_{i+1}^{k+1} \\
&\quad = W_i^{k+1} + T_d S_i^{k+1}(\Delta x)^3 + \frac{T_i^k}{\Delta t}
\end{aligned} \tag{3.2}$$

where k and i refer to the indices of time and mixture fraction respectively. In the above equation, it is implied that N, T, S and W are all conditional upon Z. When put into matrix form, the equations become

$$\begin{bmatrix} 1 & 0 & 0 & 0 & 0 & 0 \\ A & B & C & 0 & 0 & 0 \\ 0 & A & B & C & 0 & 0 \\ & \vdots & & & \vdots & \\ & \vdots & & & \vdots & \\ 0 & 0 & 0 & 1 & -2 & 1 \end{bmatrix} \begin{bmatrix} T_1^{k+1} \\ T_2^{k+1} \\ T_3^{k+1} \\ \vdots \\ \vdots \\ T_n^{k+1} \end{bmatrix} = \begin{bmatrix} 0 \\ W_2^{k+1} + \frac{T_d S_2^{k+1}}{(\Delta x)^3} + \frac{T_2^k}{\Delta t} \\ W_3^{k+1} + \frac{T_d S_2^{k+1}}{(\Delta x)^3} + \frac{T_3^k}{\Delta t} \\ \vdots \\ \vdots \\ 0 \end{bmatrix} \tag{3.3}$$

where

$$A = \frac{-N_{i-1}^{k+1}}{(\Delta Z)^2} + \frac{(Z_{i-1} - 1)\, S_{i-1}^{k+1} (\Delta x)^3}{2\Delta Z}, \tag{3.4}$$

$$B = \left(\frac{1}{\Delta t} + \frac{2N}{(\Delta Z)^2} + \frac{S_i^{k+1}}{(\Delta x)^3} \right), \tag{3.5}$$

and

$$C = \frac{-N_{i+1}^{k+1}}{(\Delta Z)^2} + \frac{(Z_{i+1} - 1)\, S_{i+1}^{k+1} (\Delta x)^3}{2\Delta Z} \tag{3.6}$$

The above matrix solves for all temperatures with respect to mixture at one point in time.

The initial and boundary conditions for the temperature are:

- initially, the conditional temperature was obtained from the DNS data,
- the gradient at $Z = 0.15$ is equal to that of the adjacent data point, that is the curvature of the temperature is zero,
- the conditional temperature at $Z = 0$ is zero.

3.1.4 Calculation of the source term

The source term, $\langle W|Z \rangle$ contains both the spark source and the chemical source,

$$\langle W|Z \rangle = \langle W_{sp}|Z \rangle + \langle W_{\alpha}|Z \rangle \tag{3.7}$$

The chemical source term, $\langle W_\alpha|Z\rangle$ where α denotes the species, is given by,

$$\langle W_\alpha|Z\rangle = B_\alpha \langle Y_f Y_o|Z\rangle \exp\left[\frac{-\frac{\beta}{\tau}(1+\tau)^2}{1+\tau\langle T|Z\rangle}\right] \tag{3.8}$$

where:

- B_α is a constant related to the activation energy and heat release of the species,
- $B_f = 2.5 \times 10^7$,
- $B_o = 9.996 \times 10^7$,
- Y_f, Y_o are the conditional mass fractions of the species,
- β is the Zel'dovich factor and is equal to 6,
- τ is the heat release parameter and is equal to 4,
- T is a non dimensional temperature.

The source term to be used when calculating the conditional temperature is:

$$\langle W_T|Z\rangle = \langle W_f|Z\rangle \tau(1+AFR) \tag{3.9}$$

where AFR is the air-to-fuel ratio.

Most of the parameters of the above equations are defined in the DNS and are therefore easily obtained if the program that ran the DNS is accessible. To obtain the chemical source term, an estimate for the mass fractions of both species and the normalised temperature can be obtained from the values of these parameters at the previous time-step.

The spark source term, $\langle W_{sp}|Z\rangle$, is obtained from the DNS data.

3.1.5 Calculation of the mass fractions of fuel and oxidiser

The equation used for the calculation of the mass fractions of fuel and oxidiser is equation (1.5) with neglible terms neglected.

The numerical form of this equation is:

$$\frac{-N_{i-1}^{k+1}}{(\Delta Z)^2}Y_{i-1}^{k+1} + \left(\frac{1}{\Delta t} + \frac{2N_i^{k+1}}{(\Delta Z)^2}\right)Y_i^{k+1} - \frac{N_{i+1}^{k+1}}{(\Delta Z)^2}Y_{i+1}^{k+1} = W_i^{k+1} \tag{3.10}$$

The above equation contains less terms than that of the temperature equation, and the quantities needed to model the above equation are $\langle N|Z\rangle$ and $\langle W|Z\rangle$. In a similar fashion to the calculation of the conditional temperature, the implicit numerical solution to the above equation is found.

The initial and boundary conditions for the mass fraction of fuel are:

- initially, mass fraction of fuel is equal to the mixture fraction (this is by definition true because no fuel has been consumed),
- the gradient at $Z = 0$ and $Z = 0.15$ is equal to that of the adjacent data point, that is the curvature of the curve is zero at both boundaries.

The initial and boundary conditions for the oxidiser mass fraction are:

- $Y_o(Z = 0)$ = the mass fraction of oxygen in air,
- the initial conditional mass fraction is a function of the mass fraction of oxygen in air, $\langle Y_o|Z\rangle = (1 - Z)Y_o(Z = 0)$, and
- the gradient at the boundaries of Z is zero.

3.1.6 Determination of mean values for normalising quantities

In some instances, the normalised conditional scalar dissipation and normalised conditional generation due to droplet evaporation was modelled, rather than the absolute values of these quantities. Therefore, the mean values of these quantities at any point in time must be known in order to convert the normalised values to absolute values. While the mean values of most of the quantities of the combustion are normally modelled, for the purposes of checking the validity of the CMC model the mean values will be extracted from the DNS data.

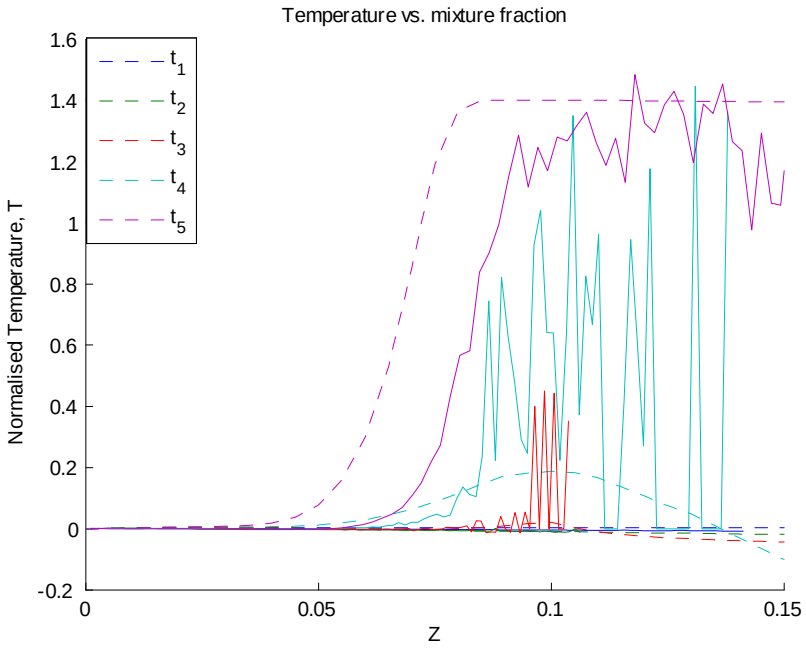

Figure 3.2: Conditional temperature calculated by the first order CMC model (dashed line) versus the the DNS data (solid line) over one quarter of the life of the simulation.

Furthermore, the mean mixture fraction also needs to be known. While this could be obtained through integration of the probability density function, which has been modelled, for simplicity of validating the CMC equation, the mean mixture fraction will also be identified from the DNS data.

3.2 Results

3.2.1 Temperature

The temperature for the first quarter of the time over which the DNS took place is shown in figure 3.2. It can be seen that the calculated values of temperature take a similar shape to what is expected for some values of time, as can be seen by the behaviour at t_4 and t_5. However, at the greatest value of time, the CMC model incorrectly identifies the critical value of mixture fraction needed for combustion. The CMC model suggests that combustion takes place at significantly leaner areas ($Z \approx 0.055$) than is indicated

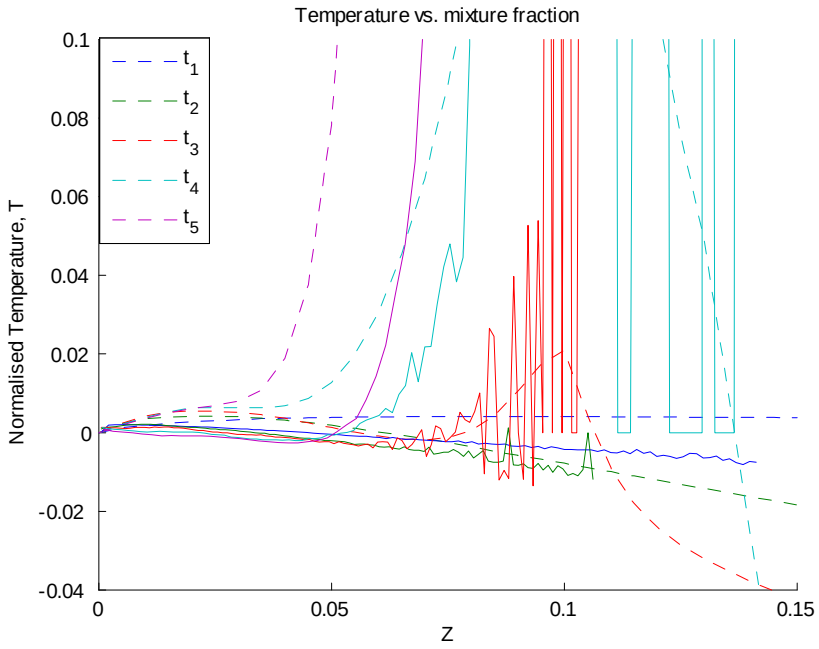

Figure 3.3: A plot of figure 3.2, zoomed in.

by the DNS data ($Z \approx 0.08$).

Figure 3.3 shows the same data as that of figure 3.2 but zoomed in. It can be seen that the first order CMC model does not accurately calculate the conditional temperature for all of the five points in time. The most encouraging aspect of this graph is the behaviour at t_3 and t_4. At this point in time the CMC model identifies the combustion (or the localised peak at $Z \approx 0.1$) quite accurately. However in subsequent points in time, it again predicts that combustion occurs in much leaner regions than suggested by the DNS data.

The conditional temperature for the whole length of the simulation is shown in figure 3.4. As expected, the calculated conditional temperature becomes more erroneous with time. The calculated temperatures after the first quarter of the time over which the calculations take place are of little semblance to the DNS values. This may be attributed to the tendency of the single order CMC model to predict the combustion occurs in much leaner regions than is possible; the graph indicates that the CMC model predicts combustion across all of the values of mixture fraction, with a peak occurring

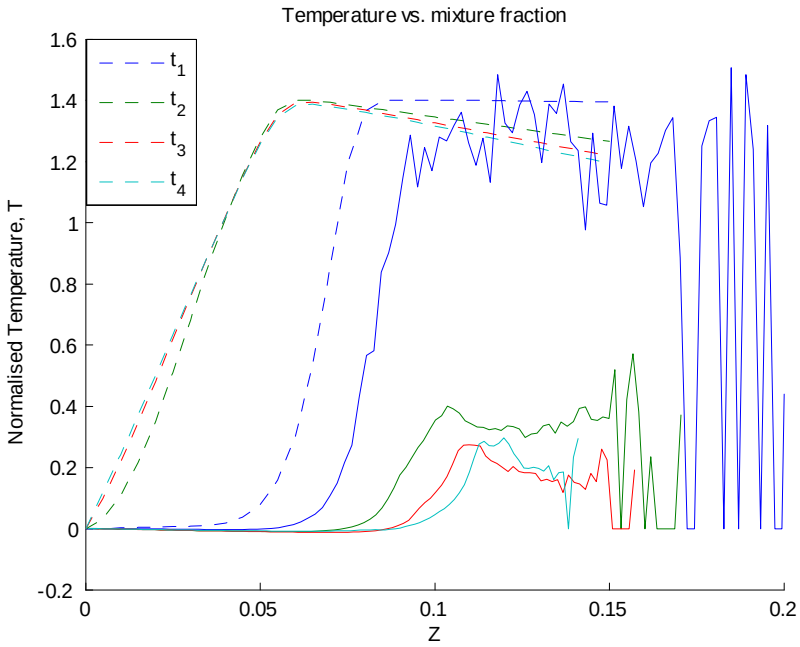

Figure 3.4: Conditional temperature calculated by the first order CMC model versus the the DNS data over the life of the simulation.

at $Z \approx 0.04$. This leads to a much greater rate of combustion and therefore higher temperature.

Because the CMC model overestimates the conditional temperature at moderate to large values of time, a maximum temperature condition had to be put in place to ensure that the temperature was not grossly over predicted. The maximum temperature condition was $T_{max} = 1.4$ which can be seen on the graph. Again, this highlights the tendency of the CMC to overestimate the conditional temperature.

3.2.2 Mass fraction of fuel

Figure 3.5 shows the conditional mass fraction of fuel for the first quarter of the combustion. The blue dots represent no combustion, the broken lines the CMC estimation and the solid lines the DNS data. At small times, (t_1 to t_3), there is little combustion (due to the energy from the spark evaporating droplets rather than initiating combustion), which the CMC model identifies correctly. However, at t_4 a slight deviation from

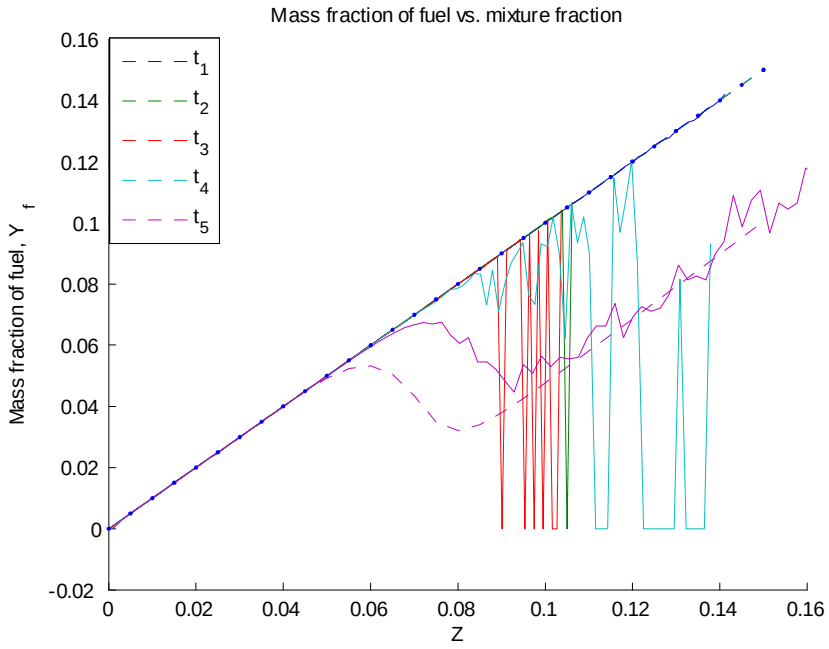

Figure 3.5: Conditional mass fraction of fuel calculated by the first order CMC model versus the the DNS data over one quarter of the life of the simulation.

the dots indicates that some combustion is starting to occur within the system, which is not reflected in the CMC estimation. Therefore the CMC model does not correctly identify the start of combustion. At the last point in time on the graph, t_5, the CMC model overestimates the combustion markedly. However of note is that the general shape of the mass fraction of fuel at this time is quite similar to that of the DNS data; the location of combustion, characterised by the local maxima and minima, seems to be transposed towards a leaner value of mixture fraction. This agrees with the trend observed in the calculation of the conditional temperature that the first order CMC model tends to predict that combustion occurs in much leaner regions than is possible.

Figure 3.6 shows the mass fraction of fuel at large values of time. The estimation of the mass fraction of fuel by the CMC model at large values of time shows a large overestimation of combustion. At high values of time, when there is an abundance of fuel, it stands to reason that the flame kernel would only expand to regions of stoichiometric or richer mass fractions of fuel. However, similar to the analysis of the temperature shown previously, the CMC model suggests that combustion occurs at almost any value of mixture fraction.

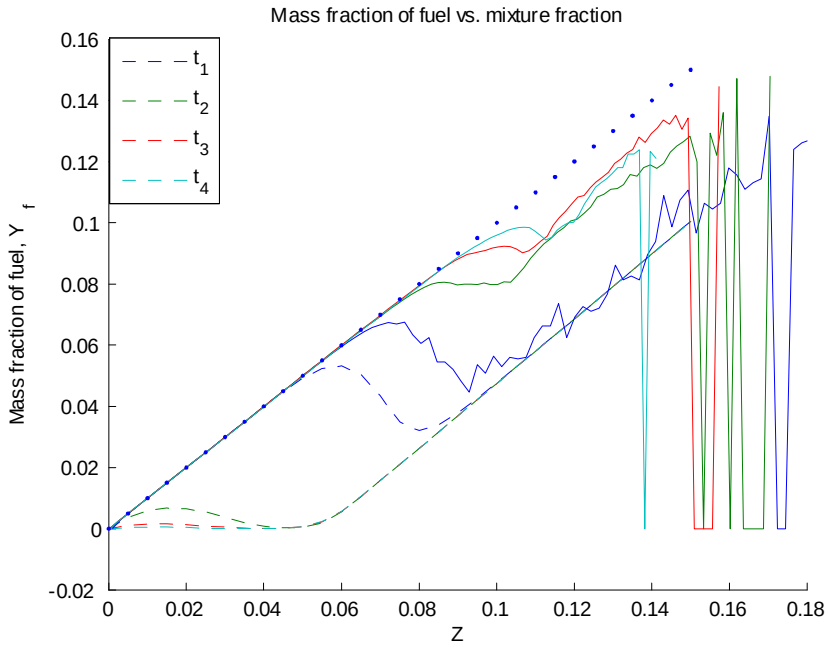

Figure 3.6: Conditional mass fraction of fuel calculated by the first order CMC model versus the the DNS data over the life of the simulation.

3.2.3 Mass fraction of oxidiser

The mass fraction of oxidiser for the first quarter of combustion is shown in figure 3.7. Again, the dots represent no combustion. The graph of the mass fraction of oxidiser shows the same behaviour as that observed in the mass fraction of fuel; the combustion is slow to occur, but once occurring the combustion takes place far too rapidly. Some of the broad behaviour of the system is captured to an extent as can be seen by comparison of the CMC and DNS estimations at time t_5.

As with the mass fraction of fuel at large times, the mass fraction of oxidiser over predicts the rate of combustion (figure 3.8).

3.2.4 Sources of errors

Analysis of the three main quantities of combustion, the mass fractions of both species and the temperature, has revealed that the first order CMC model has been unable to

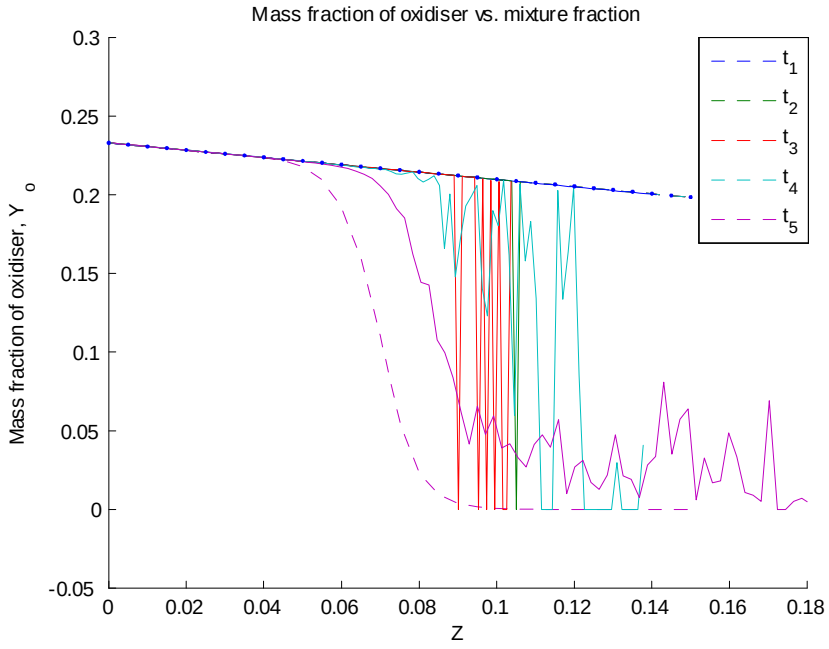

Figure 3.7: Conditional mass fraction of oxidiser calculated by the first order CMC model versus the the DNS data over one quarter of the life of the simulation.

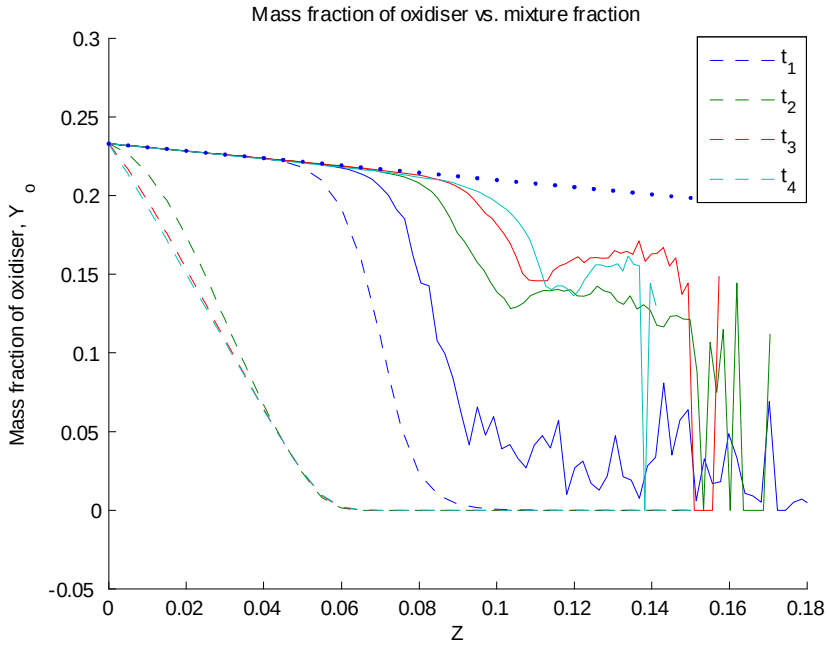

Figure 3.8: Conditional mass fraction of oxidiser calculated by the first order CMC model versus the the DNS data over the life of the simulation.

predict the behaviour of the spark assisted spray combustion that was analysed using DNS. The main error is the inclination of the CMC model to predict combustion in lean areas.

The source of the error is in the calculation of the temperature, which has a flow on effect to the other quantities. As time passes, the error becomes larger until the behaviour reported by the CMC model bears little resemblance to the behaviour reported by the DNS. This is because the errors in the calculation of the temperature, chemical source and mass fractions as shown in figure 3.1 are compounded with each step in time. For example, any error in the calculation of the temperature is then used in the calculation of the source term, which is then used in the calculation of the mass fractions. These values are then used in the next timestep.

Variance of temperature

Analysis of the DNS data reveals that there is quite a high variability of the conditional temperature. The inability of the first order CMC model to accurately predict the mean conditional temperature may be due to this variability.

Figure 3.9 shows the mean conditional temperature, and one standard deviation either side of this mean, as calculated by the DNS. The graphs shown are for the first quarter of time. It can be seen that the temperature deviates from this mean quite substantially. This may be attributed to the effect of the spark and the flame kernel. For example, in the domain, there may be several areas which have a mixture fraction which is conducive to combustion, however these areas may be far from the effects of the spark or flame kernel and therefore do not combust. These areas remain relatively cold. Likewise, there may be areas of the same mixture fraction which do indeed combust as they are in close proximity to an energy source. These areas are therefore relatively hot. This explains why, at a certain mixture fraction, there exists quite a large variation in the conditional temperature.

The CMC values of conditional temperature are also shown on figure 3.9. For the first three points in time, the CMC values of temperature are quite close to the known

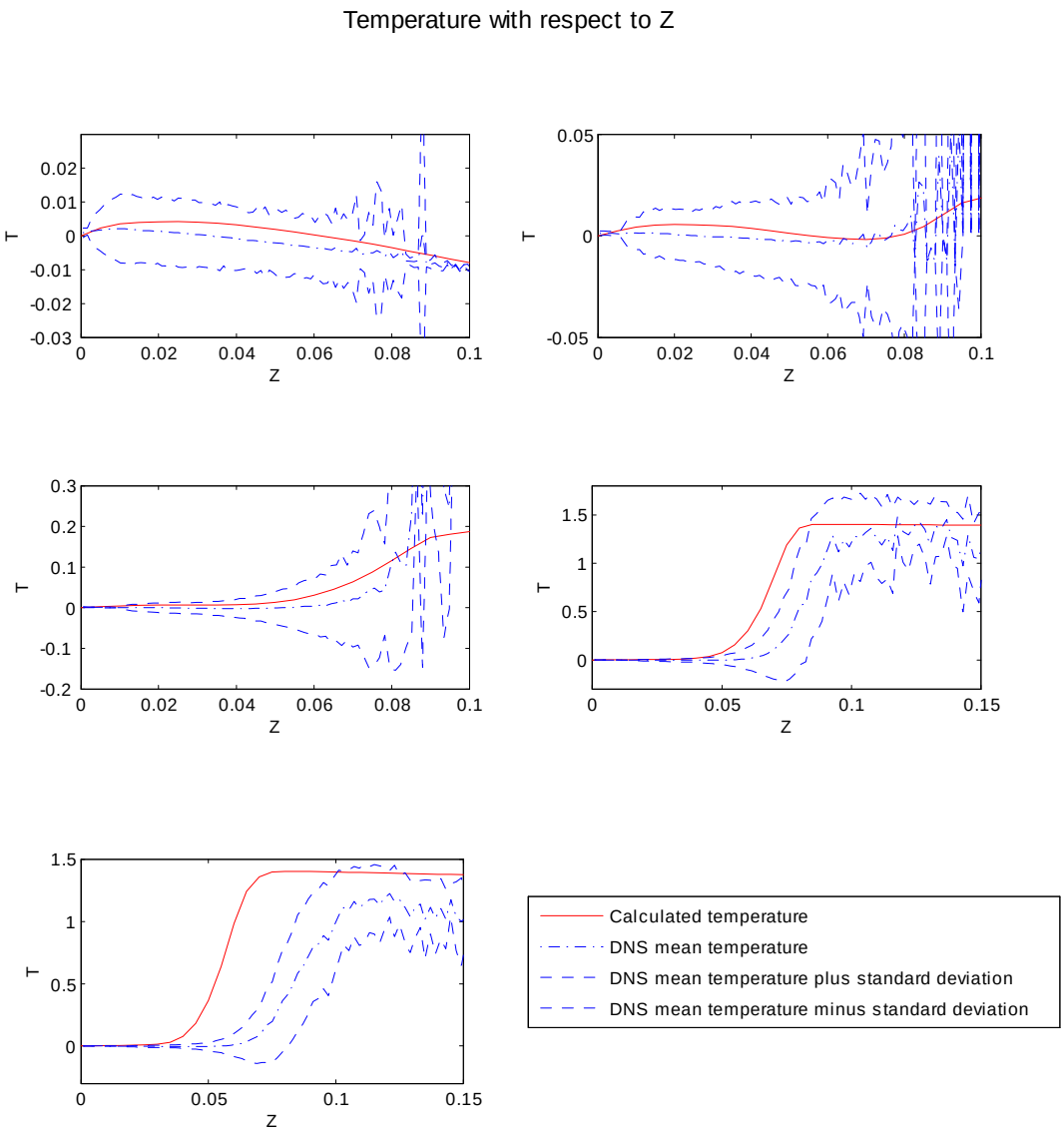

Figure 3.9: Variance of the conditional temperature as calculated from DNS data and the mean conditional temperature calculated from the CMC model.

mean and represent an encouraging fit. The maximum error for these first three graphs is approximately one half of a standard deviation. However, as time progresses, the calculated temperature becomes more erroneous and breaks out of the range of one standard deviation.

3.2.5 Comments on the validity of the first order CMC model

The ability of the first order CMC model to model the temperature at small values of time is quite encouraging. However, once combustion begins to occur and a flame kernel forms, the accuracy of the first order CMC model is compromised. It can be seen from the previous analysis that during the middle and latter stages of combustion, the CMC model grossly overestimates the rate of combustion.

In the current form of the CMC model, the results are not satisfactory. Further work will need to be undertaken to allow for the modelling of spark assisted spray combustion.

The work presented in this thesis serves more than disproving the ability of the first order CMC to accurately model two-phase spark assisted combustion. The techniques developed for the first order CMC model may be transferred towards the use of a doubly-conditioned CMC model.

One of the core assumptions of the first order CMC model is one conditioning variable, most commonly mixture fraction, is able to fully characterise the behaviour of most of the critical quantities of combustion. Implied in this assumption is that the variance of each conditional variable is quite small. For example, for all the areas within the domain that share a common mixture fraction, the conditional quantities at these points vary little. So for a given mixture fraction, say $Z = 0.06$, one would expect that the conditional temperature at these points would have a distinct mean and small variance.

The variance of the conditional temperature has already been discussed in the analysis of the CMC results. The variance of the mass fraction of fuel over the length of the simulation is shown in figure 3.10. It can be seen that at areas with high values of mixture fraction, there is a large variance of fuel mass fraction. This suggests that some of those areas are undergoing combustion while others are yet to become ignited.

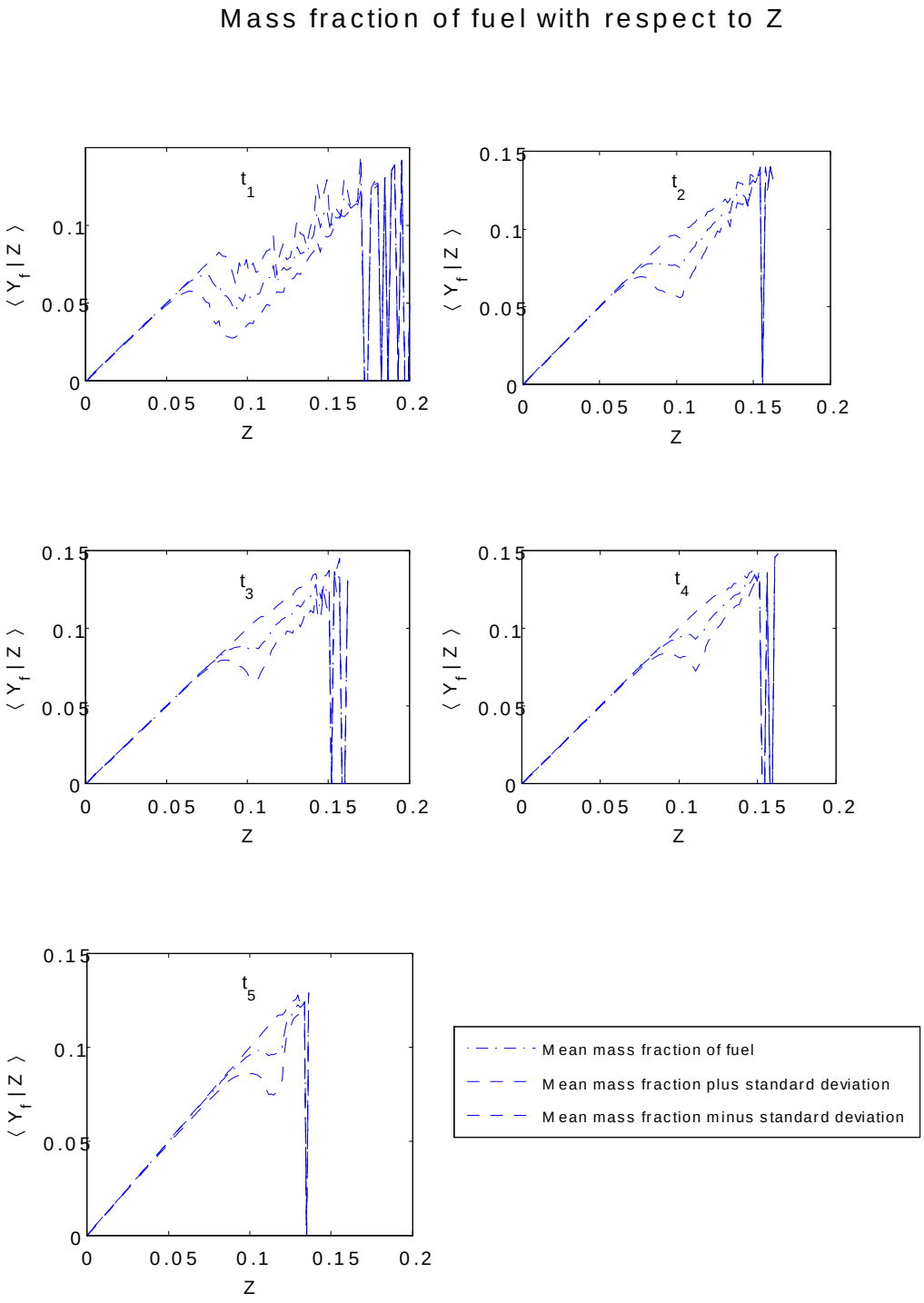

Figure 3.10: Variance of the conditional mass fraction of fuel as calculated from DNS data.

The large variance of conditional temperature and conditional mass fraction of fuel suggests that all the other quantities included in the CMC equations also exhibit high variance. Therefore, the assumption that one conditioning variable, mixture fraction, is able to fully characterise each quantity is most likely invalid. Therefore, in order to model the system using the CMC model, it seems that a doubly-conditioned CMC model is required.

3.2.6 Use of a doubly-conditioned CMC model

The inability of the first order CMC model to accurately model certain types of spray combustion has been recognised before. Kronenburg & Papoutsakis (2005) investigated the use of the doubly-conditioned CMC model to model local extinction and reignition in two phase compression ignition systems.

The work suggested that the localised extinction and reignition points cause large variations in the CMC terms. The variance was found to be 'associated with non-negligible fluctuations around the conditional mean due to local extinction, i.e., fluctuations of reactive scalars cannot be associated with those of mixture fraction only', and therefore the assumptions of the first order CMC model become invalid.

In addition to the conditional mass fractions and conditional temperature varying about a single conditional variable, it was also demonstrated how variables of the CMC equation, such as scalar dissipation, also showed high variance.

There are some parallels between the presence of local extinction and reignition events and the addition of a spark to a system. The variation occurring due to the presence of local reignition is likely to be similar to the variation caused by the addition of the spark, and the presence of local extinction is akin to the removal of the spark.

In order to account for the fluctuations about the mean at the locations of extinction and reignition, a second conditioning variable was added, creating a doubly-conditioned CMC model. The second conditioning variable which was used was sensible enthalpy, ξ.

The use of a doubly-conditioned CMC model led to the accurate prediction of extinction and reignition events, whereas the first order CMC model could not. Given that there are some similarities between the work performed by Kronenburg & Papoutsakis (2005) and the work in this thesis, it is likely that the addition of a second conditioning variable would allow for the accurate modelling of spark assisted spray combustion.

Form of the doubly-conditioned CMC model

The form of the CMC equation used in the work of Kim et al. (2002) was

$$\begin{aligned} \langle \rho|\eta,\xi\rangle \frac{\partial Q_\alpha}{\partial t} &= \langle W_\alpha|\eta,\xi\rangle + \langle W_h|\eta,\xi\rangle \frac{\partial Q_\alpha}{\partial \xi} \\ &\quad + \langle \rho D_\alpha \nabla\xi\nabla\xi|Z,\xi\rangle \frac{\partial^2 Q_\alpha}{\partial \eta^2} \\ &\quad + \langle \rho D_\alpha \nabla h\nabla h|\eta,\xi\rangle \frac{\partial^2 Q_\alpha}{\partial \xi^2} \\ &\quad + 2\langle \rho D_\alpha \nabla\xi\nabla h|\eta,\xi\rangle \frac{\partial^2 Q_\alpha}{\partial Z \partial \xi} + e_y \end{aligned} \tag{3.11}$$

where

- η is the fully conserved mixture fraction,
- ξ is the sensible enthalpy, and
- e_y is a term which accounts for the variance about the two conditioning variables.

The use of this equation is much more complex and computationally intense than the first order CMC equation, but the solving time is still many magnitudes less than is needed for a DNS. The introduction of a second conditioning variable makes the current work much more complex. The presence of three independent variables, namely mixture fraction, enthalpy and time, makes modelling of all terms of the CMC equation more difficult and beyond the scope of this thesis.

Chapter 4

Conclusions and further work

4.1 Conclusions

Data obtained from several Direct Numerical Simulations has been gathered in order to characterise the terms of the CMC model. The DNS data is from the spark ignition of n-heptane fuel in droplet form. The quantities modelled were for use in the first order CMC model.

The use of different forms of the CMC model in literature was investigated. It was found that in many different scenarios of combustion, such as jets, counterflow, compression ignition and spray combustion, the CMC model was able to predict the behaviour with varying degrees of accuracy. The versatility of the CMC model suggested that it would be well suited to the simulation of spark assisted spray combustion.

Some of the assumptions of the first order CMC model were outlined. One of the assumptions is that the quantities present in the CMC equation did not fluctuate greatly around a single conditioning variable (mixture fraction). In some cases, this assumption was found to be false (Kronenburg & Papoutsakis 2005). In order for the simulation in Kronenburg & Papoutsakis (2005) to be successful, a second conditioning variable, sensible enthalpy, was added. This accounted for the significance variance encountered in the single conditioned data.

Some of the applications of the work to be undertaken was discussed. Perhaps the most relevant application of the CMC model to spark assisted spray combustion is the use of partial or full stratification. Stratification refers to the process of centring a high density of fuel about the spark, while leaving the rest of the combustion chamber lean or void of fuel. This essentially creates a lean burn, which is advantageous for increasing fuel efficiency and reducing pollutants. The implications of the work towards the academic community was also discussed.

The selection of DNS was the next step in the process. The data was investigated to determine a case of combustion which was typical of most combustion, namely premature global extinction did not occur. This was done by checking the maximum temperature of the domain. The case chosen for further analysis was for combustion with an equivalence ratio of 2 and a droplet diameter of 3.936um.

Four distinct zones of combustion were identified. These different zones were characterised in turn. Models for the mixture fraction probability density function were developed first. The Favre averaged probability density function was used as it resulted in the behaviour becoming self similar over time. It was found that at small values of time, the mixture fraction pdf was a β-function and closely resembled the initial conditions of the DNS data as significant amounts of fuel had yet to be burnt. As time progressed, two Gaussian peaks emerged. The most prominent peak showed most fuel to occur at a mixture fraction near stoichiometric. The secondary peak linked the behaviour of the β-function with the primary peak.

The conditional scalar dissipation was the first quantity of the CMC model to be characterised. At small values of time, a single polynomial was used to describe the behaviour. Zone 1 was a transient stage between the relatively stable zones 0 and 2. Because the scalar dissipation was a function of both the mixture fraction and time, the characterisation had to be more thorough. The locations of a local maxima and minima were modelled with respect to time. These two known points, as well as the origin, where then joined with the use of two cubic splines. The tail of the curves all passed through a common point, allowing a quadratic to be used to join the local minima and the common point. The behaviour in zone 2 became more self similar. The locations of the maxima and minima remained constant, allowing for the use of two

cubic splines over the whole zone. The tail of the graph showed transient behaviour and the coefficients of a cubic used to describe the tail were modelled with respect to time. Zone 3 showed some decay of the system, but one curve was used to approximate the behaviour for all points in time.

The conditional generation due to droplet evaporation was characterised. Zone 0 was approximated with the use of one cubic and one straight line. All of the other zones could be characterised by the use of a constant, 'base' function, while upward branches from this function were described with straight lines. The 'base' function was described with the use of an error function. The coefficients of the straight lines were a function of time.

The characterisation of the CMC terms with respect to one conditioning variable was relatively easy to perform and proves the validity of using DNS data to develop models for the CMC terms.

Once all of the terms of the single order CMC equation were defined, the accuracy of the CMC model had to be determined. This could be achieved by comparing the outputs of the CMC model (conditional species mass fractions and conditional temperature) against the DNS data. A MATLAB script was developed to perform the CMC calculations.

In order for the CMC and DNS outputs to be compared, the initial conditions of the system had to be identical for both cases. In addition, the timestep of the CMC solution was the same as that of the DNS in order to directly compare the outputs of both methods at the same points in time. Solving the CMC equations required a numerical solution, in particular the implicit numerical solution as the explicit method encountered stability problems.

In order to reduce the complexity of trying to validate the CMC model, some of the quantities needed were accessed from the DNS data. These quantities included droplet temperature, density, mean scalar dissipation and mean generation due to droplet evaporation.

Using the temperature form of the CMC equation, the conditional temperature was

the first quantity to be calculated after incrementing the time. The terms of the CMC equation were accessed from the previous timestep.

Using the temperature from the same timestep, and the species mass fractions from the previous timestep, the source term was calculated. The source term is a combination of the spark source, which was obtained from the DNS data, and the chemical source, derived from an Arrhenius equation. The species mass fractions were then calculated using an implicit version of the CMC equation.

The results were compared to the DNS data in order to determine if the first order CMC equation is a valid method of predicting the behaviour of spark assisted spray combustion. The first order CMC model captured some of the behaviour of the system, with encouraging results from the conditional temperature and mass fractions, but overall the first order CMC model was quite poor. The rate of combustion was over-predicted, especially in lean areas.

Upon further investigation, one of the key assumptions of the CMC model was determined to have been broken. The assumption states that one conditioning variable is adequate to describe the behaviour, and that the variance about the mean of the quantities is small. Analysis of the DNS data showed this to be incorrect. The temperature and species mass fractions showed high variance when the mixture fraction was used as a conditioning variable. This indicates that a doubly-conditioned CMC model is required.

Comparisons were made between other cases where a doubly-conditioned CMC model was required. One such case was Kronenburg & Papoutsakis (2005), where local extinction and reignition caused fluctuations about the mean. This is somewhat similar to the addition and removal of the spark, which may have also caused high variance.

Overall, the work in this project aims to highlight the processes required for the analysis of DNS data to develop models for the CMC terms. It has been shown that all of the terms of the first order CMC equation were able to be modelled with a high degree of accuracy. Some of the techniques for developing these models, such as normalising certain quantities by their mean values, may also be used when characterising the data

with respect to two conditioning variables.

4.2 Further work

4.2.1 Further work required for doubly-conditioned CMC modelling

The analysis of DNS data in order to characterise the terms of the CMC model becomes much more complex when another conditioning variable is used. In addition to characterising each of the quantities (scalar dissipation, generation due to droplet evaporation and chemical source) with respect to time and mixture fraction, they must also account for variations with respect to enthalpy. In addition, the enthalpy probability density function must be characterised.

There are several factors which may reduce the complexity of the doubly-conditioned CMC model. For example, the most significant events which cause the quantities to have large fluctuations from the mean are the addition, and removal, of the spark. The residual effect of these events on the variation of the quantities is at this stage unknown. If the residual effect is small, the use of a second conditioning variable may only be necessary in close proximity to these events. The stages in the combustion where the combustion becomes somewhat steady may only require the use of a single order CMC model.

Characterising the terms of the CMC equation with respect to mixture fraction and enthalpy would require the DNS data to be more comprehensive. The terms would have to recorded with respect to both the mixture fraction and enthalpy.

In order to characterise the CMC quantities with respect to both the mixture fraction and enthalpy, a systematic approach would need to be implemented. The steps taken may be similar to:

1. Choose a zone of combustion (for example, zone 1).

2. Check the variability of the each of the quantities over that zone.

3. If the variability is small for each of the terms, the first order CMC model may be used. However, if there is significant variance in any one of the terms, higher order modelling is required:

4. Choose one point within the Z domain. For that point in time, at that specific value of Z, plot the terms with respect to the enthalpy and characterise this graph.

5. Choose other Z points and determine if the behaviour is similar for various values of Z. If not, approximations for the behaviour conditional upon enthalpy will need to be used.

6. Move on to another zone.

It is difficult to say whether the above steps will be difficult at this stage without having access to data which has been recorded with respect to two conditioning variables.

4.2.2 Further work required for the coupling of CMC and CFD

Further work also needs to be undertaken to couple the CMC model with CFD software. The process of coupling CMC and CFD has been discussed previously. The first step required is to find a suitable CFD program which allows the user the flexibility to code in the CMC models. The software used in both Wright (2010) and De Paola et al. (2008) was STAR-CD. As the license of CFD software is often expensive, the analysis would have to be performed with the most readily available product. The University of Southern Queensland is licensed to provide both Fluent and CFX, so both of these options would be thoroughly investigated in order to determine which would allow the most seamless integration of the CMC model.

The CMC model would take as input certain aspects of the flow field like velocity and pressure. The CMC code may then be run in the CFD environment, or in an external environment such as MATLAB. The results of the CMC analysis would then be used by the CFD software in order to determine the flow field at the next timestep. When determining which program would best suit this analysis, the ability of the program to perform the above steps would be the critical factor. The ease with which the

code is written in the CFD environment, or the ease with which an external coding environment is linked to the CFD program, would be a major aspect to consider.

Another complex aspect of coupling CMC with CFD is the determination of the mesh for each process. The process which De Paola et al. (2008) used is quite robust. A separate mesh is used for each process, with the CFD grid determined by the CFD software. An algorithm is then used at each timestep to map the behaviour of the dynamic CFD grid to a stationary, predefined CMC grid. While some accuracy may be lost when using this process, the method is proven and at this stage would be the easiest path to take.

The determination of the initial conditions would also have to be undertaken from known experimental data. Parameters such as droplet density, size and spray pattern could be investigated from experimental analysis of injector behaviour. Other important conditions, such as initial temperature, pressure and the behaviour of the flow of the incoming air would also need to be approximated.

4.2.3 Further work required on the MATLAB scripts

The development of the models for the terms of the CMC model is an integral part of the process outlined in this project. Therefore, the streamlining of this process would be quite useful.

Currently, in order to develop models for the conditional scalar dissipation, conditional generation due to droplet evaporation and the mixture fraction pdf, several MATLAB scripts are used. These scripts focus on developing models for one quantity at a specific zone. The value of these scripts could be greatly increased if one script fully defined every zone for a conditional quantity. Furthermore, if the scripts were made to be function files, these functions could be called from within the script shown in Appendix A, rather than manually coding in the values of each model.

However, the most important objective would be to make the scripts as robust as possible when investigating other cases of combustion. For example, some of the important characteristic of the curves are currently coded in manually by the user after graph-

ically analysing the data. One such characteristic is the determination of the 'zones' of combustion. Further versions of the scripts should be able to identify all important characteristics of the graph without help from the user. Furthermore, they should be robust enough to identify the different behaviour of different cases of combustion.

However none of the above may be performed without first characterising the CMC terms with respect to two conditioning variables, mixture fraction and enthalpy. This is where the further work should be focussed on first.

References

Bini, M. & Jones, W. P. (2008), 'Large-eddy simulation of particle-laden turbulent flows', *Journal of Fluid Mechanics* **614**, 207–252.

Crawley, J. (current May 2010), *U.S. unveils new push for more efficient cars, trucks*, `http://www.reuters.com/article/idUSTRE64K4JK20100521`.

De Paola, G., Mastorakos, E., Wright, Y. M. & Boulouchos, K. (2008), 'Diesel engine simulations with multi-dimensional Conditional Moment Closure', *Combustion Science and Technology* **180**, 883–899.

Fairweather, M. & Woolley, R. M. (2004), 'First-order contitional moment closure modeling of turbulent, nonpremixed flames', *Combustion and Flame* **138**, 3–19.

Gillard, J. (current August 2010), *Emissions Standards for Cars*, `www.alp.org.au`.

Girimaji, S. S. (1991), 'Assumed β-pdf model for turbulent mixing: Validation and extension to multiple scalar mixing', *Combustion Science and Technology* **78**, 177–196.

Kim, I. S. & Mastorakos, E. (2006), 'Simulations of turbulent non-premixed counterflow flames with first-order conditional moment closure', *Flow, Turbulence and Combustion* **76**, 133–162.

Kim, K. H., Huh, K. Y. & Bilger, R. W. (2002), 'Second-order conditional moment closure modeling of local extinction and reignition in turbulent non-premixed hydrocarbon flames', *Proceedings of the Combustion Institute* **29**, 2131–2137.

Klimenko, A. Y. & Bilger, R. W. (1999), 'Conditional moment closure for turbulent combustion', *Progress in Energy and Combustion Science* **25**, 595–687.

Koss, H. J., Bruggemann, D., Wiartalla, A., Backer, H. & Breuer, A. (2010), 'Investigations of the influence of turbulence and fuel type on the evaporation and mixture formation in fuel sprays', *Integrated Diesel European Action* .

Kronenburg, A. & Papoutsakis, A. E. (2005), 'Conditional moment closure modeling of extinction and re-ignition in turbulent non-premixed flames', *Proceedings of the Combustion Institute* **30**, 759–766.

Lebas, R., Menard, T., Beau, P. A., Berlemont, A. & Demoulin, F. X. (2009), 'Numerical simulation of primary break-up and atomization: DNS and modelling study', *International Journal of Multiphase Flow* **35**, 247–260.

Lu, T., Law, C. K., Yoo, C. S. & Chen, J. H. (2009), 'Dynamic stiffness removal for direct numerical simulations', *Combustion and Flame* **156**, 1542–1551.

Massebeuf, V., Bedat, B., Helie, J., Lauvergne, R., Simonin, O. & Poinsot, T. (2006), 'Direct numerical simulation of evaporating droplets in turbulent flows for prediction of mixture fraction fluctuations: application to combustion simulations', *Journal of the Energy Institute* **79**, 212–216.

Mortensen, M. & Bilger, R. W. (2009), 'Derivation of the conditional moment closure equations for spray combustion', *Combustion and Flame* **156**, 62–72.

Nabi, N. (2010), 'Theoretical investigation of engine thermal efficiency, adiabatic flame temperature, $_x$ emission and combustion-related parameters for different oxygenated fuels', *Applied Thermal Engineering* **30**, 839–844.

Reynolds, C. C. O. B. & Evans, R. L. (2003), 'Improving emissions and performance characteristics of lean burn natural gas engines through partial stratification', *Internation Journal of Engine Research* **5**, 105–114.

Sreedhara, S. & Huh, K. Y. (2007), 'Conditional statistics of nonreacting and reacting sprays in turbulent flows by direct numerical simulation', *Proceedings of the Combustion Institute* **31**, 2335–2342.

Taymaz, I., Cakir, K. & Mimaroglu, A. (2005), 'Experimental study of effective efficiency in a ceramic coated diesel engine', *Surface and Coatings Technology* **200**, 1182–1185.

Wandel, A. P., Chakraborty, N. & Mastorakos, E. (2009), 'Direct numerical simulations of turbulent flame expansion in fine sprays', *Proceedings of the Combustion Institute* **32**, 2283–2290.

Wang, Y. & Rutland, C. J. (2007), 'Direct numerical simulation of ignition in turbulent n-heptane liquid-fuel spray jets', *Combustion and Flame* **149**, 353–365.

Wright, Y. M. (2010), 'Experiments and simulations of n-heptane spray auto-ignition in a closed combustion chamber at diesel engine conditions', *Flow Turbulence Combust* **84**, 49–78.

Appendix A

Project Specification

University of Southern Queensland

FACULTY OF ENGINEERING AND SURVEYING

ENG4111/4112 Research Project
PROJECT SPECIFICATION

FOR: Jason Peter CLARKE

TOPIC: ANALYSIS OF DATA TO DEVELOP MODELS FOR SPRAY COMBUSTION

SUPERVISOR: Dr. Andrew WANDEL

PROJECT AIM: To develop models for spark assisted spray combustion through analysis of data generated by Direct Numerical Simulations performed by Dr. Andrew Wandel.

PROGRAMME: **(Issue A, 22 March 2010)**

1. Research past attempts to characterise spray combustion.

2. Analyse a set of Direct Numerical Simulation (DNS) data to discover underlying trends that can be used to produce models for certain terms in the Conditional Moment Closure (CMC) equation for spray combustion. This is to be done by displaying the data graphically in an attempt to visualise how different input parameters (such as droplet size and spacing, and spark duration) affect the combustion process.

3. Investigate how the mass release of fuel through evaporation of droplets by the spark affects different aspects of combustion.

4. Identify trends in the data.

5. Develop curve-fits to characterise the combustion through the different stages of combustion.

6. Use CFD software to apply the developed models to larger simulations.

As time permits:

7. Apply the models to actual physical combustion, such as in the combustion chamber of a petrol engine.

8. Investigate conditions which lead to the most efficient combustion of fuel.

AGREED *Jason Clarke* (student) *Andrew Wandel* (supervisor)
22/03/2010

Examiner/Co-examiner: _____

Appendix B

MATLAB script

The following is the MATLAB script used to validate the first order CMC model. The terms of the CMC model have been modelled beforehand through analysis of the DNS data. The validation of the outputs of the CMC model is done graphically and is not shown in this script.

```
% Important time indexes
starttime = 300;
endtime = 4000;
indexstep = 500;
t2 = 1300;
t3 = 2350;

% Spark duration
tsp = 0.00952;

% Maximum allowable temperature
Tmax = 1.4;

% Load conditional scalar dissipation from DNS
load n_z.dat

% Define Z and t from DNS data
dZ=(n_z(:,4)-n_z(:,3)) / (size(n_z,2)-4);
Zmin = n_z(:,3);
Zmax = n_z(:,4);
tnorm = n_z(:,2)/tsp;
time = n_z(:,2);
% Number of nodes in Z-direction
nZ = size(n_z,2)-4;
% Create array containing all the Z-values for all timesteps
Zplot = repmat(Zmin+dZ/2,1,nZ) + ...
    repmat(0:nZ-1,size(n_z,1),1).*repmat(dZ,1,nZ);
% Conditional scalar dissipation
NZ = n_z(:,5:end);
% Probability density function of mixture fraction
load zpdf.dat
PZ = zpdf(:,5:end);
% Mean scalar dissipation
load nstat.dat
Nmean = nstat(:,3);
% Mean mixture fraction
load zstat.dat
Zmean = zstat(:,3);
% Mean density
load d_z.dat;
dZ = d_z(:,5:end);
load dstat.dat;
dmean = dstat(:,3);
% Droplet liquid temperature
load dtstat.dat;
Td = dtstat(:,3);
% Spark source
load sp_z.dat
WspZ = sp_z(:,5:end);

% Define indepedant variables
dZ = 0.005;
Z = 0:dZ:0.15;
nZ = length(Z);
dt = (time(2)-time(1))/1;
t = dt:dt:time(end);
tn = t/tsp;
```

```
nt = length(t);
Yf = zeros(nt,nZ);
Yo = zeros(nt,nZ);
% Initial conditions of Yf and Yo
Yf(1,:) = Z;
Yo(1,:) = 0.23295 - 0.2302246 * Z;
SZdata = zeros(1,nZ);
NZdata = zeros(1,nZ);
PZdata = zeros(1,nZ);
TZ = zeros(nt,nZ);
TZ(1,:) = 1/9.13144876325088*Z;
Yf_data = 0;

% Constants
beta = 6;
tau = 4;
Bf = 2.5e7;
Bo = 9.9956997e7;
AFR = 17.16;
gamma = 1.4;

A = zeros(nZ,nZ);
B = zeros(nZ,1);
i = 2:nZ;

for k = 2:endtime;  % For all time
% Calculate mean and normalised values for DNS
Zn = Z./interp1(time,Zmean,t(k));
dm = interp1(time,dmean,t(k));
meanZ = interp1(time,Zmean,t(k));
meanN = interp1(time,Nmean,t(k));

% Calculate source term
if k < 478;     % Spark Source
    Wsp = interp1(Zplot(k,:),WspZ(k,:),Z);
    Wsp(isnan(Wsp)) = 0;
else
    Wsp = zeros(size(Z));
end
Wf = -Bf*dmean(k)*Yf(k-1,:).*Yo(k-1,:).*exp(-(beta/tau*(1+tau)^2)./(1+tau*TZ(k-1,:)));
Wo = -Bo*dmean(k)*Yf(k-1,:).*Yo(k-1,:).*exp(-(beta/tau*(1+tau)^2)./(1+tau*TZ(k-1,:)));
Wt = -Wf*(1+AFR)*gamma;

if k < starttime;  % Calculations at zone 0

NZ = (0.3282*Zn.^2 + 0.2706*Zn) * meanN;
SZ = zeros(size(Z));
f = find(Z>0.025 & Z<0.045);
SZ(f) = 6.68257271143619e5*Z(f).^3 - 0.42963524576816e5*Z(f).^2 ...
    + 0.00916632257700e5*Z(f) - 0.00006493293492e5;
f = find(Z>=0.045);
SZ(f) = 1.10957796798435e3*Z(f) - 0.04128204389030e3;

PZ = 902.395888329216 * betapdf((Zn+eps-0)/(8-0), ...
      0.0380689651575583, 2.905061771776) / (8-0);
PZ = PZ.*meanN./dm;
end

if k >= starttime & k < t2;     % Calculations at zone 1
% Find position of minima and maxima
x1 = (-0.12666274950986/(tn(k)).^2+0.01687501733376/(tn(k))+1)*meanZ;
```

```
x2 = (-0.36336196647208/(tn(k)).^2 + 0.13198443568512/(tn(k)) + 1.65)*meanZ;
y1 = (polyval([0.20803613776866 -1.62401156204858 4.21584585067841  ...
       -1.33845333094621],tn(k)))*meanN;
y2 = (polyval([0.06392292923108 -0.67240394983682 2.77771157873551  ...
       -5.61510528788125 5.52341953543007 -1.14505276874137],tn(k)))*meanN;
x3 = x1;
x4 = x2;
y3 = 0;
y4 = 0;
x0 = 0;
y0 = 0;
xzone3 = 2.187*meanZ; yzone3 = 2.221*meanN;
ydash0 = 0;
Acoeffs = [x1^3 x1^2 x1 1; x2^3 x2^2 x2 1; 3*x3^2 2*x3 1 0; 3*x4^2 2*x4 1 0];
Xcoeffs = [y1;y2;y3;y4];
coeffmid = (Acoeffs^-1*Xcoeffs)';  % Coefficients of middle cubic

B = [x0^3 x0^2 x0 1; x1^3 x1^2 x1 1; 3*x0^2 2*x0 1 0; 3*x1^2 2*x1 1 0];
Y = [y0;y1;ydash0;y3];
coeffstart = (B^-1*Y)';  % Coefficients of start cubic

C = [x2^2 x2 1; 2*x2 1 0; xzone3^2 xzone3 1];
ZZ = [y2; 0; yzone3];
coeffend = (C^-1*ZZ)';  % Coefficients of end cubic

% Scalar dissipation
NZ = zeros(size(Z));
f = find(Z<=x1);
NZ(f) = polyval(coeffstart,Z(f));
f = find(Z>x1 & Z<x2);
NZ(f) = polyval(coeffmid,Z(f));
f = find(Z>=x2);
NZ(f) = polyval(coeffend,Z(f));

% Conditional generation
SZ1 = (erf(4.11334079702044*(Z*10-0.49494449696130))+1)*0.5*1.4; % Base function

% Transient function
M = polyval([-2.55331491948866 58.6011026879749 -457.940364175283 ...
     1363.80799296097],tn(k));
c = polyval([0.00010424159276 -0.00214147549725235 0.0172408639514765 ...
     0.0247155820294859],tn(k));
SZ2 = M*(Z - c);

SZ = max([SZ1 ; SZ2],[],1); % Composite function

% Mixture fraction pdf
gauss3 = 23.1701331855219*normpdf(Zn,1.80908873046397,sqrt(0.194257861080933));
gauss2 = 3.73697193354983*normpdf(Zn,0.470029675139587,sqrt(0.107330863128369));
beta1 = 18.9136524191883 * betapdf((Zn+eps-0)/(0.3-0), ...
          0.952941284730441, 5.65580680750951) / (0.3-0);
PZ = (gauss3+gauss2+beta1)*meanN./dm+eps;
end

if k >= t2 & k < t3;  % Zone 2
% Coefficients of cubic d
coeffd = [0.973799583824862 -21.4985048121448 180.641214571967 ...
           -724.359583760126 1381.78701880408 -961.730472229017];

% Location of points of interest
xmax = 0.9919568*meanZ;
```

```
xmin = 1.6649288*meanZ;
ymin = 0.941120507902074*meanN;

% Scalar dissipation
NZ = zeros(size(Z));
f = find(Z<=xmax);
NZ(f) = (polyval([-3.8549160112568 5.3555471568870 0.7545182072174 0],Zn(f)))*meanN;
f=find(Z>xmax & Z<xmin);
NZ(f) = (polyval([8.62532117782214 -34.37473781428536 42.73512344157097 ...
          -14.73071855964037],Zn(f)))*meanN;
f = find(Z>=xmin);
% Constant coefficients
a = -0.15536151155019;
b = -0.49082203616733;
d = polyval(coeffd,tnorm(k));
% Correction of c to ensure curve passes through minima
c = (ymin/meanN - d)/(a*b*d*(xmin/meanZ)^3+b*d*(xmin/meanZ)^2+d*(xmin/meanZ));
NZ(f) = (a*b*c*d*Zn(f).^3 + b*c*d*Zn(f).^2 + c*d*Zn(f) + d)*meanN;
f=find(NZ<0); NZ(f) = 0;

% Conditional generation
SZ=zeros(size(Z));
SZ1 = (erf(4.11334079702044*(Z*10-0.49494449696130))+1)*0.5*1.4;
M = polyval([-2.55331491948866 58.6011026879749 -457.940364175283 ...
      1363.80799296097],tn(k));
cc = polyval([0.00010424159276 -0.00214147549725235 0.0172408639514765 ...
      0.0247155820294859],tn(k));
SZ2 = M*(Z - cc);
SZ = max([SZ1 ; SZ2],[],1);

% pdf
gauss3 = 12.8574342579664*normpdf(Zn,1.77259587267161,sqrt(0.0930379251931375));
gauss2 = 2.39009161654828*normpdf(Zn,1.05149635568527,sqrt(0.0573191516519168));
beta1 = 27.6221660904781 * betapdf((Zn+eps-0)/(0.9-0), ...
          0.153551056468068, 1.61900335333552) / (0.9-0);
PZ = (gauss3+gauss2+beta1)*meanN./dm;
end

if k >= t3;  % Zone 3
xmax = 0.904174168*meanZ;
xmin = 1.738884098*meanZ;

NZ = zeros(size(Z));
f = find(Z<=xmax);
NZ(f) = polyval([-4.7031815180410 5.9381380704338 0.79676693239664 0],Zn(f))*meanN;
f = find(Z>xmax & Z<xmin);
NZ(f) = polyval([4.49085881278609 -17.8044022665395 21.1823133240837 ...
          -5.81796930196766],Zn(f))*meanN;
f=find(Z>=xmin);
NZ(f) = polyval([1.52737006864932 -5.31183905015193 5.41092880747833],Zn(f))*meanN;

SZ = zeros(size(Z));
SZ1 = (erf(4.11334079702044*(Z*10-0.49494449696130))+1)*0.5*1.4;
M = polyval([-2.55331491948866 58.6011026879749 -457.940364175283 ...
      1363.80799296097],tn(k));
c = polyval([0.00010424159276 -0.00214147549725235 0.0172408639514765 ...
      0.0247155820294859],tn(k));
SZ2 = M*(Z - c);
SZ = max([SZ1 ; SZ2],[],1);

gauss3 = 9.63390164624745*normpdf(Zn,1.67810825120131,sqrt(0.0880827539466074));
```

```
gauss2 = 2.72352456577655*normpdf(Zn,1.02508301616646,sqrt(0.0515322898900093));
beta1 = 9.45856515202054 * betapdf((Zn+eps-0)/(1.1-0), ...
          0.598418714494375, 1.93434196853147) / (1.1-0);
PZ = (gauss3+gauss2+beta1)*meanN./dm;
end

% To create the diagonal elements of the matrix A (mass fraction of fuel)
diag0 = [1 ; [1/dt + 2*NZ(2:end-1)/dZ^2]' ; 1];
diagn1 = [[-NZ(2:end-1)/dZ^2]'; -2];
diag1 = [0; [-NZ(2:end-1)/dZ^2]'];

% To construct A from the diagonal elements
A = diag(diag0,0) + diag(diagn1,-1) + diag(diag1,1);
% To insert boundary conditions
A(end,end-2) = 1;
A(1,2:end) = 0;
A(1,1) = 1;

% To create matrix B (Yf)
B = [0; [Yf(k-1,2:end-1)/dt + Wsp(2:end-1) + Wf(2:end-1)]' ;0];
B = [0; [Yf(k-1,2:end-1)/dt + Wf(2:end-1)]' ;0];

% To create the diagonal elements of the matrix A (mass fraction of oxidiser)
diag0ox = [1 ; [1/dt+2*NZ(2:end-1)/dZ^2]' ; 1];
diagn1ox = [[-NZ(2:end-1)/dZ^2]'; -2];
diag1ox = [2; [-NZ(2:end-1)/dZ^2]'];

% To construct A from the diagonal elements
Aox = diag(diag0ox,0) + diag(diagn1ox,-1) + diag(diag1ox,1);
% Boundary conditions
Aox(end,end-2) = 1; Aox(1,3) = -1;
Aox(1,2:end) = 0;
Aox(1,1) = 1;

% To create matrix B (Yo)
Box = [Yo(1,1); [Yo(k-1,2:end-1)/dt + Wsp(2:end-1) + Wo(2:end-1)]' ;0];
Box = [Yo(1,1); [Yo(k-1,2:end-1)/dt + Wo(2:end-1)]' ;0];

% To create the diagonal elements of the matrix A (normalised temperature)
diagT0 = [1 ; [1/dt + 2*NZ(2:end-1)/dZ^2 + SZ(2:end-1)/128^3 + ...
           (-1+Z(2:end-1)).*SZ(2:end-1)/(dZ*128^3)]' ; 1];
diagTn1 = [[-NZ(2:end-1)/dZ^2]'; -2];
diagT1 = [0; [-NZ(2:end-1)/dZ^2 + (1 - Z(2:end-1)).*SZ(2:end-1)/(dZ*128^3)]'];

% To construct A from the diagonal elements
TA = diag(diagT0,0) + diag(diagTn1,-1) + diag(diagT1,1);
TA(end,end-2) = 1;

% To create matrix B (T)
TB = [0; [Wsp(2:end-1) + Wt(2:end-1) + Td(k)*SZ(2:end-1)/128^3 + ...
       TZ(k-1,2:end-1)/dt]'; 0];
TB = [0 ;[Wsp(2:end-1) + Wt(2:end-1) + Td(k)*SZ(2:end-1) + TZ(k-1,2:end-1)/dt]'; 0];

% To find the mass fraction of fuel at the specified time
row = A\B;
% Save this to an array
Yf(k,:) = row;

% To find the mass fraction of oxidiser at the specified time
rowox = Aox\Box;
% Save this to an array
```

```
Yo(k,:) = rowox;

% To find the normalised temperature at the specified time
Trow = TA\TB;
% Ensure temperature doesn't get too high
Trow = min( Tmax,  Trow );
% Account for any NaN/Inf results
Trow( ~isfinite(Trow) )  =  Tmax;
TZ(k,:) = Trow;

% To find the average Yf over the whole range.
Pnorm = trapz(Z,PZ);
Yf_mean = trapz(Z,Yf(k,:).*PZ/Pnorm);
Yf_data = [Yf_data;Yf_mean];

SZdata = [SZdata;SZ];
NZdata = [NZdata;NZ];
PZdata = [PZdata;PZ];
end
```